Molecular Interactions Between Xanthan Gum, Psyllium, Milk Proteins and Starches, and Their Implications on Gluten-Free Bakery Products

Carolin Bischoff

Department of Food Technology, Engineering and Nutrition
KLGM01 Master Thesis in Food Technology

LUND
UNIVERSITY

MAX PLANCK INSTITUTE
FOR POLYMER RESEARCH

Jungbunzlauer
From nature to ingredients®

November 2021

Lund, Sweden

Subject: KLGM01 Degree Project in Food Technology
Examiner: Associate Prof. Dr. Ingegerd Sjöholm
Supervisor: Dr. Jeanette Purhagen

Assistant-Supervisor (Max Planck Institute for Polymer Research):
Prof. Dr. Thomas A. Vilgis
Assistant-Supervisor (Jungbunzlauer Ladenburg GmbH):
Dr. Natalie Dietz

Abstract

Gluten in bread can cause severe health problems in patients with celiac disease. However, gluten-free substitutions often show impaired quality characteristic like a liquid dough because of a missing gluten-network or accelerated staling due to the high amount of gluten-free starch. Therefore, hydrocolloids are considered to improve gluten-free bread quality characteristics. The idea of this degree project was to understand the interactions between xanthan gum and specific bread ingredients on a molecular basis with subsequent analysis of xanthan gum's function in gluten-free dough and bread. The molecular interactions between xanthan gum, psyllium, starches and milk powder were tested as model systems in water-salt solutions and analysed by rheological measurements, i.e. amplitude sweep, temperature sweep and apparent viscosity profile. Based on these analyses, two types of gluten-free doughs and breads were prepared, one of which contained 1.2% xanthan gum and the other not. The doughs were analysed using rheometry, moisture analysis, texture analysis and kneading behaviour. Moisture analysis as well as texture analysis was performed after baking bread loafs of both types of dough. The analysis of molecular interactions showed that the addition of xanthan gum increased the overall rigidity and viscosity when mixed with starches and psyllium. Also, the combination of xanthan gum with starches resulted in a lower pasting temperature compared to starches without xanthan gum probably due to enhanced starch granule swelling. In contrast to that, the behaviour of the xanthan gum and milk powder formulation seemed to be xanthan-gum driven. The derived effects on gluten-free dough and bread based on the molecular interactions in solution could be partially confirmed in the analysis of dough and bread. For example, the incorporation of xanthan gum to gluten-free dough resulted in a more rigid dough with less moisture release during moisture analysis compared to the gluten-free dough without xanthan gum. The different properties of both tested gluten-free breads showed the thickening effect of xanthan gum, which led to lower baking loss and higher loaf weight with a firmer bread texture in comparison. Also, the observed lower moisture content in the crust of the bread with xanthan gum could probably delay retrogradation and bread staling. From these results it can be concluded that xanthan gum can act as a moisturizer and thickener for gluten-free bread and affects the molecular behaviour of gluten-free starches and psyllium.

Preface

This master thesis was performed within the Master's Program of Food Technology and Nutrition at the Department of Food Technology, Engineering and Nutrition at the Faculty of Engineering (LTH) of Lund University. The project took place between June and November 2021 in cooperation with the Max Planck Institute of Polymer Research (MPI-P) where the practical work was carried out in collaboration with Jungbunzlauer Ladenburg GmbH.

First, a special thank goes to my LTH supervisor Dr. Jeanette Purhagen for taking the time to guide me through the whole project, for the valuable comments and feedback. Secondly, I would like to thank Dr. Thomas A. Vilgis for the insight into the field of rheology, the useful suggestions and the interesting discussions. Thanks also to Andreas Hanewald for the instruction on the equipment and the help in the mechanics lab. Furthermore, thank you to the Foodies Group at MPI-P, especially Hannah and Marta for the kind help and support.

I would also like to express my sincere gratitude to Dr. Natalie Dietz from Jungbunzlauer Ladenburg GmbH for making the project possible, for the guidance through the project and for providing the raw materials.

Lastly, thank you to Associate Prof. Dr. Ingegerd Sjöholm for being the examiner of the project.

Thank you!
Carolin

Abbreviations and Symbols

A	Area
Å	Ångström
Da	Dalton
Eq.	Equation
F	Force
FDA	Food and Drug Administration
G'	Storage modulus
G''	Loss modulus
GdL	Glucono-delta-lactone
GmbH	Limited liability company (german: Gesellschaft mit beschränkter Haftung)
G1	Goal 1
G2	Goal 2
G3	Goal 3
H	Gap size
h	Shear gap width
LVR	Linear Viscoelastic Region
M	Torque
mNm	Millinewton metre
MP	Skim milk powder
MPI-P	Max Planck Institute for Polymer Research
N	Newton
n	Rotational speed
nm	Nanometre
NRRL	Northern Regional Research Laboratories
Ns	Newton second
Pa	Pascal
Pa.s	Pascal-second
Psy	Psyllium
R	Rest
R	Radius
R_i	Bob radius
R_e	Cup radius
rpm	Revolutions per minute
S	Deflection

SAOS	Small Amplitude Oscillatory Shear
SSL	Sodium Stearoyl Lactylate
St	Starch blend
T_g	Glass transition temperature
tanδ	Loss factor
Temp.	Temperature
TPA	Texture Profile Analysis
V	Volume
W	Weight
w/w	Weight by weight
XG	Xanthan gum
Y	Yeast
δ	Phase shift
η	Viscosity
$\eta(\dot{\gamma})$	Apparent viscosity or shear viscosity
$\vec{p}$	Momentum
φ	Deflection angle
τ	Shear stress
υ	Velocity
ω	Frequency
γ	Shear strain
$\dot{\gamma}$	Shear strain rate
γ_A	Strain amplitude

Contents

1. Introduction

1.1 Background and Relevance of the Project

Traditional wheat bread is mainly composed of wheat flour, water, yeast and salt. During mixing, these ingredients form a viscoelastic dough which, under heat treatment, develops into a bread with a spongy, soft crumb and a crispy crust. This viscoelastic property is attributable to the protein gluten contained in wheat flour and its interaction with other ingredients. However, gluten can cause severe health problems like celiac disease in individuals (Hamer, 2005). This chronic disease is characterized by inflammations in the small intestine after ingestion of gluten from wheat, rye or barley (Schuppan, Junker & Barisani, 2009). Only a lifelong elimination of gluten in the diet recovers the intestinal mucosa and reduces the progression of this disease (Gallagher, Gormley & Arendt, 2004).

However, the development of gluten-free bakery products introduces technological challenges regarding texture. The fact that the final texture of the product influences sensory attributes and hence consumer acceptance makes the imitation of a gluten network a major challenge (Saha & Bhattacharya, 2010). Research has shown that hydrocolloids such as xanthan gum are commonly used in gluten-free bakery products which directly affect the rheology of doughs and final bread quality characteristics (Crockett, Ie & Vodovotz, 2011; Saha & Bhattacharya, 2010). Although extensive research has been carried out on xanthan gum in gluten-free products, little is known about the molecular interactions of xanthan gum between starches, psyllium and milk powder and the resulting bread properties. The knowledge gained from this degree project will be used to extend the area of application of xanthan gum in gluten-free baked products and to offer more alternatives to people suffering from coeliac disease.

1.2 Aim of the Project

The overall aim of the degree project was to understand the function and interactions of xanthan gum in gluten-free bread. This was examined based on the following research questions:

- How does xanthan gum interact with psyllium, milk proteins and a gluten-free starch blend in solution under heat treatment?
- How can the viscoelastic behaviour of gluten-free doughs be described?
- What are the resulting textural bread properties?

The first research question referred to the rheological analysis of different combinations of the four ingredients in salt-solution. This was performed to understand the molecular interactions between xanthan gum + gluten-free starch blend, xanthan gum + psyllium and xanthan gum + milk powder. The second question aimed to investigate the function of xanthan gum in gluten-free dough by studying the rheological behaviour, kneading behaviour, texture and moisture retention of gluten-free doughs with and without xanthan gum. Lastly, on basis of the second question, the two gluten-free doughs (with and without xanthan gum) were baked to understand the implications of xanthan gum on gluten-free bread.

1.3 Scope and Delimitations

The investigation of the influence of hydrocolloids on gluten-free dough and breads is an extensive and complex topic. Therefore, this degree project was performed within delimitations. Overall, the degree project was adapted to meet the requirements of the Lund University, Max Planck Institute for Polymer Research (MPI-P) and Jungbunzlauer Ladenburg GmbH. All written parts and experimental analyses were completed within a given time period. Because of this defined period the project focused on rheology and textural parameters so that neither chemical nor sensory analyses were performed. Moreover, the focus of this degree project was the analysis of three molecular interactions, namely xanthan gum - starch blend, xanthan gum - psyllium and xanthan gum - milk proteins. This means that the analysis of further molecular interactions between e.g. psyllium and milk proteins was out of scope. In addition, improvements in the nutritional value of the gluten-free breads were also not considered as the composition and recipe for the gluten-free bread was already predefined by the company Jungbunzlauer Ladenburg GmbH. As the degree project at the MPI-P was conducted on behalf of Jungbunzlauer Ladenburg GmbH the experiments were chosen based on availability of instruments and feasibility. Finally, the laboratory work had to be adapted to the measures against the Covid-19 pandemic.

2. Theoretical Background

This chapter gives an overview why hydrocolloids are important in gluten-free bread. It starts by explaining the function of gluten in bread and the resulting textural consequences in gluten-free bread. As this investigation focuses particularly on xanthan gum and its molecular interactions with specified ingredients, the molecular structure and resulting properties will be explained individually for all four ingredients with focus on xanthan gum. After that, the theory of rheological analysis methods used in this degree project is explained.

2.1 Gluten in Bread

To understand the properties of gluten-free bread it is important to know the function of gluten. Gluten is a non-water-soluble protein that occurs in wheat flour and makes up the largest proportion (85%) of wheat proteins (Veraverbeke & Delcour, 2002). The remaining 15% consist of a mix of e.g. albumins and globulins (Appell et al., 2018). Gluten consist of the proteins glutenin and gliadin which bring viscoelasticity and structure to the dough after hydrating and kneading dough (Anton & Artfield, 2008). This is enabled by the formation of a 3D-network surrounding starch granules and entrapping gas within the proofing and baking steps (Gan et al., 1989; Zandonadi, Botelho & Araújo, 2009). Consequently, it prevents the diffusion of carbon dioxide (CO_2) from the dough resulting in higher bread specific volume and favourable crumb characteristics (Arendt et al., 2008; Crockett, Ie & Vodovotz, 2011; Gallagher, Gormley & Arendt, 2004; Preichardt et al., 2011). It gives structure to form a soft, loose and fine-pored crumb (Crockett, Ie & Vodovotz, 2011). Whereas glutenins contribute to elastic behaviour and provide strength to the network through polymerization by sulfhydryl-disulphide interactions, gliadins contribute to viscous behaviour making gluten strains more extensible (Arendt et al., 2008; Clare Mills et al., 1990). Their lack in gluten-free bread provides challenges to mimic their unique viscoelastic properties as can be seen in the next chapter.

2.2 Gluten-Free Bread

In general, bread is classified as a soft solid (Sherman, 1969). However, the texture of gluten-free breads can differ from wheat flour breads since gluten-free flours do not contain structural proteins (Crockett, Ie & Vodovotz, 2011). The lack of the viscoelastic property of gluten leads to a liquid dough and low gas retention which results in deteriorated processing and impaired bread quality characteristics like a dense, crumbly texture with poor mouthfeel and low bread volume (Gallagher, Gormley & Arendt, 2004; Sciarini et al., 2010). As a result, the impaired mouthfeel and flavour release reduce the acceptance of gluten-free bread. Especially, the liquid dough highlights the need for hydrocolloids to absorb free water. Moreover, as gluten-free breads mainly consist of gluten-free flours like rice-, corn-, or buckwheat flour with a high starch proportion, they are subjected to a higher staling rate due to quick retrogradation (Korus & Achremowicz, 2004, as cited in Ziemichód, Wójcik & Różyło, 2018). Therefore, also the properties of starches and their interaction with further ingredients like xanthan gum contributes to the characteristics of gluten-free bread.

2.3 Starch

In nature, starch functions as main energy storage in plant tissue (Coultate, 2009). Its molecular conformation can be explained chemically and in terms of structural arrangement.

Chemically, starch consists of the two main fractions amylose (15–30%) and amylopectin (about 70%) and small amounts of proteins and lipids (Huber, McDonald & BeMiller, 2005; Taggart, 2009). Figure 1 presents both polymers which are made up of D-glucopyranosyl monomers but differ in linkage and resulting properties (Coultate, 2009). Amylose is composed of linearly linked monosaccharides with α-1→4 glycosidic linkages and a total molecular weight of approximately 500,000 Da (Taggart & Mitchell, 2009). This molecular set-up leads to amylose forming a double helix as the α-1→4 glycosidic linkages enable to rotate freely (Edwards, 2007). It is hot-water soluble and forms gels (Niba, 2005; Wang & Wood, 2005). In contrast, amylopectin is a branched polysaccharide with α-1→4 and α-1→6 glycosidic linkages which results in a higher molecular weight than amylose (up to 10^9 Da) (Huber, McDonald & BeMiller, 2005; Taggart & Mitchell, 2009).

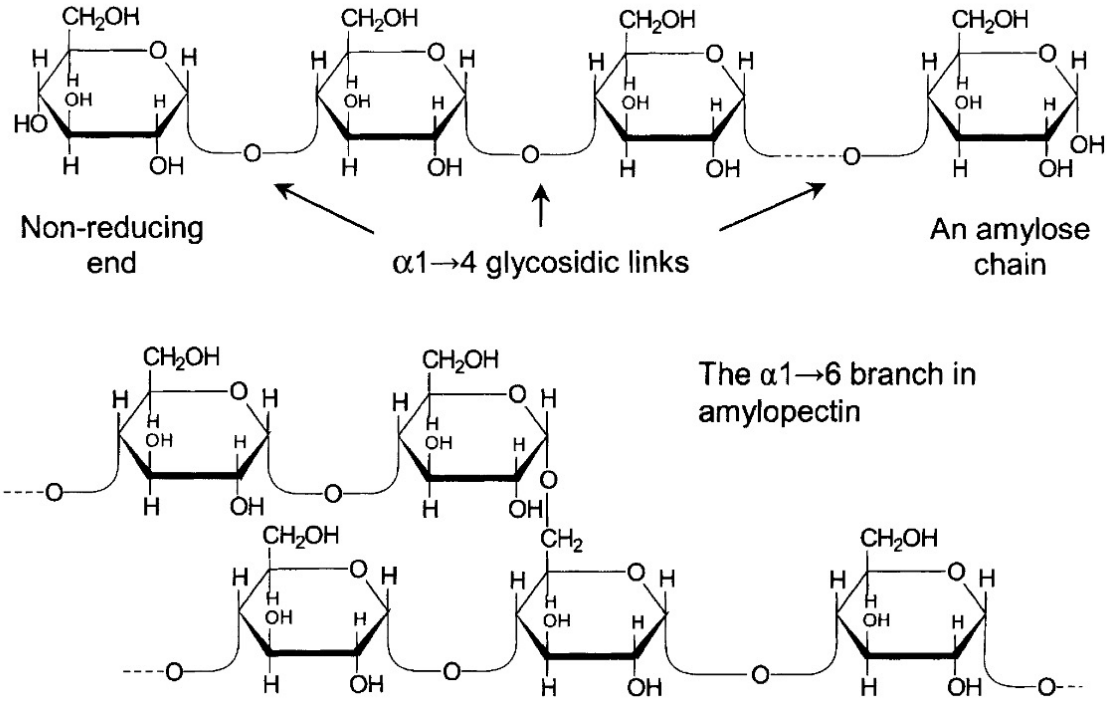

Figure 1: The upper chemical structure shows the linear amylose and below is the branched amylopectin chain (Coultate, 2002).

In terms of structural arrangement, native starch occurs as dense, semicrystalline starch granule of up to 100 µm in case of potato starch (Taggart & Mitchell, 2009). The granule is built up of changing amorphous and crystalline layers (Figure 2). Amylose is located in the amorphous region where its helices stabilize the branching points (α-1→6 glycosidic linkages) of the branched amylopectin chains (Coultate, 2009; Eliasson, 2006). Accordingly, the crystalline region mainly consists of the continuous amylopectin branches (Taggart & Mitchell, 2009).

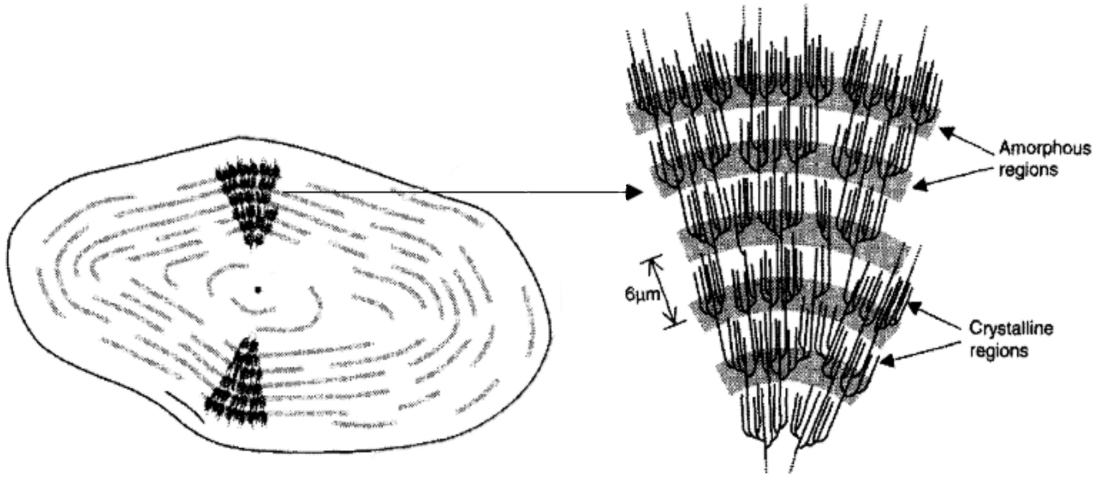

Figure 2: Localization of the amorphous and crystalline regions in starch granules. Adapted and modified from Coultate (2002).

Native starch granules are insoluble in cold- or lukewarm water because of their semicrystalline nature and inter-/intramolecular hydrogen bonds (Eliasson, 2006). However, with increasing water temperature, starch can be dissolved by gelatinization which is further explained in the next chapter.

2.3.1 Starch gelatinization and retrogradation

Gelatinization occurs at temperatures of about 58°C (wheat starch) or 68°C (rice starch) in enough water when the crystalline starch granules start to dissolute (Taggart & Mitchell, 2009). This process is characterized by the loss of the crystalline structure and birefringence as water begins to accumulate in the amorphous region with subsequent non-reversible swelling of the starch granule (Taggart & Mitchell, 2009; Zhang et al., 2018). Continuous swelling of granules ruptures hydrogen bonds between starch molecules and releases amylose into solution (gelatinization) (Coultate, 2009; Edwards, 2007; Vaclavik, Christian & Campbell, 2021). With further heating the viscosity increases as swollen starch granules occupy a larger volume (pasting) (Coultate, 2009; Vaclavik, Christian & Campbell, 2021). However, a continued heating and mixing, destabilizes the granules with a resulting decrease in viscosity (Coultate, 2009). With falling temperatures to 25°C, the paste becomes viscous again as amylopectin and amylose form new hydrogen bonds (Coultate, 2009; Levine & Finley, 2018). After complete cooling within several hours, dissolved amylose double-helices recrystallize again under water expulsion and form a firm, clear continuous gel (gelation) which is also called retrogradation (Arendt et al., 2008; Niba, 2005; Taggart & Mitchell, 2009).

In the bread making process, the retrogradation of amylose contributes to a large extent to the formation of a firm but spongy crumb structure (Coultate, 2009; McGee, 2004). This spongy structure is enabled by the solid gel network which stabilizes the wall of embedded small CO_2 bubbles and thus prevents their coalescence (McGee, 2004). Additionally, in presence of gluten, starch also softens its rigid network by sticking on the gluten's surface and slightly permeating it (McGee, 2004). However, after several days, staling occurs in form of amylopectin recrystallization which can be observed by additional firming of bread due to water migration to the crust (Coultate, 2009; McGee, 2004).

2.3.2 Influencing factors on starch gelatinization

Since in this degree project the gluten-free starch base consisted of a mixture of different starches, it is important to mention the influence of the different starch sources on the granule composition and subsequent gelatinization process.

First, the temperature at which the starch granules disrupt can be influenced by the source of starch (Taggart & Mitchell, 2009). Depending on its origin the amylose:amylopectin fractions and their chain-length can vary (Arendt et al., 2008). A longer amylopectin chain length requires a higher temperature to break down amylopectin aggregates and hydrogen bonds between their molecules (Edwards, 2007; Taggart & Mitchell, 2009). The rate of gelation is influenced by the amylose content whereby the larger the amylose proportion, the faster the gel is formed (Niba, 2005). The form of the starch granules (morphology) additionally influences the arrangement of gels and pastes (Niba, 2005). Some shapes can bed together better than others during swelling. Table 1 presents an overview of the gelatinization and pasting temperatures and the morphology of wheat and starches of gluten-free flours.

Table 1: Gelatinization- and pasting temperature, and amylose content of different starches (5% starch suspension). Adapted from Hoover et al., 2003, p. 255ff., 259[a]; Taggart, 2009, p.110, 114.

Starch type	Gelatinization temp. [°C]	Pasting temp. [°C]	Amylose content [%]	Morphology
Wheat	58–64	77	25	Round lenticular
Rice	68–78	81	19	Polygonal spherical compound granule
Tapioca	62–73	63	17	Oval truncated "kettle drum"
Potato	59–68	64	20	Oval spherical
Oat[a]	56–74	84–94	20–29	Irregular, Polygonal

Apart from the mentioned intrinsic factors, additional ingredients in the starch dispersion can also alter the gelatinization process. For example, the presence of ionic substances like sodium chloride controls the gel strength as starch can be anionic (Niba, 2005). In addition, the overall extent of granule swelling can differ with presence of further ingredients. Starch can accumulate nearly half (45%) of the present water during bread manufacturing (Belitz, 2009). This can be reduced if starch needs to compete for water with hydrocolloids (chapter 2.5) and water-binding milk proteins (chapter 2.4). Consequently, limited water availability in the amorphous regions can increase the melting temperature of crystallites since water acts plasticizing on starch (Eliasson, 2006).

2.4 Milk Powder Proteins

This chapter focuses on milk proteins in bovine milk and milk proteins occurring in non-fat milk powder as the gluten-free bread composition in chapter 3 included skim milk powder as ingredient.

Amino acids contain a carboxylic group (COOH), an amino group (NH_2) and a rest R. At the isoelectric point (pH) amino acids have zero charge which makes them a Zwitterion with a dipolar property. Below the isoelectric point, amino acids are mainly cationic and above the isoelectric point, amino acids are mainly anionic so that they can bind anionic and cationic polyelectrolytes respectively (Coupland, 2014; Park et al., 1992). Linking numerous amino acids by peptide bonds forms proteins like casein and whey proteins which mainly consist of glutamic acid, leucine, aspartic acid and lysine (Belitz, 2009). The formation of proteins can be described by four types: The amino acid series is called primary structure, the secondary structure is the folding of these amino acid sequences into β-sheets, α-helix (helical structure) or random coils by hydrogen bonds, their three-dimensional arrangement is described by the tertiary structure and the linkage of several chains defines the quaternary structure (Appell et al., 2018).

Non-fat milk powder or skim milk powders are produced by cream separation and dehydration of milk (Goulding, Fox & O'Mahony, 2020). The remaining constituents are mainly lactose (49.6%), milk proteins (38.4%), minerals (8%), residual water (3–4%) and no or small amounts of fat (Belitz, 2009). The major fraction of milk proteins is the phosphoprotein casein (80%) while the remaining 20% are whey proteins which include mainly lactalbumin and lactoglobulin and minor fractions of serum albumin as well as immunoglobulins (Belitz, 2009). In skim milk powder, whey proteins can be present as native or denatured proteins depending on the processing parameters which can range for example between 75°C–120°C for a holding time of seconds to minutes (Goff, 2014; Kelly, O'Connell & Fox, 2003). For example, high-heat treated skim milk powders are often used in bakery products (Kelly, O'Connell & Fox, 2003).

The main constituent lactose contributes to Maillard reactions leading for example to the browning of bread crust and flavour development during baking (Goulding, Fox & O'Mahony, 2020). Blood serum albumins and immunoglobulins are considered to have no importance in physicochemical properties of milk compared to caseins or whey proteins (Fox, 2003; Fox et al., 2015).

Caseins can be divided into α_{S1}-, α_{S2}-, β- and κ-casein of which α_{S2}- and κ-casein are considered the most water-soluble due to more sugars, less sulphur comprising amino acids and more phosphate groups (Ebermann & Elmadfa, 2011; Fox et al., 2015; Goulding, Fox & O'Mahony, 2020). The molecular weight of caseins differs since they are build-up of varying amount of amino acids: α_{S1}-casein consists of 199 amino acids (23 kDa), α_{S1}-casein of 207 amino acids (25 kDa), β-caseins of 209 amino acids (24 kDa) and κ-caseins of 169 amino acids (18 kDa) (Belitz, 2009). α_{S1}- and β-caseins are considered mainly water-insoluble due to the higher presence of nonpolar amino acids like valine or leucine (Fox et al., 2015). Since amino acids also contain parts with positive and negative charge, caseins are amphiphilic proteins

with hydrophobic and hydrophilic parts (Singh & Flanagen, 2005). Therefore, caseins self-assemble to spherical casein micelles with an average size of 120 nm (10^8 Da) in milk where hydrophobic parts are on the inside and hydrophilic parts (κ-casein) on the outside stabilizing the micelle itself by steric hindrance (Goff, 2014; Goulding, Fox & O'Mahony, 2020).

In addition, aggregation of casein micelles in milk is prevented by electrostatic repulsion since the C-terminal part of κ -casein is slightly negatively charged resulting in an overall negative charge of casein micelles (Fox, 2003; Singh & Flanagen, 2005). However, precipitation occurs for example at the isoelectric point at pH 4.6, by the addition of calcium or milk saturation with NaCl (sodium chloride) (Goff, 2014; O'Mahony & Fox, 2013; Singh & Flanagen, 2005). Caseins have incomplete secondary and tertiary structures due to the presence of the structure-interrupting proline which allow caseins to tolerate high temperatures up to 140°C without coagulation (Goulding, Fox & O'Mahony, 2020). Consequently, they do not form firm gels but rather increase the viscosity of food systems. This is because their secondary structure resembles expanded random coils due to the destabilizing amino acid proline in their structure so that the coils increase the specific volume (Goff, 2014; Goulding, Fox & O'Mahony, 2020; Singh & Flanagen, 2005). Because of the amphiphilic character, caseins can bind 2g water/g casein protein, are surface-active and widely used as emulsifiers or foam stabilizer in food applications (Fox et al., 2015; Houben, Höchstötter & Becker, 2012). In addition, its heat stability favours their usage in foods which require heat treatment like soups and bakery products (Singh & Flanagen, 2005).

Whey proteins consist mainly of β-lactoglobulin which makes up half of the total whey proteins and α-lactalbumin (20%) as well as further minor constituents like immunoglobulins (e.g. IgG, IgA) and blood serum albumin (Fox et al., 2015). The primary structure of β-lactoglobulin consists of 162 amino acids (18 kDa) and its isolelectric point is at pH 5.2 where in the range of pH 5.5 up to 7.5 two β-lactoglobulins form a dimer (Belitz, 2009; Fox et al., 2015). α-lactalbumin consists of 123 amino acids (14 kDa) and the isolelectric point is at pH 4.8 (Belitz, 2009; Fox et al., 2015). The secondary structure of α-lactalbumin and β-lactoglobulin occurs as β-sheets, α-helixes and further miscellaneous structures of which β-lactoglobulins form a globular structure in the tertiary structure (Fox et al., 2015). Moreover, native β-lactoglobulins showed to bind sodium ions at pH 7.5 although there is no high negative net charge (Carr, 1956). At neutral pH (pH 7), the addition of salt (NaCl) contributes to an even enhanced aggregation rate as well as larger aggregates of native β-lactoglobulins during heating due to a screening of charges and subsequent decrease in electrostatic repulsion (Singh & Havea, 2003; Verheul, Roefs & de Kruif, 1998).

The modification of environmental conditions like heating during spray drying can induce whey protein denaturation which includes two processes, first the unfolding of the proteins and second their (permanent) aggregation by maintaining their secondary structure (Singh & Havea, 2003; Stathopoulos, 2008). The denaturation of β-lactoglobulins in milk occurs at around 65–70°C where it dissociates into two monomers which strongly, irreversibly interact with κ-casein, α-lactalbumin and eventually α_{S2}-casein via sulfhydryl-disulphide reactions and hydrophobic interactions (Anema, 2020; Dalgleish, Senaratne & Francois, 1997; Fox et al., 2015). Especially the reaction with further caseins is enabled by the dissociation of κ-casein

during heating (Anema & Klostermeyer, 1997). Another study found that this complexation is pH-dependent where in reconstituted milk at pH 6.8 85% of the β-lactoglobulins react with casein whereas at pH 7.1 it is only 15% (Anema, 2007). This author also observed that at pH 7.0 casein-whey protein complexes make up a particle volume of 3–5 $nm^3/10^6$ in reconstituted unheated milk of low heat-treated skim milk powder. The heating of already denatured, aggregated β-lactoglobulins in combination with NaCl resulted in small aggregates possibly because of charge screening effects of already aggregated β-lactoglobulins which showed a higher negative net charge, however (Ryan et al., 2012).

Denaturation of α-lactalbumin occurs at around 62°C with no aggregation but rather a tendency to renaturation (Hines & Foegeding, 1993; Rüegg, Moor & Blanc, 1977). However, its aggregation can be also enhanced by NaCl addition (Vardhanabhuti & Allen Foegeding, 2008). Its isoelectric point is at around pH 4.5 (Belitz, 2009). According to the denaturation temperatures of β-lactoglobulin and α-lactalbumin, whey proteins in skim milk powder may already denature after spray drying initiating mostly irreversible bonds with α-lactalbumin and κ-casein (Ako et al., 2009). Depending on the pH, theses complexes either attach to micelle surfaces (pH < 6.8) or are present in the serum phase at e. g. pH 7 (Mohammad & Fox, 1987). However, all the mentioned mechanisms and properties depend strongly on pH, ionic strength, temperature and further aspects.

At temperatures of above 80°C native whey proteins can develop fine-stranded or particulate gels at concentration >8% where the tertiary globular structure unfolds and aggregation occurs which traps water inside the 3D-network (Goff, 2014; Singh & Flanagen, 2005). This results in almost 12.5 to 50 times the amount of water being absorbed compared to native whey proteins (0.2–2.5g water/g protein) (Augustin, Clarke & Craven, 2003; Carr, 2003, as cited in Stathopoulos, 2008). Overall, the water-binding property with subsequent increase in viscosity favours the usage of milk proteins in bread. A study conducted by Gallagher, Gormley & Arendt (2003) found that the addition of milk powder altered the rheological behaviour of gluten-free doughs by increasing their viscosity. An important aspect here is that skim milk powder in general can bind 0.96–1.28g water/g powder (Augustin, Clarke & Craven, 2003). Also, this functionality makes gluten-free doughs not only easier to handle but also reduces staling by preventing water migration (Gallagher, Gormley & Arendt, 2003; Gallagher, Gormley & Arendt, 2004; Stathopoulos, 2008). Further, milk proteins are mainly incorporated in gluten-free bread to moist the bread crumb due to the water-holding ability of proteins with their (non-) polar and charged amino acids (Belitz, 2009; Singh & Flanagen, 2005; Vaclavik, Christian & Campbell, 2021).

The overall function of milk proteins to bind water depends on many factors in the food system (Singh & Flanagen, 2005). As mentioned in the chapter 2.3.1, especially water availability can be crucial in presence of starches (chapter 2.3.1) and hydrocolloids.

2.5 Hydrocolloids

Apart from milk proteins, attempts have also been made by adding hydrocolloids (hydrophilic colloids) to mimic the viscoelastic network of gluten-free bread since they contain many hydroxyl groups (OH) with a high water-binding ability (Saha & Bhattacharya, 2010). This property can modify the viscosity of food products and consequently favours their usage as thickener or gelling agent in many products. In the present chapter, the chemical structure and the resulting properties of psyllium and xanthan gum will be presented.

2.5.1 Psyllium

The polysaccharide psyllium, also known as Isabgol or Ispaghula, can be isolated from the seed husk or leaves of the plant *Plantago ovata L.* which belongs to the genus *Plantago* and family *Plantaginaceae* (Franco et al., 2020; Fratelli et al., 2018; Pawar & Varkhade, 2014). Around 200 different species can be summarized under *Plantago* of which the most common ones are *Plantago ovato L.*, *Plantago asiatica L.* or *Plantago depressa L.* (Zhang et al., 2019). Consequently, the molecular organization of psyllium and the resulting functional properties depend not only on the raw material used but also from applied methods like extraction or purification (Nie, Cui & Xie, 2018). Additionally, its overall very complex structure contributes to the fact that the molecular composition and the resulting properties of psyllium have not been fully investigated (Fischer et al., 2004; Nie et al., 2014; Zhang et al., 2019). However, some studies show that the highly branched polysaccharide mainly composes of a xylopyranose backbone with β-1→4 linkage (Nie, Cui & Xie, 2018). The side chains also include mainly xylopyranose, arabinofurose and minor components like rhamnose, glucose, galactose and galacturonic acid (Franco et al., 2020; Nie et al., 2014; Pawar & Varkhade, 2014). Figure 3 exemplifies the branched structure of *Plantago asiatica L.* seeds.

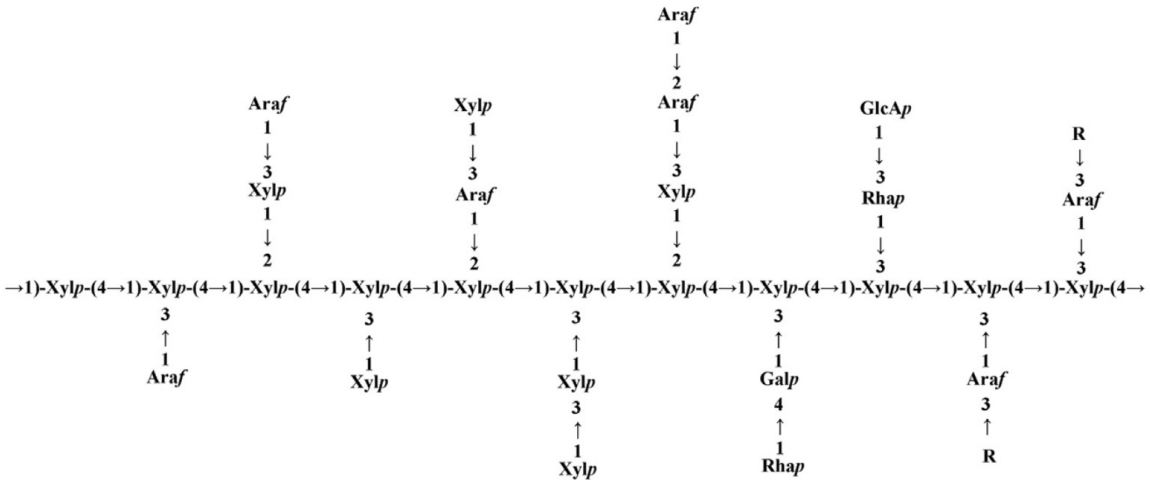

Figure 3: Exemplary polysaccharide structure of *Plantago asiatica L.* seeds (Nie, Cui & Xie, 2018).

Depending on the used measurement method, the overall composition results in a high molecular weight of up to e. g. $7x10^6$ Da for *P. ovato* which is also the cause for its highly viscous property (Al-Assaf et al., 2003; Fischer et al., 2004; Nie et al., 2014). Its gel-like behaviour in water is attributed to the alkali-soluble part of the psyllium husk which amounts to 25–28.5% (*w/w*) of extractable mucilage (Farahnaky et al., 2010; Fischer et al., 2004). It is

widely accepted that arabinose has a positive influence on psyllium's water solubility (Izydorczyk, 2009). The water solubility may also be enhanced by the presence of carboxyl groups in the molecular structure characterizing psyllium as anionic (Farahnaky et al., 2010). In addition, this negative charge causes electrostatic repulsion and results in elongated chains which initiate gelation by cross-linking to form filamentous gels with single strains having a length of 20–30 µm in deionized water (Farahnaky et al., 2010; Guo et al., 2009; Haque, Richardson & Morris, 1993). However, the hydrophilicity depends also on the respective psyllium structure in terms of chain length or arabinose allocation throughout the xylopyranose main chain (Izydorczyk, 2009). The addition of salt in turn does not affect its water solubility (Cui & Wang, 2005). Apart from these properties, psyllium also withstands a wide pH and temperature range (Ngemakwe, Le Roes-Hill & Jideani, 2015).

In gluten-free products, psyllium functions as gluten replacer due to its stability and thickening property (Zandonadi, Botelho & Araújo, 2009). For example, 1g psyllium can bind ten times the amount of water (Sosulski & Cadden, 1982). According Mariotti et al. (2009), it also improves the dough structure by film formation. Results of further studies show that psyllium in gluten-free dough can increase the stability of gas cell walls by gelling and thereby contributes to a higher bread volume (Haque, Morris & Richardson, 1994). In addition to its function as a thickener, psyllium is also used as dietary fibre in gluten-free products. It is the viscous rheological functionality of the high soluble fibre content that provides health benefits like improving the blood glucose and cholesterol level or stimulating digestion in case of obstipation (Belorio & Gómez, 2020; Franco et al., 2020). Therefore, psyllium is often used in combination with further hydrocolloids like xanthan gum which do not have these additional health benefits.

2.5.2 Xanthan gum

Xanthan gum is a biopolymer and was detected as polysaccharide B-1459 around 60–70 years ago by the American Northern Regional Research Laboratories (NRRL) in Peoria, Illinois (Côté & Finkenstadt, 2008; Kang & Pettitt, 1993). It is secreted by the bacterial species *Xanthomonas campestris* of which the genus *Xanthomonas* is considered as plant pathogen occurring on e.g. cabbage leaves which belongs to the family *Pseudomanceae* (García-Ochoa et al., 2000).

The main steps of commercial manufacturing since the start in the 1960s can be summarized as follows: Xanthan gum is extracted from *Xanthomonas campestris* during aerobic fermentation at neutral pH with an optimum temperature of 28°C (García-Ochoa et al., 2000; Palaniraj & Jayaraman, 2011). After that, *Xanthomonas campestris* bacteria are inactivated in the pasteurization step following a flocculation of xanthan gum by the addition of e.g. isopropyl alcohol (Galindo & Albiter, 1996; García-Ochoa et al., 2000). Finally, the wet precipitation is dehumidified and ground to a white-yellowish, fine powder. Depending on the environmental conditions, 30–50 g/L xanthan gum can be achieved after the last processing step (Caggianiello, Kleerebezem & Spano, 2016).

Today, xanthan gum is regulated as food additive by the American Food and Drug Administration (FDA) which allows unlimited use of xanthan gum in food applications ("Xanthan gum," 2021). According to Annex II and III in *Food Additives* (Regulation 1333/2008), xanthan gum is regulated as E415 in Europe with a maximum level of e.g. 20,000 mg/kg for gluten-free cereal products intended for infants and *quantum satis* when used as a liquid table-top sweetener. Although both USA and Europe mostly allow the unlimited use of xanthan gum in food, a typical use is a concentration of 0.03–1% (*w/w*) (García-Ochoa et al., 2000).

Due to its versatile properties, which will be explained in the next chapters, xanthan gum can be used in numerous products. For example, it is used as a thickener in salad dressings or binds water in baked goods and thus improves stability (Sworn, 2009). Especially, in a study conducted by Lazaridou et al. (2007) it was shown that the addition of xanthan gum to gluten-free dough exerted the highest viscoelastic effects amongst other hydrocolloids.

Chemical structure and properties

Figure 4 shows the chemical composition of xanthan gum. The primary structure of the heteropolysaccharide composes of a linear β-D-glucose 1→4-linked chain with a trisaccharide side chain at every second glucose unit (García-Ochoa et al., 2000). This sidechain glycosidically branches off at O-3 of the respective β-D-glucose unit and is made up of a D-mannose unit 1→2-linked to D-glucoronic acid which in turn is bound (1→4) to another D-mannose unit (García-Ochoa et al., 2000; Melton, Mindt & Rees, 1976). In addition, the non-terminal D-mannose unit carries an acetyl attachment whereas terminal D-mannose units have a pyruvic acid attachment (García-Ochoa et al., 2000; Sworn, 2009). This conformation results in a relatively high molecular weight which ranges between $2x10^6$–$20x10^6$ Da (García-Ochoa et al., 2000).

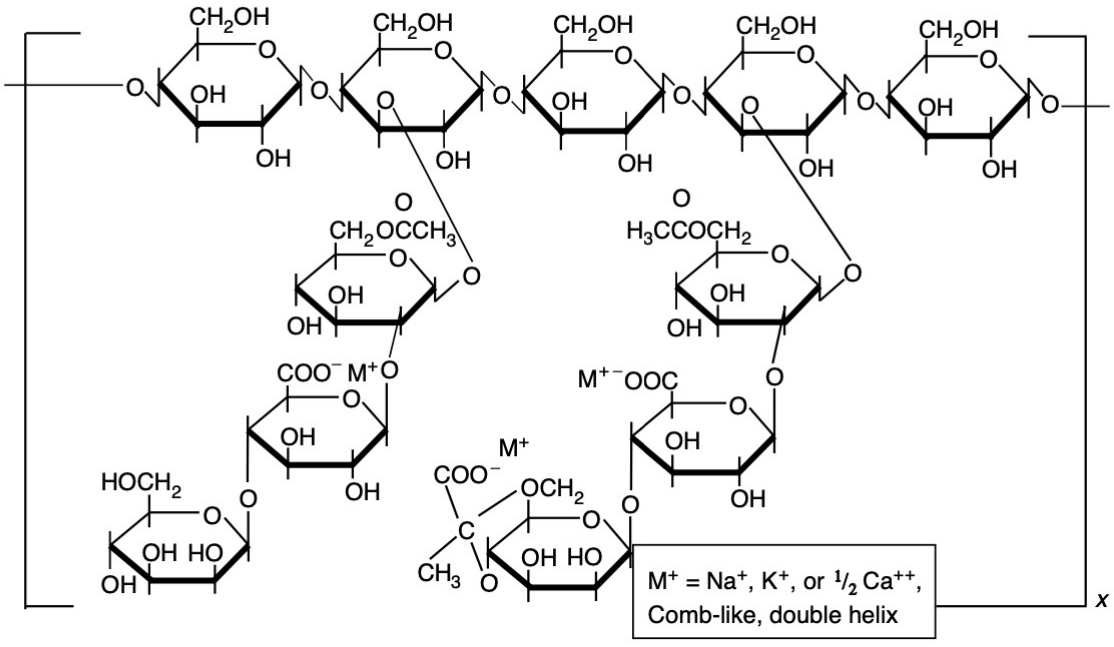

Figure 4: Chemical structure of xanthan gum (Ward, Hanway & Ward, 2005).

Previous research has established, that the secondary structure of xanthan gum naturally occurs as a helix (Bercea & Morariu, 2020; Chazeau, Milas & Rinaudo, 1995). The anionic property of xanthan gum is determined by the carboxylic groups of the side chains like the above mentioned 4,6-acetal-linked pyruvic acid (Chawla & Patil, 2010; García-Ochoa et al., 2000; Huber, McDonald & BeMiller, 2005; Jansson, Kenne & Lindberg, 1975; Kang & Pettitt, 1993). These charged side chains explain xanthan gum's water solubility independent of the water temperature by forming hydrogen bonds with water molecules (Anton & Artfield, 2008; García-Ochoa et al., 2000). However, the two carboxylic groups favour different interactions: Whereas pyruvate causes electrostatic repulsion between the charged trisaccharide side chains preventing intermolecular linkage and thus securing the disordered conformation of xanthan, acetate promotes intramolecular interactions which strengthens the rod-like form of xanthan gum and therefore sustains the ordered conformation (Callet, Milas & Rinaudo, 1987). Its anionic property is also the reason for xanthan gum's salt tolerance towards sodium chloride (Sworn, 2009). The high stability of xanthan gum to enzymes like amylases and proteases, alkalis and acids may result from the trisaccharide side chains swathing the linear β-D-glucose chain and thus forming a protective layer over the weak β-1→4-linkages (BeMiller, 2019b; Sworn, 2009). Especially its resistance to active enzymes is the reason why xanthan gum is perfectly suitable for the application in high-starch products like bread as the viscosity will not be impaired (Sworn, 2009). Finally, chemical analysis revealed that xanthan gum consists of approximately 85% complex carbohydrates (soluble dietary fibre), 0–2% protein, 10% ash, 5% others (mainly moisture) and 5 mg/100g sodium (Ward, Hanway & Ward, 2005).

Rheological functionality

The high viscosity at already low concentrations can be explained by xanthan gum's helical structure where the steric hindrance between side chains keeps the stiff structure and consequently maintains the linear shape of the helices (Huber, McDonald & BeMiller, 2005). Consequently, this takes up more space in solution than other secondary structures like random coils (BeMiller, 2019a). Combined with the high molecular weight of the heteropolysaccharide, xanthan gum solutions show a highly viscous flow behaviour (Sciarini et al., 2010). Therefore, xanthan gum is non-gelling and its solutions exhibit highly pseudoplastic (shear-thinning) flow with Newtonian viscosity at low shear stress and non-Newtonian viscosity with rising shear stress (BeMiller, 2019b; García-Ochoa et al., 2000; Sciarini et al., 2010; Sworn, 2009). In addition, xanthan gum shows thixotropic behaviour characterized by a viscosity increase after the removal of shear stress (Goff & Guo, 2020; Sworn, 2009). This can be explained by the spatial molecular arrangement of xanthan gum molecules during shear stress as mentioned by Nordqvist and Vilgis (2011) introducing the jamming transition theory in deionized water: At low concentrations highly charged xanthan gum molecules do not approach each other due to electrostatic repulsion. As soon as a certain concentration is exceeded, the molecules cannot move freely anymore because the electrostatic repulsion between these molecules becomes stronger and the molecules are thereby fixed in one position. Only sufficient stress (yield stress) can cause the system to move. An increase in shear stress makes the molecular arrangement more flexible or even parallelizes the stiff rods which reduces the flow resistance and leads to a liquid-like flow behaviour (Kasapis, 2005; Mezger, 2016; Nordqvist & Vilgis, 2011; Whaley, Templeton & Anvari, 2019). After releasing the stress xanthan gum molecules can rearrange freely again and thus increase the viscosity in contrast to the parallel arrangement.

Although the viscosity of xanthan gum can also change in dependence of temperature, xanthan gum solutions are relatively stable to a wide temperature span due to hydrogen bonds between side chains which stabilize the helical structure (García-Ochoa et al., 2000; Mezger, 2016). This is enhanced by electrostatic repulsion between the anionic side chains. Increasing the temperature leads to an increase in thermal energy and molecular movement so that the side chains can move more freely (T. A. Vilgis, personal communication, November 9, 2021). This initiates a conformation transition from a helix to a coil within a temperature range of 37–50°C in distilled water leading to a slight reduction in viscosity (Brunchi et al., 2019). Nevertheless, during cooling, xanthan gum in salt-solution transforms to the helical state again with slightly stiffer molecules probably due to a more elongated backbone (persistence length 1000 Å) in the renatured state compared to the native state (persistence length 300Å) (Brunchi et al., 2019; Milas, Reed & Printz, 1996; Milas & Rinaudo, 1986). During this process, the original pattern of the side-chain-backbone association is not completely restored but the doubling in mass per unit length from the native to the renatured state (200 Da/Å) suggests a transformation from a single to a dimer, i.e. a double-stranded helix (Milas, Reed & Printz, 1996; Milas & Rinaudo, 1986; Morris, 2019).

Since in this study, NaCl is a part of each formulation it is important to also mention the influence of salt on xanthan gum. As explained in chapter 2.5.2 the extended form of xanthan gum is caused by electrostatic repulsion between carboxylic groups of the trisaccharide side chains in a salt-free aqueous environment (Brunchi, Morariu & Bercea, 2014). The addition of salt leads to a reduction of the electrostatic repulsion between these groups due to the presence of counter ions (Na^+) (Wyatt & Liberatore, 2009). This favours a stabilized, ordered conformation by interactions between the acetyl groups of the trisaccharide chains and the main chain (Bercea & Morariu, 2020; Brunchi, Morariu & Bercea, 2014; Fitzpatrick et al., 2013). Subsequently, the transition temperature increases above 55°C up to around 90°C (Abbaszadeh et al., 2019; Brunchi et al., 2019; Sworn, 2009). Also, the lack of electrostatic repulsion leads to conformation alterations and an approach of xanthan gum molecules which results in lower apparent viscosity and differences in rheological measurements compared to salt-free formulations (Brunchi, Morariu & Bercea, 2014; Galván et al., 2018; Wyatt & Liberatore, 2009). However, the exact salt-xanthan gum interaction depends on the prevailing conditions of each experiment.

Overall, this chapter presented the composition of starch, milk powder, psyllium and xanthan and the resulting physical properties. As already mentioned, the behaviour of each substance in solution and in bread can change depending for example on the origin, water availability or interactions with other substances. Therefore, rheological measurements will be used to investigate how xanthan interacts with starches, psyllium and milk powder in solution and in gluten-free dough.

2.6 Theory of Analysis Methods

2.6.1 Rheology

Rheology is the physical science of investigating deformation and flow behaviour of materials like foods (Sahin & Sumnu, 2006). Data from rheological studies are important in food processing and engineering when it comes to e.g. pumping foods or investigating the viscoelastic behaviour of gluten-free doughs and breads (Sahin & Sumnu, 2006).

Deformation: During deformation, foods undergo stress which can be divided into normal stress (σ) and shear stress (τ) (Sahin & Sumnu, 2006). Normal stress acts vertical on the food leading to compression or pulling apart (Figure 5) whereas shear stress acts parallel to the material and results in shearing (Figure 6) (Sahin & Sumnu, 2006). Shear stress is defined as the relation of shear force (*F*) to the shear area (*A*) in Equation 1 (Eq. 1) (Mezger, 2016):

$$\text{Shear stess } \tau = \frac{F}{A} \text{ in } \frac{N}{m^2} = Pa \qquad \text{(Eq. 1)}$$

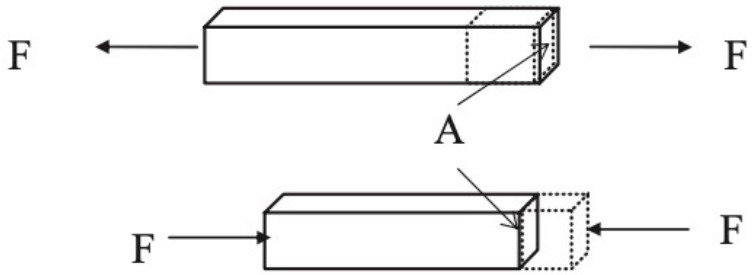

Figure 5: Normal stress leading to stretching or compression of the material. *F* describes the force [N] and *A* the area [m^2] (Sahin & Sumnu, 2006).

The relation between the change in shape when the material is deformed compared to its original position is described by the strain (Sahin & Sumnu, 2006). The shear strain is the angle difference (φ) of an orthogonal during deformation (Sahin & Sumnu, 2006). Figure 6 shows the two-plates model with a fixed lower plate (s=0) and an upper plate which is movable by shear force (*F*) exerting shearing by deflection (*S*) (Mezger, 2016; Zheng, 2019). It illustrates the definition of the shear strain by bringing the deflection (*S*) and shear gap (*h*) into relation (Eq. 2). As the shear strain is dimensionless it is often presented as percentage (Mezger, 2016).

$$\text{Shear strain } \gamma = \frac{S}{h} \text{ in } \frac{m}{m} = \text{dimensionless} \qquad \text{(Eq. 2)}$$

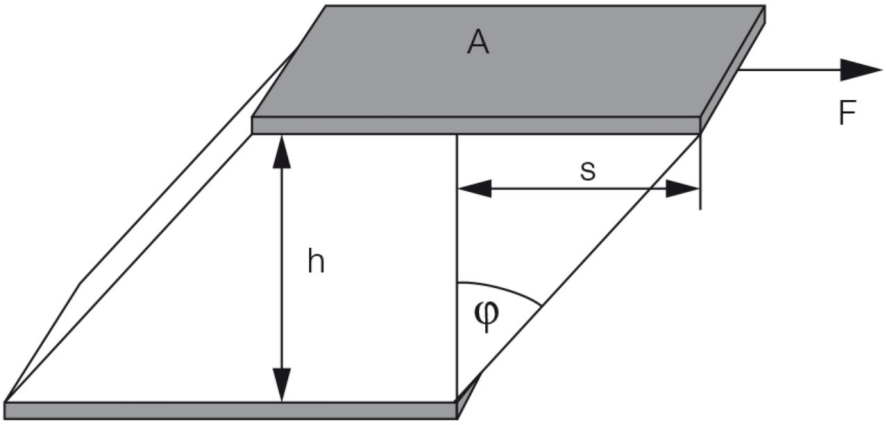

Figure 6: Two-plates model showing shear stress leading to shearing of the material. *F* describes the (shear) force [N], *A* is the shear area [m²], *S* is the deflection [m], *h* is the shear gap width [m] and φ is the deflection angle [degree] (Anton Paar, n.d-a).

Hookean solids show elastic behaviour meaning that the material deforms under applied stress but recovers to its original size after the stress is taken off (Sahin & Sumnu, 2006). However, the network of numerous materials can be destroyed in case of great shear stress which can lead to flow (Moreno, 2001).

Flow: When it comes to the flow behaviour of a material the (shear) viscosity (η) is a characteristic parameter of viscous fluids and describes the resistance to flow (Sahin & Sumnu, 2006). At the molecular level it is described by the friction between the molecules during flow resulting in flow resistance, namely viscosity, which is defined by the relation of the shear stress τ to the shear rate $\dot{\gamma}$ (Eq. 3, 4) (Mezger, 2016):

Viscosity $\eta = \frac{\tau}{\dot{\gamma}}$ in Pa s^{-1} (Eq. 3)

Shear rate $\dot{\gamma} = \frac{v}{h}$ in $\frac{m/s}{m} = \frac{1}{s}$ or s^{-1} (Eq. 4)

Generally, the flow behaviour of viscous fluids can differ from each other.

Flow behaviour of fluids: Viscous fluids describe two types of fluids: Newtonian and non-Newtonian fluids. For example, water and oil are ideal viscous substances (Newtonian fluids) as they obey Newton's law of Viscosity meaning that their viscosity does not depend on shear rate ($\dot{\gamma}$) (Moreno, 2001). If the viscosity of a viscous fluid depends on the shear rate it can be classified as a non-Newtonian fluid where the viscosity is referred to as 'shear viscosity' or 'apparent viscosity' $\eta(\dot{\gamma})$ at a defined shear rate (Barnes, Hutton & Walters, 1989b). The overall flow behaviour of non-Newtonian fluids can be influenced for example by the molecular conformation of the material and ambient factors like temperature (Barnes, Hutton & Walters, 1989b; Sahin & Sumnu, 2006). As mentioned in chapter 2.5.2, xanthan gum solutions behave shear-thinning (pseudoplastic) where the apparent viscosity decreases with increasing shear rate. Contrary to this, the apparent viscosity of shear-thickening (dilatant)

non-Newtonian fluids increases with increasing shear rate (e.g. corn starch in water) (Sahin & Sumnu, 2006).

However, apart from materials which are either solid or viscous, there are many substances which inhere both properties. These materials exhibit viscoelastic behaviour.

2.6.2 Viscoelasticity

Viscoelastic materials like dough show both elastic and viscous rheological behaviour (Barnes, Hutton & Walters, 1989a). The elastic behaviour serves as an energy storage whereas the viscous part releases energy (Zheng, 2019). The stored energy acts as operating power as soon as the deformation diminishes to help the material return to its original shape while the energy supplied to viscous components during deformation is completely used for the flowing so that there is no energy left for re-deformation (Zheng, 2019). Depending on the predominance of either the elastic or viscous components, viscoelastic or semisolid foods can be divided into viscoelastic solids (energy storage is higher than energy release) and viscoelastic liquids (energy release is higher than energy storage) (Zheng, 2019). After deformation, viscoelastic liquids (e.g. silicon) do not completely return to their original shape as the elastic component is underlying the viscous component whereas viscoelastic solids return completely to their original position (Mezger, 2016). Since these viscoelastic materials inhere both elastic and viscous properties of which the viscous component is temperature-dependent, the rheological behaviour of viscoelastic materials and semisolid foods is also more or less under the influence of heat depending on the extent of viscous properties (Zheng, 2019). Whereas rotational tests investigate the viscous behaviour (viscosity), dynamic tests in oscillation can be used to analyse the viscoelastic behaviour of foods (chapter 2.6.4) (Sahin & Sumnu, 2006).

2.6.3 Rotational tests

The aim of the rotational test is to analyse the viscous behaviour of fluids where the time is plotted on the x-axis versus the viscosity (η) on the y-axis (Mezger, 2016). Especially, temperature-dependent properties can be examined by conducting a steady shear rate rotational test under heat treatment (Mezger, 2016).

Rotational tests at constant shear rate operate at a pre-set rotational speed n [min^{-1}] where the torque M [mNm] is measured (Mezger, 2016). Here, the given speed n corresponds to the shear rate and the torque can be converted into shear stress (τ) (Mezger, 2016). Depending on the properties of the fluid an appropriate measuring system is used for the test (Figure 7). For example, cone-plates are commonly used for samples with low-high viscosity and small particle size, plate-plate systems measure samples with low viscosity or soft solids and concentric cylinders are used for low-medium viscous samples (Whaley, Templeton & Anvari, 2019).

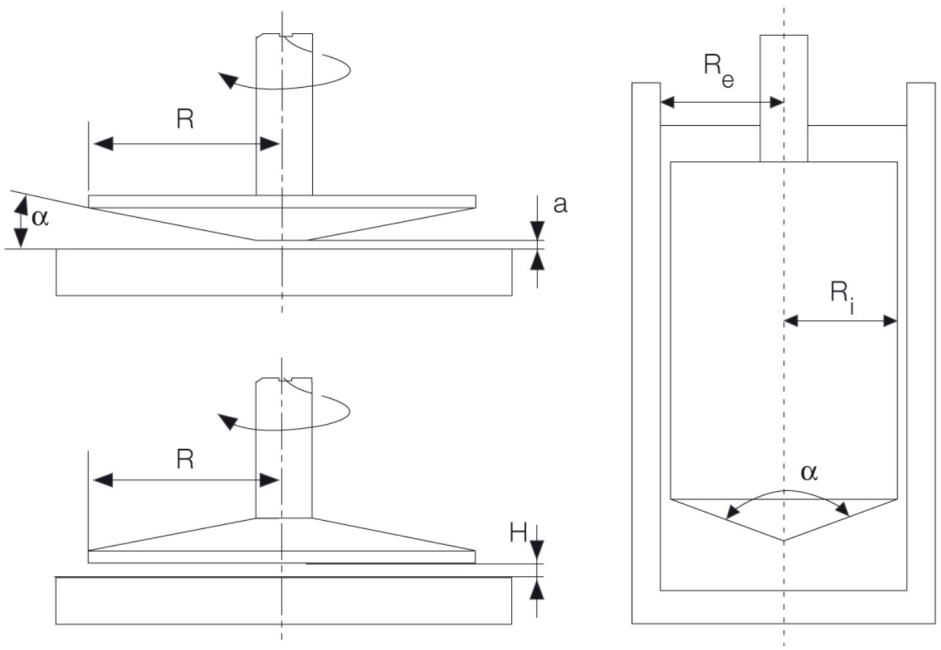

Figure 7: Measuring systems. Top left: Cone-plate (α = cone angle), down left: plate-plate, right: concentric cylinder (α = internal angle). R = radius H = gap size, R_i= bob radius, R_e= cup radius (Anton Paar GmbH, n.d.-b).

In all these measuring systems, the upper plate respectively the concentric cylinder is movable whereas the bottom plate is stationary (see two-plate model in Figure 6). In rotational tests, the movable part rotates continuously around its own axis. In oscillation tests it moves back and forth at a certain frequency (e.g. temperature sweep).

Apart from the molecular interactions in gluten-free dough which may increase its overall viscosity, these doughs also need a viscoelastic network to resist deformation during processing in order to exhibit the same properties like gluten-bread (Saha & Bhattacharya, 2010). As rotational tests are limited to measuring just the viscous part and thus do not consider elasticity it is recommended to also perform oscillation tests which are suitable for viscoelastic samples (Zheng, 2019).

2.6.4 Oscillatory tests

Viscoelasticity of samples can be analysed by oscillatory shear tests (dynamic tests) (Zheng, 2019). These tests are also called small amplitude oscillatory shear (SAOS) as they are performed within the linear viscoelastic region (LVR) without destroying the structure of the sample (Whaley, Templeton & Anvari, 2019).

The LVR can be determined with an amplitude sweep. After that, the viscoelastic behaviour of a sample can be characterized by further oscillatory tests which measure for example the moduli G' and G''. According to Rao (2014) and Whaley, Templeton & Anvari (2019) there are three oscillatory tests: Frequency sweeps (1) measure the moduli at varying frequency (ω) during constant temperature and strain or stress. Time sweeps (2) investigate a sample with consistent frequency (ω), strain and temperature in dependence of time. Lastly, temperature sweeps (3) measure the structural response of a material over a temperature range at constant frequency. As temperature sweeps are suitable to investigate temperature-dependent

viscoelastic behaviour (e.g. dough) it will be used in this degree project and will be explained later in this chapter. Therefore, only the parameters G', G'' and $tan\delta$ that are important for this type of investigation are explained below.

G' [Pa] is the storage modulus and determines the elastic/solid property of a sample. It marks how much energy can be saved in a sample at the same time in which stress is applied within a period while G'' [Pa] is defined as the loss modulus and introduces liquid behaviour of a sample (Mezger, 2016; Saha & Bhattacharya, 2010). The relation between these two moduli is described by the loss factor tanδ (Eq. 5):

$$tan\delta = \frac{G''}{G'} \text{ (dimensionless)} \quad \text{(Eq. 5)}$$

For example, soft and flexible polymers with a weak chemical network (low degree of cross-linking) can have a tanδ of ≤ 1 whereas polymers with a strong chemical network (high degree of cross-linking) show lower tanδ values with a tendency towards 0 (Mezger, 2016). Based on the relationships shown in Table 2, conclusions can be drawn about the viscoelastic behaviour of a sample over a defined temperature range.

Table 2: Parameters to distinguish viscoelastic behaviour. Adapted from: Mezger, 2016, p. 158; Saha & Bhattacharya, 2010, p. 592.

Behaviour	**Modulus**	**tanδ**
Viscous	$G' \rightarrow 0$	$tan\delta \rightarrow \infty$
Viscoelastic fluid	$G'' > G'$	$tan\delta > 1$
Viscoelastic with balanced viscous and elastic parts	$G' = G''$	$tan\delta = 1$
Viscoelastic solid	$G' > G''$	$tan\delta < 1$
Solid	$G'' \rightarrow 0$	$tan\delta \rightarrow 0$

Nevertheless, an amplitude test must be conducted first to define the LVR in which oscillatory tests are performed.

Amplitude sweep

Amplitude sweeps determine the rigidity of samples and the LVR for oscillatory tests by increasing the amplitude of the applied strain or stress at pre-set temperature and frequency while measuring the stress or strain response of the sample respectively (Zheng, 2019). In this investigation a strain sweep was used. This is because foods undergo stress during deformation and the strength of the sample structure is directly influenced by the extent of deformation and the resulting stress (Mezger, 2016).

The LVR is the left part of the diagram where the G' and G'' lines show a plateau with constant moduli values (Mezger, 2016) (Figure 8). In this region, the molecular arrangement of the sample can withstand strain (or stress) but as soon as the moduli values deviate by 2–10% from their previous one, the critical strain is reached (γ_c or γ_L, strain sweep) marking the limit

of the LVR after which the internal structure will be gradually destructed (Zheng, 2019). Therefore, commonly the *G′* curve is used for evaluation since it describes the solid behaviour of a sample (Mezger, 2014). The strain at which a sample starts to flow (flow point) is characterized by a crossover of the two moduli (*G′* = *G″*) (Mezger, 2016) (Figure 8, left graph).

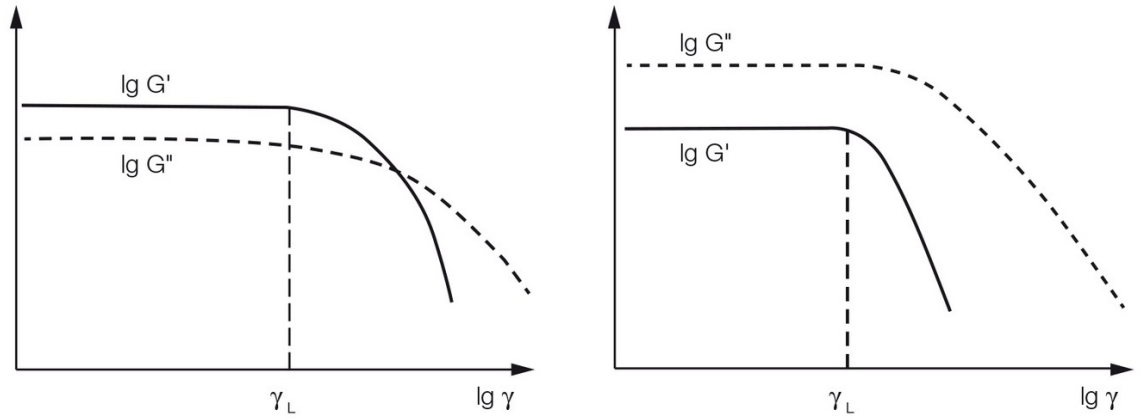

Figure 8: Two amplitude strain sweeps. The left graph shows a solid or gel-like network in the LVR (*G′* > *G″*). The right graph shows a liquid material in the LVR (*G″* > *G′*) (Anton Paar GmbH, n.d.-a).

The resulting values of *G′* and *G″* can be compared to identify if the material is viscoelastic solid or viscoelastic liquid within the LVR (Table 2). After defining the LVR for each sample, the following oscillatory test under heat treatment (temperature sweep) can be carried out.

Temperature sweep

Temperature sweeps are oscillatory tests. As previously mentioned in chapter 2.6.4, it is one way to estimate the moduli *G′* and *G″* within a temperature span. It measures the structural response of a material over a defined temperature range at constant frequency (*ω*) (Rao, 2014; Whaley, Templeton & Anvari, 2019). Solely the temperature is variable with a heating rate of usually 1–3 °C/min. As a result, *G′* and *G″* are plotted against the temperature (Figure 9).

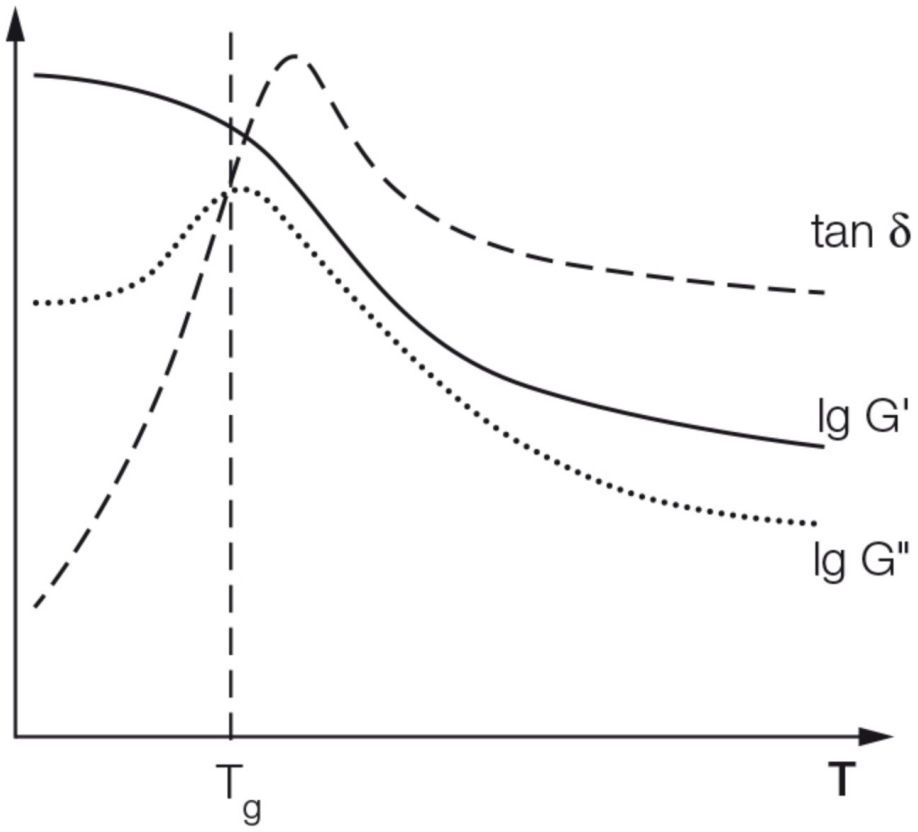

Figure 9: Example of the temperature sweep of a polymer with crosslinks. T_g is the glass-transition temperature (Anton Paar GmbH, n.d.-c).

The curve pattern in Figure 9 gives an indication of the molecular behaviour of a sample. Here, the value of the glass transition temperature (T_g) is of interest. The glass transition is characterized by an increase in G" and a subsequent decrease so that below T_g, the sample is in a glassy state and above T_g it can be deformed to a certain degree depending on the strength of the network (Mezger, 2016).

To sum up the theoretical background, apart from the internal molecular microstructure of a food substance which determines the overall response to shear stress and strain, the external factors such as temperature influences the sample's viscoelastic behaviour. This emphasizes the importance of studying the viscoelastic behaviour of the individual molecular interactions and gluten-free doughs under heat treatment by rheometry.

2.6.5 Micro mixer

A micro mixer is used to determine the optimal mixing and development time for doughs. It consists of a mixing bowl with pins and a rotating mixer head with pins. As explained by Schiedt et al. (2013), the micro mixer cannot be directly compared to a mixograph because of its immovable kneading bowl which does not allow for direct measurements of dough resistance. Generally, Gras et al. (2001) states that the bandwidth of a mixograph curve corresponds to the extension and disruption of dough strands between moving and fixed pins. Thus, it is seen as a measure of extensional viscosity where the maximum bandwidth is assumed to indicate optimal dough development, respectively cohesiveness (Gras, Carpenter & Anderssen, 2000; Schiedt et al., 2013).

2.6.6 Texture analysis

Food texture is a multidimensional term which is why 'textural properties' is often favoured describing several physical properties derived from food structure and which can be perceived through senses and quantified by objective measurement (Bourne, 1990). The main principles of these objective measurements base on the measurement of force, distance and time by e. g. cutting, puncturing or compressing a food sample (Bourne, 1990). One example of force measurement is the one-cycle compression (imitative test, Figure 10) which mimics conditions a food sample undergoes in the oral cavity, on the plate or during manufacturing (Rahman et al., 2021). Another example is the texture profile analysis (TPA) in Figure 11 which compresses the sample twice to imitate a chewing process in the mouth (Sahin & Sumnu, 2006).

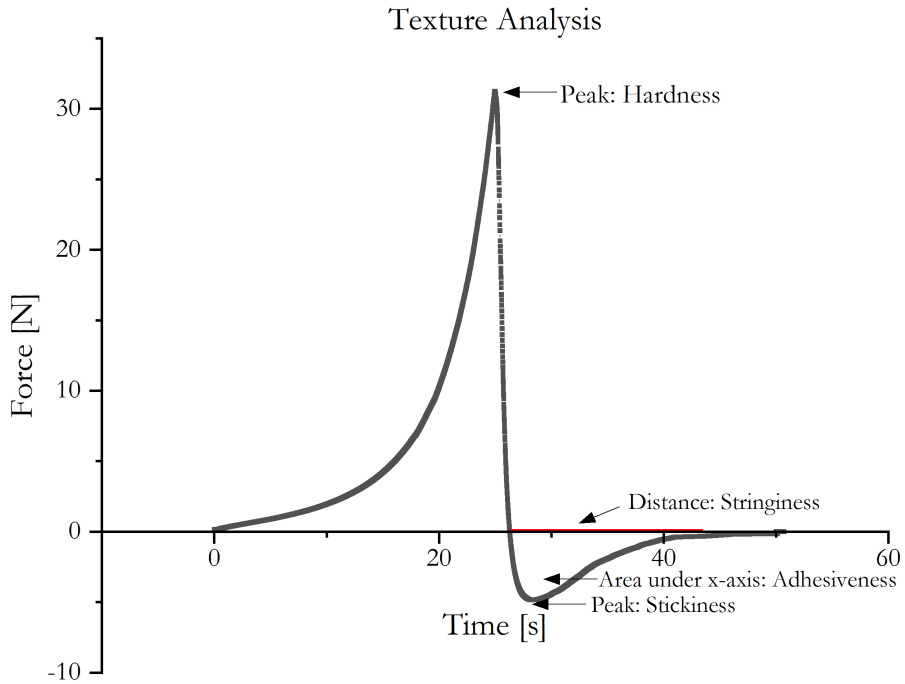

Figure 10: Example of a one cycle compression texture analysis. Adapted from Perten Instruments (n.d.-a).

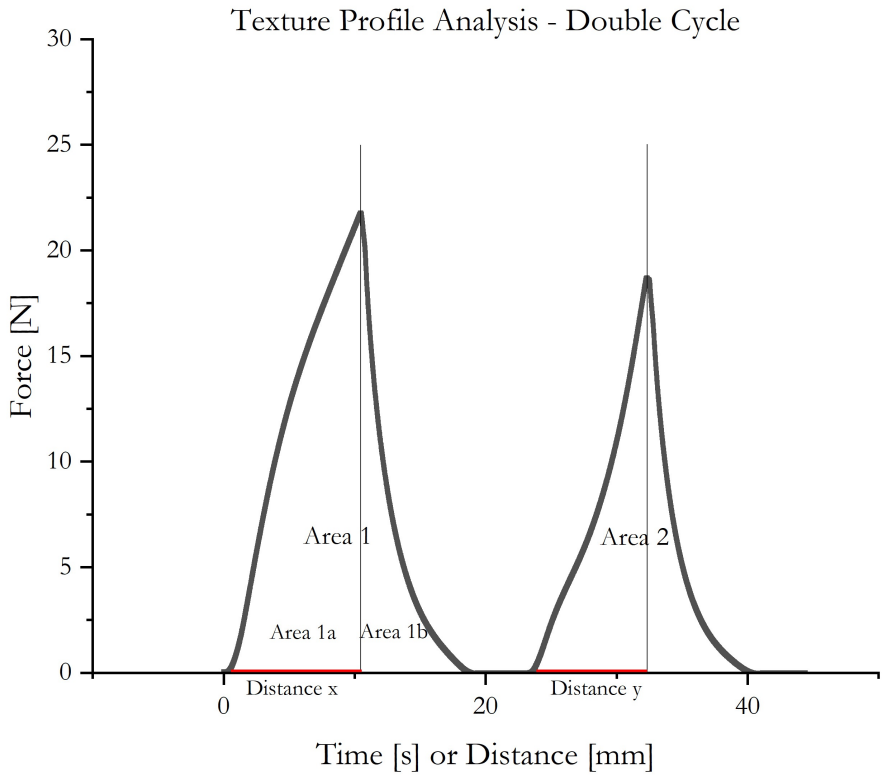

Figure 11: Example of a double-cycle compression texture profile analysis. Adapted from Perten Instruments (n.d.-b).

Table 3 lists the parameters which can be determined from mechanical measurements (Figure 10, Figure 11) and their sensory interpretation.

Table 3: Parameters based on Texture (profile) analysis. Adapted from Armero & Collar, 1997[e]; Bourne & Comstock, 1981[f]; Civille & Szczesniak, 1973[d]; Perten Instruments, n.d.-a[a], n.d.-b[a]; Sahin & Sumnu, 2006[b]; Stable Micro Systems Ltd, n.d.[g]; Szczesniak, 1963[c].

Parameter[a]	**Mechanical Measurement[a,b]**	**Sensory description[c,d,e,f,g]**
Firmness (bread)/ Stiffness (dough)	Peak force of the first compression	Force needed to break down the solid food between molar teeth or the semisolid food enclosed by tongue and palate
Cohesiveness	$\frac{\text{Area 2}}{\text{Area 1}}$	Toughness of the food's internal bonds; extent of compression until the food breaks down
Adhesiveness	Area under x-axis	Work required to detach food from oral cavity/teethes/tongue
Stringiness	Distance between the negative peak until reaching 0 N (removal of probe)	Extent to which a food sample can be stretched or pulls threads
Stickiness	Negative peak force	Force required to detach food from oral cavity/teethes/tongue
Springiness (elasticity)	$\frac{y}{x} * 100$	How much the sample springs back to its initial shape at the end of the first

		bite and the beginning of the second bite
Resilience	$\frac{Area\ 1b}{Area\ 1a}$	Fastness of a food returning to its initial shape
Gumminess	Firmness * Cohesiveness	Energy needed to chew and overcome the denseness of the semisolid food until it can be swallowed
Chewiness	Gumminess * Springiness	Time to chew a solid food until it can be swallowed

2.6.7 Statistical analysis

The Grubbs outlier test or Extreme Studentized Deviate is used for the statistical detection of outliers within a data set. It detects significant outlier by analysing the greatest absolute deviation between single values and the mean value divided by the standard deviation where the resulting value is subsequently compared to a critical value (Grubbs, 1950). After the Grubbs outlier test, further tests like the Student's t-test and an analysis of variances (ANOVA) can be performed with or without the previously analysed outlier. A Student's t-test is suitable to determine statistically significant differences in means between two independent (two-sample t-test) or dependent (one-sample t-test) groups (Kalpić, Hlupić & Lovrić, 2011). An ANOVA can investigate more than two independent group data sets by comparing differences in variances between multiple groups (Herzog, Francis & Clarke, 2019). Since the ANOVA does not show between which two particular groups the significant difference was found, a post-hoc test like the Tukey's test must be carried out to find out especially which group mean values deviate significantly (Herzog, Francis & Clarke, 2019).

3. Materials and Methods

This chapter introduces the experiments carried out during the degree project. First, the required materials are named and then the experimental set-up is explained.

3.1 Materials

Table 4 presents all food materials used. Xanthan gum, Glucono-delta lactone (GdL) and Sub4salt® were provided by Jungbunzlauer Ladenburg GmbH. The gluten-free starches, psyllium, sodium bicarbonate and sodium stearoyl lactylate (SSL) were also provided by Jungbunzlauer Ladenburg GmbH but bought from different suppliers. Here it must be noted that the gluten-free starches were mixed at defined ratios by Jungbunzlauer Ladenburg GmbH so that a starch blend was used in this project. Sodium chloride (NaCl) was used from Sigma Aldrich (CAS Number: 7647-14-5). The remaining materials were purchased at the supermarket with a focus on purchasing products with the same batch number to minimize deviations between different batches. Apart from that, Lugol's solution (Iodine/Potassium iodine solution) from Sigma Aldrich was used to stain the gluten-free starch blend (respectively amylose) for better differentiation during the microscopy. Milli®-Q water was used for the first research question (Goal 1).

Table 4: Materials for dough and bread sample preparation. *Gluten-free starch blend.

Material	**Brand/Origin**
White rice flour*	Nuts.com
Brown rice flour*	Nuts.com
Potato starch*	Nuts.com
Tapioca flour*	Nuts.com
Oat flour*	Nuts.com
Non-fat milk powder	Supermarket (Sucofin, Globus)
Psyllium husk	Nuts.com
Xanthan gum	Jungbunzlauer Ladenburg GmbH
Eggs	Supermarket
Butter	Supermarket (ja!, Rewe)
Water	Supermarket (Black Forest, Rewe)
Sugar	Supermarket (Südzucker, Rewe)
Dry yeast	Supermarket (Dr. Oetker, Rewe)
GdL	Jungbunzlauer Ladenburg GmbH
Sodium bicarbonate	Arm Hammer
Sub4salt ®	Jungbunzlauer Ladenburg GmbH
SSL	Puratos

3.2 Methods

3.2.1 Experimental set-up

In accordance with the objectives in chapter 1.2, the molecular interactions of xanthan gum with psyllium, starch and milk proteins as well as the effects on gluten-free doughs and breads were investigated in three steps: In solution (Goal 1), in dough (Goal 2) and in bread (Goal 3). The experimental set-up is shown in Figure 12.

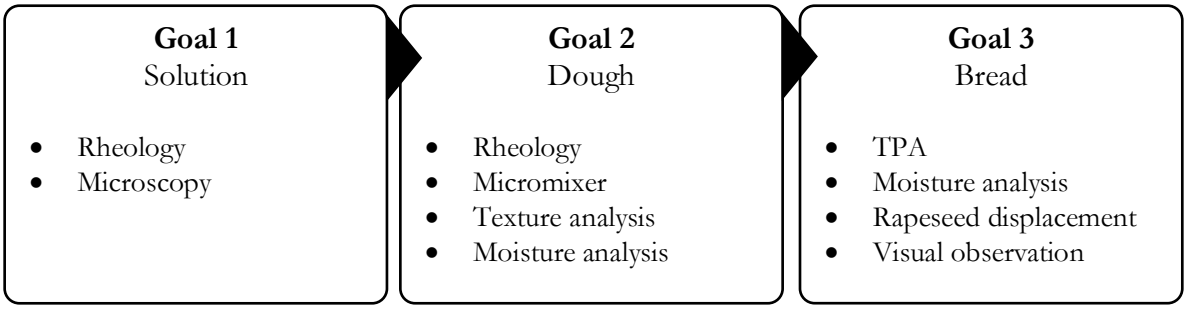

Figure 12: Experimental set-up of the degree project.

3.2.2 Formulations for rheological analysis in solution

After performing some pre-trials to define the concentrations of the dry ingredients (data not shown), Table 5 presents the final concentrations used for the rheological measurements and microscopy in Goal 1. The ratios of the dry ingredients were orientated on the ratios of the dough and bread formulations except for water and salt to investigate the molecular interactions in an ionic solution. Therefore, the water-salt solution was considered as the basis.

Table 5: Concentrations for Goal 1.

Ingredient	**Concentration [%]**
Xanthan gum	0.30
Psyllium	0.30
Starch blend	10.35
Milk powder	1.02
Sodium chloride	0.74

Table 6 presents the final formulations where the individual components such as xanthan gum, psyllium, and the gluten-free starch blend (G1XG, G1Ps, G1St) were examined first and then the combinations with xanthan gum (G1XG-Ps - G1XG-MP). Milk powder could not be examined individually, as the solution was too watery for rheological experiments.

Table 6: Formulations for Goal 1 in water-salt solution. "G1" stands for "Goal 1".

Formulation	Ingredient
G1XG	Xanthan gum
G1Ps	Psyllium
G1St	Starch blend
G1XG-Ps	Xanthan gum
	Psyllium
G1XG-St	Xanthan gum
	Starch blend
G1XG-MP	Xanthan gum
	Milk powder

The respective ingredients for each formulation were dissolved or suspended into a salt-solution consisting of Milli-Q® water and sodium chloride for a final weight of 10g or 40g. 10g samples were used for amplitude sweep and temperature sweep measurements whereas 40g samples were used for the rotational test since the concentric cylinder required a higher volume. To reduce measuring and preparation errors, all measurements were performed at least as duplicates with fresh samples in each case. The exact preparation method for these formulations will be mentioned after the importance of the moisture analysis has been explained.

Moisture analysis

The moisture content of the ingredients was measured by a Halogen Moisture Analyzer (HS153, Mettler Toledo, Columbus, USA) and can be seen in Appendix A (Table 17). This was done to consider both the inherent moisture of the ingredients and the added Milli®-Q water in the final formulations. According to the best practice instructions provided by Mettler-Toledo, the drying temperatures were 140°C for xanthan gum, psyllium as well as the starch blend and 110°C for milk powder (Mettler-Toledo GmbH, 2016). Eq. 6 shows the calculation for the subsequent weight of the contents.

$$m_{DI} = \frac{c \cdot m_{total}}{100\% - MC_{DI}} \quad \text{(Eq.6)}$$

m_{DI}: Mass of dry ingredient [g]
c: Final concentration of the dry ingredient (*w/w*) [%]
m_{total}: Sample weight [g]
MC_{DI}: Moisture content of dry ingredient [%]

The final Milli®-Q water content was then calculated according to Eq. 7 by subtracting the calculated mass of dry ingredients from the final sample weight (10g or 40g).

$$m_W = m_{total} - m_{DI} \quad \text{(Eq.7)}$$

m_W: Weight of Milli®-Q water [g]
m_{total}: Sample weight [g]
m_{DI}: Mass of dry ingredient [g]

Preparation for rheological measurements of formulations in solution
All ingredients were weighed in with an analytical scale (MS 204, Mettler Toledo, Columbus, USA). After the water-salt solutions has been prepared, further ingredients (Table 6) were added under constant stirring at 22°C. The containers were closed afterwards to prevent evaporation. Mixing speeds (rpm) needed to be adjusted for each formulation separately due to viscosity differences. In case of two or more ingredients in one formulation, the respective ingredients were dry mixed before added to the water-salt solution. G1XG, G1Ps, GXG-Ps and G1XG-MP were mixed at 400 rpm and stirred overnight. Since G1Ps developed a distinct gel lump instead of a homogeneous mix, only the gel lump was used for the rheological measurements. Starch containing formulations (G1St, G1XG-St) were prepared on the same day of rheological measurement to prevent pre-swelling into lumps. Nevertheless, sufficient hydration was ensured. G1St was stirred at 500 rpm whereas G1XG-St was stirred at 800 rpm initially with a reduction to 500 rpm after broad hydration.

Rheological measurements of formulations in solution
All rheological measurements were performed with a Discovery HR-3 rheometer from TA Instruments, New Castle, USA.

Amplitude sweeps were performed as duplicates or triplicates after a soak time of 60s within a strain range of 0.01%–1000% (G1Ps: 0.02 –2000%) at frequency ω = 1 Hz under constant temperature (25°C). For G1XG and G1XG-MP a cone-plate (40 mm diameter, cone angle 2°) measuring system was used because of the very small particle size. Since the other formulations (G1St, G1XG-Ps, G1XG-St) had a higher particle size than suitable for the cone-plate, a plate-plate geometry (40 mm diameter) was used. Here, the gap between the two plates was set to 1000 µm as default. For G1Ps, a disposable plate-plate geometry with 25 mm diameter was used because the gel lump had a small, irregular size and a higher viscosity than the other samples. Therefore, the measuring geometry was covered with sandpaper (P60) to prevent slippage. Also, the gap was manually adjusted due to the irregular size so that the top plate completely contacted the psyllium gel. Amplitude sweeps with formulations containing no starch were conducted before performing the temperature sweep to define an appropriate strain for the temperature sweep and because these ingredients already develop their potential to increase viscosity in cold water. In contrast to that, amplitude sweeps for formulations including starch were performed directly after the temperature sweep to measure the gelatinized food system and not the ungelatinized starch granules. For these samples, the respective chosen strain for the temperature sweeps was based on literature values and reasonable conclusions from other experiments already conducted at the MPI-P. However, the assumed strain was then checked in the subsequent amplitude sweep. Table 7 summarizes all final parameters for the amplitude sweeps and the strains derived from them within each LVR for the temperature sweeps.

Table 7: Summary of measuring geometries and gap sizes for the amplitude sweep. The strains in column 4 are only valid for the temperature sweeps and were defined on basis of the length of the respective LVR.

Formulation	Measuring geometry	Gap [mm]	Strain [%]
G1XG	Cone-Plate (40mm, 2°)	-	1.00
G1Ps	Disposable Plate-Plate (25mm)	1833, 1719, 1826	-
G1St	Plate-Plate (40mm)	1000	0.20
G1XG-Ps	Plate-Plate (40mm)	1000	1.00
G1XG-St	Plate-Plate (40mm)	1000	0.50
GXG-MP	Cone-Plate (40mm, 2°)	-	1.00

Temperature sweeps in oscillation were performed as duplicates or triplicates after a soak time of 60s with a plate-plate measuring geometry (40 mm diameter), a default gap size of 1000 µm and at 1 Hz. The strain within the LVR was previously determined in the amplitude sweep or checked afterwards. The samples were heated from 25°C to 90°C and kept at 90°C for 5 min. before cooling down to 25°C at a rate of 3°C/min. To prevent evaporation, a solvent trap was used and the edge of the measuring geometry and the sample in between was sealed with silicon oil. In case of formulations containing starch, an oscillation step at constant temperature (25°C) for 5 min. was directly programmed after the temperature sweep to enable relaxation of the sample before starting the amplitude sweep.

Apparent viscosity profiles in rotation were performed as duplicates or triplicates with a vane geometry (4 blades, 42 mm bob length, 28 mm bob diameter) and a concentric cylinder (30.37 mm cup diameter) at constant shear rate of 200 s^{-1}. The gap size was set to 4000 µm so that the solvent trap could still be used to prevent evaporation. With a smaller gap, the solvent trap would not have fitted into the small gap between the measuring geometry and the concentric cylinder. After that, the samples were heated from 25°C to 90°C and kept at 90°C for 5 min. before cooling down to 25°C at a rate of 3°C/min.

Optical analysis of formulations in solution

The light microscopy was performed with an Axio Scope.A1 microscope (Carl Zeiss Microscopy Deutschland GmbH, Oberkochen, Germany) and a heating stage (PE120, Linkam Scientific Instruments Ltd., Tadworth, United Kingdom). Here, only formulations with starch were used to visualize the gelatinization. The formulations were supplemented with Lugol's solution for better image contrast and placed on a microscope slide covered with a cover glass. To prevent drying/evaporation, the edges of the cover glass were sealed with nail polish. After that, the samples were heated from 25°C to 90°C at a heating rate of 3°C/min. and kept at 90°C for 5 min. Images were taken with 20x A-plan objectives every minute.

3.2.3 Dough and bread preparation

This chapter refers to Goal 2 and 3 under the overall aim on investigating the function of xanthan gum in gluten-free dough and bread. Here, mainly two gluten-free doughs/breads were investigated: with xanthan gum and without xanthan gum. Table 8 shows the respective formulations for the samples.

Table 8: Formulations for Goal 2 and 3. G2 and G3 stand for "Goal 2" and "Goal 3" respectively.

Formulation	Formulation
G2YXG	Dough with yeast and with xanthan gum
G2Y	Dough with yeast and without xanthan gum
G2XG	Dough without yeast and with xanthan gum
G2-	Dough without yeast and without xanthan gum
G3XG	Bread with xanthan gum
G3-	Bread without xanthan gum

G2YXG and G2Y were used for single cycle texture analysis, micro mixer and moisture analysis measurements whereas the doughs G2XG and G2- were used for rheological measurements since air bubbles in the dough system can disturb and impair the rheological measurements of the amplitude sweep, temperature sweep and apparent viscosity profile. G3XG and G3- had the same formulations as G2YXG and G2Y, respectively. The composition for the doughs and breads in Table 8 can be seen in Appendix B (Table 18). The preparation of the doughs for Goal 2 and final breads for Goal 3 weas based on the instructions provided by Jungbunzlauer Ladenburg GmbH. For example, the bread G3- without xanthan gum was set to a batch of 500g. The masses of the ingredients remained the same for G3XG, except that xanthan gum was added. This was also done for the doughs where just xanthan gum was added to G2Y and G2- to obtain G2YXG and G2XG. Ingredients were weighed in with a precision scale (MS4002TS/00, Mettler Toledo, Columbus, USA). First, the butter was melted to 30°C. After that, all dry ingredients were mixed and water was added. This mixture was mixed with a hand mixer (dough hooks, 450 W, Robert Bosch Hausgeräte GmbH, München, Germany) for 1 min. at level 3 out of 5. Eggs were added and the dough was again mixed for 1 min at level 3 out of 5. Lastly, the melted butter was added to the mixture and mixed for 6 minutes. Covered with a towel, the dough then proofed for one hour in a climate-controlled chamber (Binder GmbH, Tuttlingen, Germany) under constant conditions at 25°C and 60% relative humidity. The bread was baked at 175°C in a house hold oven (air circulation, Moulinex CT31, GroupSEB Deutschland GmbH, Frankfurt am Main, Germany) for 50 minutes where the bread was turned after 25 min. After baking, the bread cooled at room temperature for 10 minutes in the pan and after that the pan was removed so that the loaf cooled for another two hours at 23°C.

Micro mixer

Figure 13 shows the micro mixer used from National Manufacturing Co, Lincoln, Nebraska. The mixing bowl had two pins and the mixer head with four pins rotated at 100 rpm.

Figure 13: Micro Mixer.

The procedure according to Zheng et al. (2000) was followed who converted the current (I) consumption by the motor to voltage (U) (torque) and used the torque to record dough resistance like in a mixograph. In this study, torque was measured by a programme written by a colleague. Since the motor of the micro mixer was considered to not follow Ohm's law, the standard deviation of I/U was recorded (Schiedt et al., 2013). The dough formulations with xanthan gum (G2YXG) and without xanthan gum (G2Y) for the micro mixer can be seen in Appendix B (Table 19). The dry ingredients were mixed and filled into the kneading bowl of the micro mixer. The measurement started as soon as water was added to the dry ingredients. After 1 minute, the measurement was shortly interrupted to add the egg. Again, after 1 minute of mixing, the measurement was stopped to add the melted butter. The mixing time was then set to 25 minutes to record the mixing behaviour of the dough by the programmed computer software. The force which was required to mix the dough was reported as resistance (y-axis) dependent on the time (x-axis) in a graph.

Dough rheology

Dough rheology was performed with formulations G2XG and G2- as previously explained. Appendix B (Table 18) presents the exact formulations. Each dough replicate was directly prepared as a 70g batch before measured to avoid differences in texture and microstructure between each replicate due to intramolecular reactions. Immediately after preparation, the dough was wrapped in sufficient cling film and transported to the rheometer in a plastic tray.

The dough rheology consisted of an amplitude- and temperature sweep which were performed as duplicates or triplicates after a soak time of 60s at a frequency of 1 Hz with a disposable plate-plate geometry (25 mm diameter) and a gap of 2000 µm. To prevent slippage, the measuring geometries were covered with sandpaper (roughness 500). An enclosure with moistened tissues was placed around the geometry to prevent evaporation and to keep the

relative humidity in the air system. Amplitude sweeps were performed within strain range of 0.01%–1000% under constant temperature (25°C). The time from the end of the dough preparation until the start of the amplitude sweep (incl. soak time) was on average 5.7 min. As a result of the amplitude sweep, the strain for the temperature sweep was set to 0.03 %. The samples were heated from 25°C to 90°C and kept at 90°C for 5 min. before cooling down to 25°C at a rate of 3°C/min. The time from the end of the dough preparation until the start of the temperature sweep (incl. soak time) was on average 24.2 min. This time also included the time during which the amplitude sweep was performed.

Moisture analysis of gluten-free dough and bread

The moisture analysis was used as a measure of moisture retention and measured by a Halogen Moisture Analyzer (HS153, Mettler Toledo, Columbus, USA). The drying temperature was 135°C for both, dough and bread. For the dough, a small amount of dough (7g) was rolled out between cling film to prevent uncontrolled moisture loss. Afterwards, the sample was put on a glass fibre filter on an aluminium sample pan to increase the surface by absorbing potential water loss and to reduce the measuring time. In case of bread, three different samples were used: (i) a sample from the centre of the crumb (2.5cm x 3 cm), (ii) the crust and (iii) a thin bread slice without the crust was cut from the centre of the bread and put on an aluminium sample pan in the Halogen Moisture Analyzer. Apart from the measured moisture content, the slope of the curves for dough and bread in the graph was evaluated by means of a linear fitting with OriginPro 2021.

Texture analysis

Texture analysis tests were carried out with the material testing machine Z005 from ZwickRoell (Ulm, Germany) at initial speed of 1.0 mm/s, test speed of 1.0 mm/s and retract speed of 1.0 mm/s. The dough and bread samples were prepared according to chapter 3.2.3. Test parameters were derived from Perten Instruments Method Description TVT Method 03-01.02 and 01-03.02 (Perten Instruments, n.d.-a, n.d.-b).

Single cycle compression texture analysis was carried out with the doughs G2YXG and G2- to determine the stiffness, stringiness and adhesiveness of the dough. After proofing in the climate chamber, a 50g sample was evenly formed into a dough ball and placed centrally under the cylindrical probe (75 mm diameter). The test was performed by a 70% compression and the trigger force was set to 0.2 N.

TPA as double-cycle compression was carried out with the breads G3XG and G3- to determine the bread crumb firmness, springiness, resilience, cohesiveness and chewiness. After two hours cooling down the bread at room temperature three 2.5 cm thick slices (triplicate) were cut from the middle part of each bread replicate. Also, the crust was cut off to not distort the measurement. The TPA test was performed by using a cylinder probe (36 mm diameter) exerting a 40% compression with a trigger force of 0.05 N.

Specific bread volume and baking loss

The measurement of the specific bread volume was based on AACC International Method 10-05.01 - Guidelines for Measurement of Volume by Rapeseed Displacement (Cereals & Grains Association, 2001). The bread was weighed one hour after baking with a precision scale

(Precisa Gravimetrics AG, 321LS, 4200C, Dietikon, Switzerland). A sufficiently large rectangular container was filled with rapeseeds and the surface smoothed with a ruler. Some of the rapeseeds were then taken out again and the bread was placed in the box. Again, the box was filled with the rapeseeds and the surface smoothed with a ruler. The remaining rapeseeds were then filled into a measuring cylinder to determine the bread volume. Eq. 8 presents the calculation for the specific bread volume, where *V* is the volume [ml] and *W* the loaf weight [g]:

$$Specific\ bread\ volume\ = \frac{V}{W}\ in\ \frac{ml}{g} \quad \text{(Eq. 8)}$$

In addition, the baking loss was calculated by the total mass of ingredients after weighing-in before baking and the final loaf weight one hour after baking by the following equation 9:

$$Baking\ loss\ = \frac{Mass\ weighing-in}{Loaf\ weight}\ in\ \frac{g}{g} \quad \text{(Eq. 9)}$$

3.2.4 Statistical analysis

Assuming that the data are normally distributed, data analysis was performed by means of a one-way analysis of variance (ANOVA) at $p < 0.05$ and a two-sample/independent t-test (student's t-test). In case of three groups mainly represented in the first research question, the Tukey's Test was used as post-hoc test. For the second and third research question, a student's t-test was used instead of an ANOVA since only two groups were of interest (dough/bread with xanthan gum and dough/bread without xanthan gum). Data analysis was performed with the software OriginPro 2021 and IBM SPSS Statistics Version 27. Outliers detected by the Grubbs outlier test were not considered in the statistical analysis.

4. Results and Discussion

This section starts with analysing the individual interactions in model systems based on the rheological measurements conducted. In the following, two gluten-free doughs respectively breads where one contains xanthan gum and the other does not will be compared to investigate the viscoelastic behaviour of gluten free doughs under influence of xanthan gum and the resulting bread properties.

4.1 Molecular Interactions in Solution

4.1.1 Temperature sweep and tanδ

Figure 14 presents the temperature sweeps in the range of 25–90–25°C performed for the formulations in Table 6. All formulations can be classified as viscoelastic solids ($G' > G''$). Figure 15 presents tanδ for the temperature sweep based on which the network strength can be concluded as explained in chapter 2.6.4.

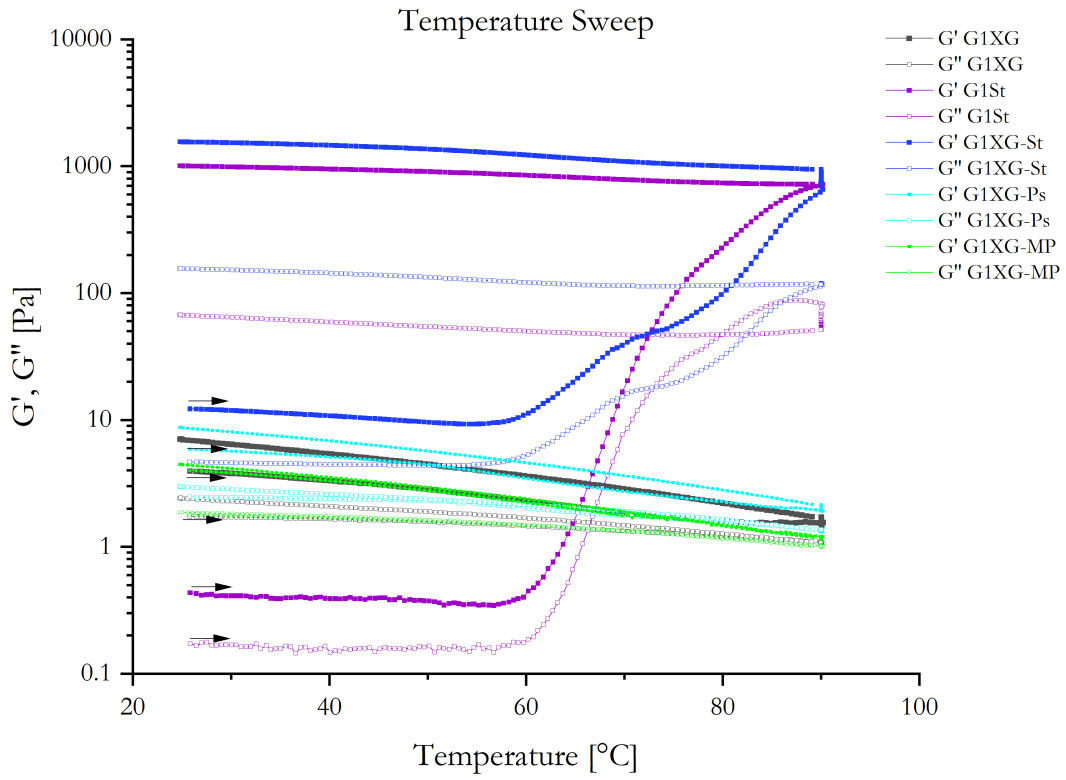

Figure 14: Temperature Sweep from 25°C to 90°C (heating rate 3°C/min.). Constant heating at 90°C for 5 min. before reducing the temperature back to 25°C. Mean graphs are based on triplicates for G1XG, G1XG-Ps, G1XG-St and on duplicates for G1St, G1XG-MP.

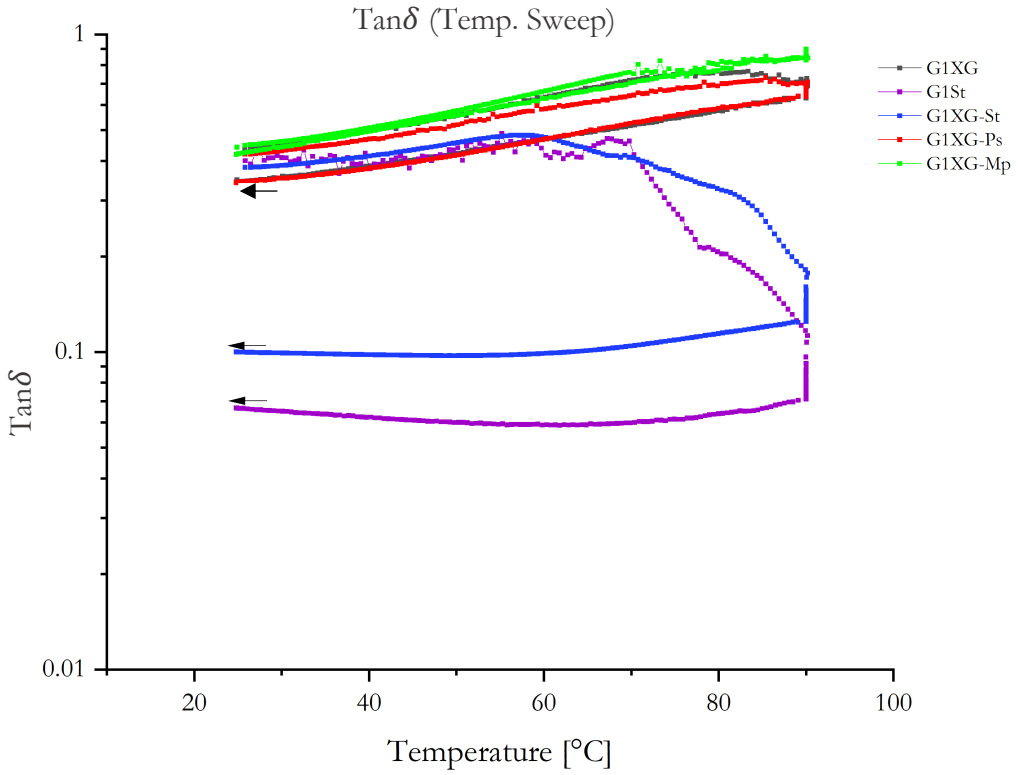

Figure 15: Tanδ with respect to temperature for the temperature sweep from 25°C to 90°C and back, as described above.

Starting with G1XG, the decrease in both moduli in Figure 14 during heating may give a hint on the helix–coil transition of xanthan gum molecules. This is supported by the relative increase in the viscous component (tan$\delta \rightarrow 1$) for G1XG in Figure 15 since coils are considered to reduce the resistance to flow by taking up less space than (entangled) helices. During cooling, the increase in rigidity, Figure 14, and elastic proportion, Figure 15, for G1XG suggests the coil–helix retransition and stiffening due to the formation of double-stranded helices. However, the curve pattern differs when xanthan gum was combined with further ingredients whose molecular interactions will be explained in the following.

Xanthan gum - starch blend:

Starting with the starch-containing formulations G1St and G1XG-St, the beginning of starch granule swelling and amylose leaching out of the granules can be seen in Figure 14 from 58°C onwards where the moduli for G1St and G1XG-St increase. The steep increase for G1St may be explained by the free movement of water molecules within the matrix enabling a fast diffusion of water into the starch granules and their swelling as well as the building of the 3D-amylose-network in the continuous phase. In contrast to that, the slope of the storage modulus for G1XG-St is less steep since xanthan gum increased the viscosity already from the beginning and competed with starch for water so that water molecules could not move as freely as in G1St. Looking at G'', for G1St a loop occurs in the range of 80–90°C. This indicates a glass transition with a T_g of around 85°C. On a molecular basis, it describes the intensification in molecular movement and friction heat until the bursting of starch granules with subsequent solubilization of amylose and amylopectin in the continuous phase which reduces friction (G'' reduction). The kink at about 70°C for G'' G1XG-St gives rise to the assumption that xanthan gum contributed to a lower T_g because the higher viscosity may have increased friction between

starch granules. Thus, swollen starch granules already disrupted at around 70°C, see Figure 18 e). The disruption can cause a short period of friction reduction and a subsequent increase in moduli due to the greater release of network-forming amylose and amylopectin, as can be seen in the range of 65–90°C for G1XG-St in Figure 14. During cooling, a small increase in the storage and loss moduli can be observed for G1XG-St compared to G1St which argues for xanthan gum's slight temperature dependence with stiffer molecules after heating as mentioned in chapter 2.5.2.

Concerning tanδ in Figure 15, both G1St and G1XG-St started with the same network properties. At around 58–70°C, the starch granule swelling and formation of the 3D-network began which can be seen in decreasing tanδ values indicating an increase in the elastic component. However, after the temperature increase to 90°C and the subsequent cooldown to 25°C, G1St develops lower tanδ showing more pronounced elastic properties than G1XG-St after cooling. These values suggest a stronger network structure with a higher degree of crosslinks, here junction zones between amylose molecules. If these crosslinks contributed to elasticity, an increased tanδ may be the result of less crosslinking. This again emphasizes that xanthan gum probably impaired the amylose/amylopectin continuous network structure by reducing the degree of crosslinking which was also found by Eidam et al. (1995) using galactomannan in starch gels. In contrast to the effect of xanthan gum on starch gelatinization, the mixture of xanthan gum and milk proteins had rather small effects.

Xanthan gum - milk proteins:

The combination of xanthan gum and milk powder (G1XG-MP) increased only slightly its initial gel strength during cooling compared to G1XG which gives rise to the assumption that the coil–helix retransition and stiffening of xanthan gum molecules during temperature reduction is limited. Assuming the coil–helix retransition being responsible for the increase in elastic proportion in G1XG, Figure 15, milk powder addition may have inhibited these mechanisms since the elastic component is less pronounced for G1XG-MP. Also, accepting the already denatured state of the whey proteins, irreversible complexation of denatured β-Lactoglobulin with α-Lactalbumin and probably caseins during spray drying as mentioned in chapter 2.4 can be assumed. In addition, the pH of G1XG-MP (6.99 $\pm$ 0.03) was above the isoelectric point of casein, α-Lactoglobulin and β-Lactoglobulin so that net negative charge of the proteins dominated which would attract cationic polyelectrolytes (Park et al., 1992). Since xanthan gum is anionic it is unlikely that coulombic interactions prevailed between xanthan gum with milk proteins or caseins over long distance. Nevertheless, positive patches on whey protein amino acids still might have been present that could attract xanthan gum. However, sodium is considered to partially screen the negative charges of xanthan gum and positively charged patches of whey protein amino acids so that they could no longer attract each other over long distances but in a short radius. Therefore, attraction could only occur at very short distances, as the positively charged patches of whey proteins may cluster around the negatively charged side chains. Consequently, milk proteins may act as obstacles which prevented complete conformational retransition during cooling. This effect is likely to be enhanced by the higher skim milk powder concentration (1.02%) than xanthan gum (0.3%) and the occupied volume of milk protein complexes reducing the volume available for the expansion of xanthan gum coils back into helices resulting in incomplete coil–helix

retransition. This could explain why there is no increase in rigidity for G1XG-MP in Figure 14 and no increase in the elastic proportion for G1XG-MP in Figure 15 during cooling.

Xanthan gum - psyllium:
As for G1XG, the curve for G1XG-Ps shows a decrease in storage and loss moduli during heating and an increase in both moduli during cooldown. This suggests that a complete helix –coil–helix transition of xanthan took place. However, the moduli for G1XG-Ps are slightly higher than for G1XG which shows that the addition of psyllium contributed to rigidity probably by water binding. Tanδ revealed no big differences except that G1XG showed a slightly higher viscous proportion than G1XG-Ps during heating. As soon as the temperature decreased from 90°C both formulations showed the same ratio of viscous to elastic proportions in Figure 15. This implies that the addition of psyllium to xanthan gum did not greatly influence the ratio of viscous to elastic proportions in the formulation during heating in oscillation. No temperature sweep was conducted for G1Ps since the gel aggregate required a different measuring geometry (disposable plate-plate, chapter 3.2.2) for which no suitable solvent trap was available.

Usually, temperature sweeps are performed after amplitude sweeps (chapter 2.6.4). However, in this degree project, the amplitude sweep was carried out after the temperature sweep for the starch-containing formulations so that the results of the amplitude sweep are presented in the following.

4.1.2 Amplitude sweep

Figure 16 presents the amplitude sweeps for all formulations at 25°C. All formulations can be characterized as a viscoelastic solid since the elastic behaviour dominated the viscous behaviour within the LVR ($G' > G''$). Overall, xanthan gum (G1XG) showed the lowest gel strength which could be derived from its inability to form firm networks on its own. As for the temperature sweep, the combination of xanthan gum with further ingredients resulted in different curve patterns of which the molecular interactions will be explained in the following.

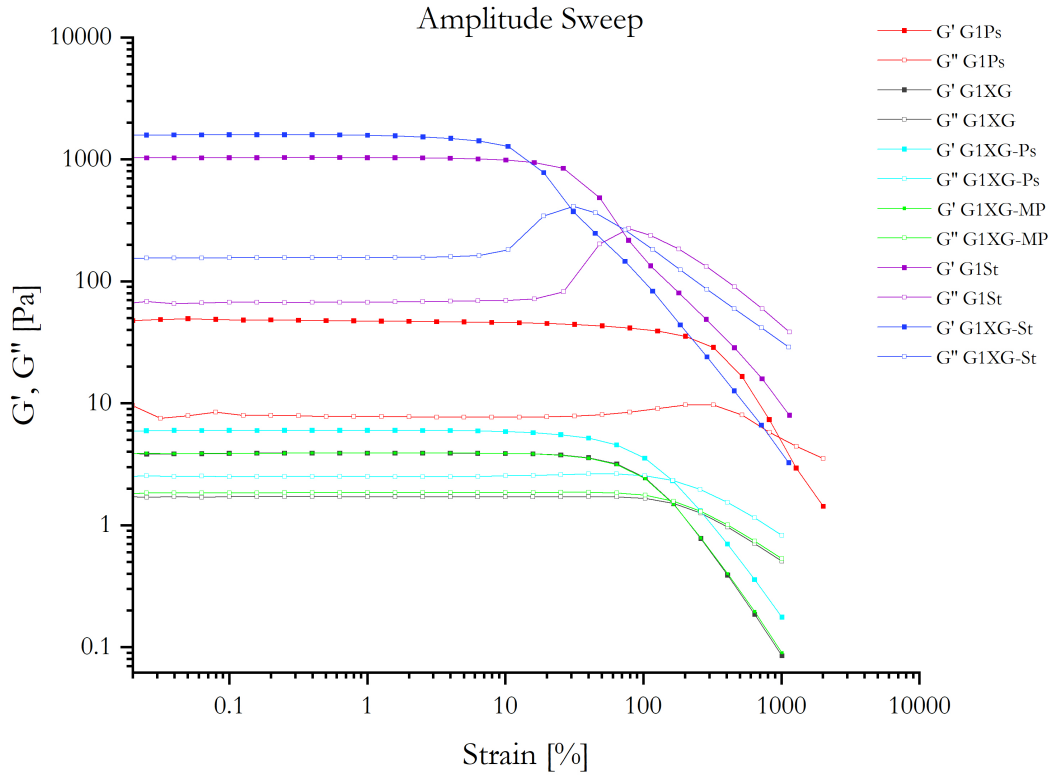

Figure 16: Amplitude Sweeps at 25°C. Mean graphs are based on triplicates for G1XG, G1Ps, G1XG-Ps, G1XG-St, G1XG-MP and on duplicates for G1St.

Xanthan gum - starch blend:

The amplitude sweeps for G1St and G1XG-St were performed directly after the temperature sweep, so gelatinization had already taken place. Thus, G1St showed a higher gel strength than G1XG probably because of short-term retrogradation of leached amylose that led to a stronger 3D-network and dispersed, swollen starch granules taking up more space (intrinsic viscosity) in the continuous phase than xanthan gum molecules (G1XG). The combination of starch and xanthan gum (G1XG-St) increased the elastic and viscous properties compared to the single formulations (G1XG, G1St). The increase in *G'* for G1XG-St may be due to larger starch granules, the slight entanglement of linear xanthan gum molecules resulting in an additional thickening effect and a higher total dry matter concentration. Consequently, the system's resistance to flow is enhanced and shows higher moduli. The lengths of the LVRs between the formulations showed significant differences with G1XG > G1St > G1XG-St in descending order as can be seen in Table 9.

Table 9: LVR and gel strength in the amplitude sweep for G1XG, G1St and G1XG-St. Statistical Analysis by means of an ANOVA and Tukey-HSD Post-hoc test, $p < 0.05$.

Formulation	**LVR ($G'_{95\%}$)**	**Gel strength**
G1XG	30.18 ± 0.57^{a}	3.87 ± 0.14^{a}
G1St	10.75 ± 0.01^{c}	1036.02 ± 29.52^{b}
G1XG-St	3.24 ± 0.37^{b}	1579.17 ± 117.62^{c}

The shorter LVR deformation limit for G1XG-St as compared to G1St may be attributed to local xanthan gum phases interfering the continuous entanglement of leached amylose/amylopectin in the continuous phase. Xanthan gum is a highly anionically charged polyelectrolyte so that a phase separation between xanthan gum and amylose/amylopectin in the continuous phase is assumed due to repulsion respectively thermodynamic incompatibility (Mandala & Palogou, 2003). This is also supported by BeMiller (2011) who states that polyelectrolytes induce a more pronounced demixing in starch pastes than non-charged polymers. This emphasizes that even the presence of salt, which in the extreme case would shield the charge of xanthan gum completely, demixing would still not be prevented. Solely potato starch is also negatively charged which even may increase the thermodynamic incompatibility with xanthan gum (Gibiński et al., 2006). As a consequence, local regions where xanthan gum, amylose or amylopectin dominate respectively could be present in the starch-xanthan gum formulation (Mandala & Palogou, 2003). This is supported by Eidam et al. (1995) who reported that the increased viscosity of the continuous phase induced by hydrocolloids like xanthan gum hinders the movement of amylose. This can impair the formation of a continuous network leading to a system being more susceptible to deformation represented in shorter LVR and small G" maximum as discussed below.

Looking at the curve pattern for G1St and G1XG-St, it is striking that G'' shows a clear maximum. G" maxima are a sign for a network where a high G" maximum indicates an increase in energy loss due to the onset of fine cracks in the existing network (Mezger, 2016). This network was probably formed by realigned amylose molecules connected via hydrogen bonds embedding starch granule ghosts. With increasing strain, the hydrogen bonds broke leading to a disrupted network which can no longer stabilize the embedded starch granule ghosts so that the starch granules started to slide past each other. This can be seen in the decreasing curve directly after the G" maximum (G1St). Looking at G1St and G1XG-St one can assume that the G'' maximum of G1XG-St is somewhat less pronounced than for G1St. This again suggests that xanthan gum may have reduced the extent of deformation energy needed to deform the network, suggesting an impairment of the overall network formation of leached amylose and amylopectin chains as previously explained. Therefore, less deformation energy is necessary to disrupt the internal structures which is reflected in the lower G'' maximum for G1XG-St. According to Mezger, 2006, a system's structure does not disintegrate suddenly but begins to disrupt by micro-cracks which leads to an increase in G'' by higher energy dissipation. These micro cracks then develop into greater cracks until the system starts to flow at $G' = G''$ followed by a decrease in G''. Looking at G'' for G1XG-St, especially the areas where xanthan gum and amylose/amylopectin phases were adjacent may be susceptible for micro-cracks due to the lack of interaction initiating an earlier rupture compared to G'' of G1St. This may also be an additional explanation for the shorter LVR of G1XG-St. Conversely, G'' for G1XG does not present any maximum which shows that xanthan gum did not form crosslinks (Mezger, 2016). In contrast to the moduli for starch and xanthan gum + starch formulations the interaction of xanthan gum and milk proteins resulted in different curve patterns.

Xanthan gum - milk proteins:

Comparing the mixture G1XG-MP to G1XG there are no significant differences neither between the gel strength nor between the LVR length. The reason for this was already mentioned in the temperature sweep section and can be transferred to the amplitude sweep. Solely *G″* values were slightly higher for G1XG-MP suggesting that the addition of skim milk powder brought more dry matter to the formulation and thus slightly increased friction.

Xanthan gum - psyllium:

Psyllium, G1Ps, developed a separate psyllium gel clot in the water-salt solution during formulation so that only the gel aggregate has been used for rheological measurements because the surrounding water-salt solution was too watery. The unequal polymer-water ratio did not allow a comparison with G1XG and G1XG-Ps which is why G1Ps only serves as illustration for the gel strength and LVR of the psyllium gel aggregate. The development of the distinct gel aggregate could be explained by crosslinking and swelling of elongated polysaccharide chains forming a 3D-network which can be seen in a *G″* maximum for G1Ps. In contrast to that, G1XG and G1XG-Ps do not have a *G″* maximum which indicates that these formulations did not form a significant amount of crosslinks. It is assumed that both polyelectrolytes were still slightly negatively charged despite NaCl so that electrostatic repulsion still occurred and restricted the movement of molecules. Therefore, xanthan gum and psyllium did not interact but were well mixed throughout the continuous phase which is supported by the parallel curve pattern of G1XG and G1XG-Ps with increasing strain in Figure 16. Although there are significant differences in the LVR between xanthan gum, G1XG, and the combination with psyllium, G1XG-Ps, these differences do not strike in Figure 16 with the logarithmic scale. No differences in LVR and gel strength were observed between G1XG and G1XG-Ps, Table 10. Since the rheometry results show no indication of crosslinking of molecules, i.e. no *G″* maximum (Figure 14) and no increase in elastic proportion after heating (Figure 15) a direct interaction in form of crosslinking between psyllium-psyllium and psyllium-xanthan gum molecules is not assumed and strengthens the assumption that a good mix has been achieved.

Table 10: LVRs in the amplitude sweep for G1XG, G1Ps and G1XG-Ps. Statistical Analysis by means of an ANOVA and Tukey-HSD Post-hoc test, $p < 0.05$.

Formulation	**LVR ($G'_{95\%}$)**	**Gel strength (LVR)**
G1XG	30.18 ± 0.57^{a}	3.87 ± 0.14^{a}
G1Ps	18.89 ± 3.22^{b}	47.38 ± 3.33^{b}
G1XG-Ps	18.63 ± 6.31^{b}	5.69 ± 0.51^{a}

In general, the amplitude sweeps revealed differences in gel strength and LVR during oscillation especially for starch- and psyllium-containing formulations. Differences in viscosity during rotation will be analysed in the following chapter.

4.1.3 Viscosity profile

The apparent viscosity profile of the formulations within the temperature range of 25–90–25°C can be seen in Figure 17 with the respective pasting properties in Table 11. Pasting properties describe the alterations in viscosity of a starch suspension during heating (Ai & Jane, 2016). Xanthan gum, G1XG, and the combination with milk proteins, G1XG-MP, showed the lowest viscosity whereas the combination of xanthan gum with starch, G1XG-St, had the highest viscosity. In addition, only starch-containing formulations showed pasting behaviour.

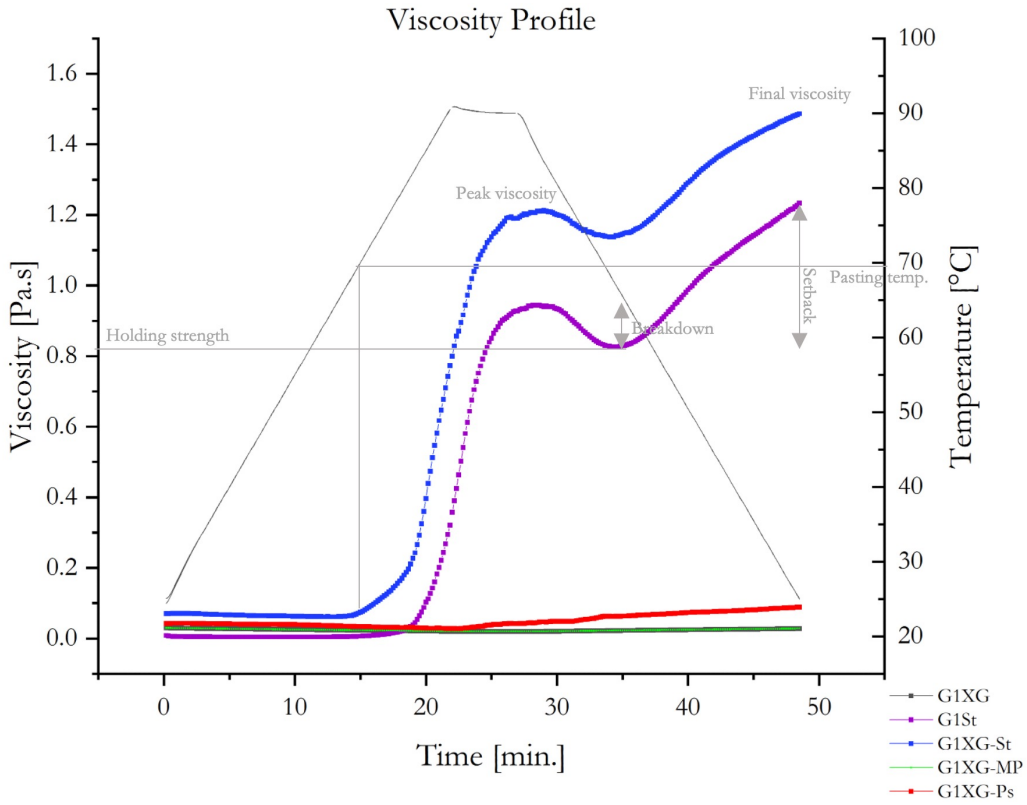

Figure 17: Apparent viscosity of G1XG, G1St and G1XG-t from 25°C to 90°C (heating rate 3°C/min.). Mean graphs are based on triplicates for G1St, G1XG-MP and on duplicates for G1XG, G1XG-Ps, G1XG-St.

Xanthan gum - starch blend:

The data in Figure 17 and Table 11 reveal a significantly lower pasting temperature for G1XG-St (70.00°C ± 0.70) than for G1St (81.20°C ± 0.32) which correlates with the microscopy pictures b) and e) in Figure 18 showing larger, swollen starch granule sizes for G1XG-St than for G1St at 70°C. Supported by Eidam et al. (1995), the thermodynamic incompatibility prevents the free movement of starch granules into xanthan gum-rich parts so that the granules accumulate around xanthan gum phases. As for the temperature sweep, the earlier disruption of starch granules due to increasing shear forces may have also resulted in significant differences in the pasting temperature between G1St and G1XG-St. This is also supported by Christianson et al. (1981) who stated that thickener increase the forces on starch granules compared to a water.

Table 11: Pasting properties for G1St and G1XG-St. Statistical analysis by means of t-test. Different letters in the same row indicate significant differences ($p < 0.05$).

Pasting properties	**G1St**	**G1XG-St**
Pasting temp. [°C]	81.20 ± 0.32^{a}	70.00 ± 0.70^{b}
Peak viscosity [Pa.s]	0.95 ± 0.20^{a}	1.21 ± 0.01^{b}
Holding strength [Pa.s]	0.83 ± 0.01^{a}	1.14 ± 0.01^{b}
Breakdown [Pa.s]	0.12 ± 0.13^{a}	0.07 ± 0.00^{b}
Final viscosity [Pa.s]	1.23 ± 0.06^{a}	1.49 ± 0.01^{b}
Setback [Pa.s]	0.41 ± 0.05^{a}	0.35 ± 0.13^{a}

The peak viscosity describes the extent to which starch granules become larger due to gelatinization before they finally disrupt (Lazaridou & Biliaderis, 2009). The higher peak viscosity of G1XG-St is reflected by larger starch granules for G1XG-St than for G1St in Figure 18 c) and f). This could be caused by the earlier onset of pasting due to xanthan gum so that the granules have more time to swell. After that, the viscosity decreased due to friction reduction and solubilization of amylose/amylopectin after final granule disruption (breakdown viscosity). Different mechanisms may have contributed to the flow inhibition regarding breakdown viscosity and overall viscosity in G1St and G1XG-St. In G1St, the amylose network and swollen starch granules can be assumed to mainly have contributed to flow inhibition. In G1XG-St the additional higher viscosity of the continuous phase caused by xanthan gum plus the greater starch granule swelling is also involved which led to a significant lower breakdown viscosity and overall higher viscosity. Also, this contributed to the significantly higher viscosity after disruption in G1XG-St (holding strength). Nevertheless, non-significant differences in the setback can be interpreted as xanthan gum having no crucial influence on the short-term retrogradation process at this concentration since setback describes the short-term retrogradation process of amylose chains aligning next to each other (Lazaridou & Biliaderis, 2009). According to the rheometry results it can be concluded that xanthan gum contributed to an overall higher viscosity of the starch system but not to an increase in network strength. However, in contrast to starch-containing formulations the mixtures of xanthan gum and psyllium or milk proteins resulted in less steep viscosity increases.

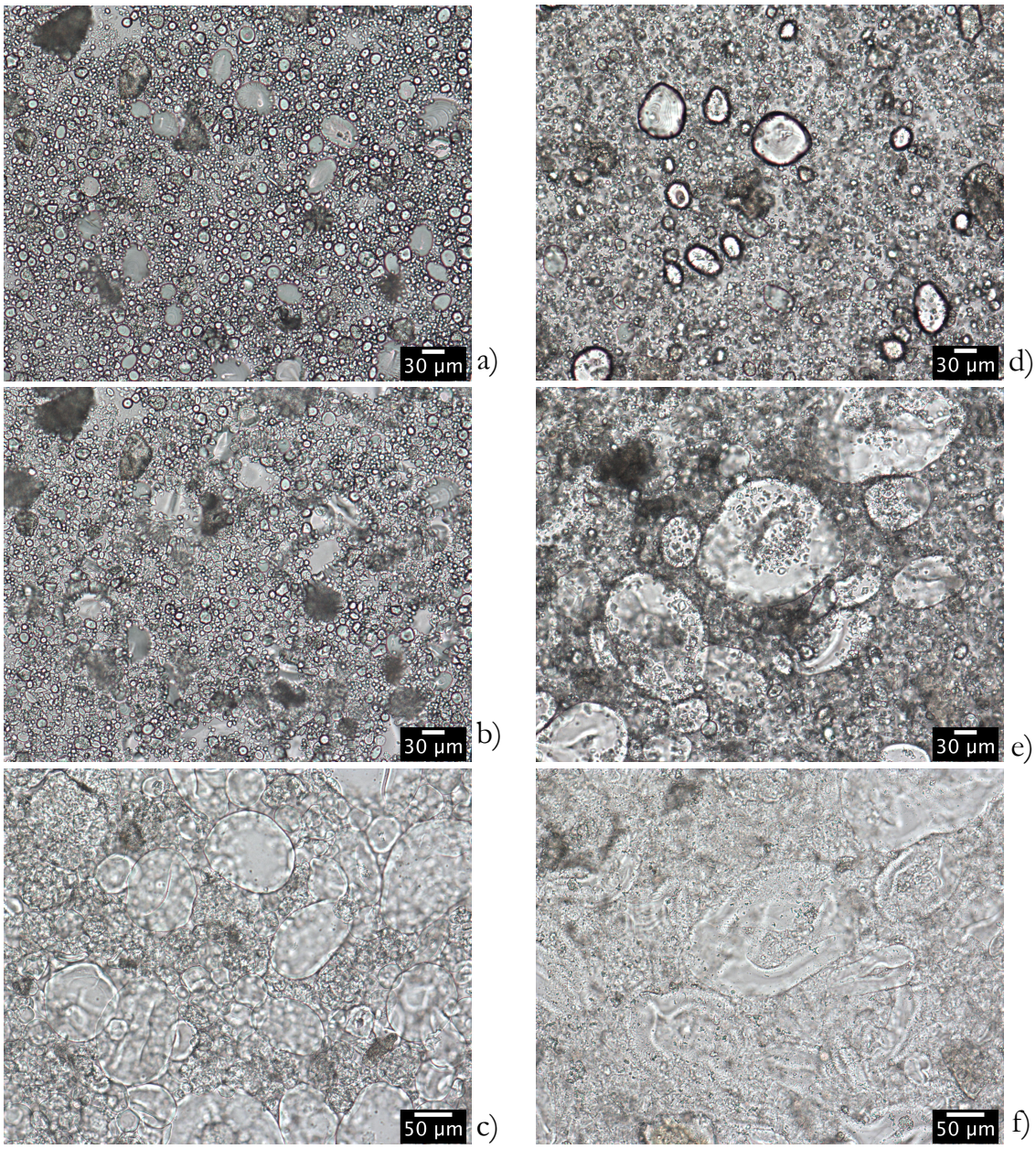

Figure 18: Microscopy of G1St and G1XG-St (20x). Left: G1St Starch at a) 25°C, b) 70°C, c) 90°C after 5 min. Right: G1XG-St Xanthan gum + Starch at d) 25°C, e) 70°C, f) 90°C after 5 min. The diameter was determined by ImageJ software.

Xanthan gum - milk proteins:

In contrast to the combination of xanthan gum with the starch blend, the apparent viscosity profile in Figure 17 of G1XG-MP shows no significant differences (Appendix C, Table 21) in viscosity which correlates with the findings of Hemar et al. (2001). This implies that milk powder had no influence on viscosity (G1XG-MP). Also, whey proteins were probably already present in the denatured state because otherwise the heating of native proteins would have resulted in a steeper viscosity increase at around 62–70°C due to protein unfolding and aggregation. However, the concentration of skim milk powder or whey proteins in this study might have been too low to result in measurable viscosity differences induced by denaturation.

Xanthan gum - psyllium:
Finally, the combination of xanthan gum and psyllium, G1XG-Ps, had a significantly higher viscosity than G1XG in Figure 17 and showed a decrease in viscosity during heating with a pronounced increase during cooling. This increase indicates shear-dependent demixing. Xanthan gum is a rather stiff molecule whereas psyllium is more flexible. During shearing, xanthan gum assumably followed the movement of the vane geometry and may have formed small xanthan gum parts. Likewise, psyllium chains probably moved also towards each other and formed a pronounced, partial viscosity.

Overall, there are limitations in the design of the rheological measurements. The apparent viscosity profile cannot be directly compared to the temperature sweep since they underly different mechanisms – the first one exerting rotation and the latter oscillation with different measuring geometries. Therefore, the storage and loss moduli cannot be directly compared to the apparent viscosity profile. Also, since the usage of measuring geometries depends on many factors of the formulations like the particle size or gel strength, different measuring devices for G1XG, G1Ps and G1XG-MP have been used in the amplitude sweep. This can result in differences in the measured values based on differences in the contact area of the measuring device to the sample and the angle of shearing. However, comparison of the moduli in the amplitude sweep with the starting moduli in the temperature sweep of the three formulations showed no differences so that the influence of different geometries can be considered insignificant for the purpose of this analysis.

To sum up, the results of the interactions between xanthan gum + starch and xanthan gum + psyllium showed an increase in viscosity and rigidity compared to xanthan gum alone. Only the interaction between xanthan gum + milk proteins did not show greater rigidity and viscosity values and thus did not provide a measurable improvement.

4.1.4 Molecular interactions and bread characteristics

Based on the results of the previous chapter, this chapter illustrates the presumed molecular interactions after heating and their implications on gluten-free bread.

Starting with the interactions between xanthan gum and starch, Figure 19 depicts a model of the continuous amylose network on the left side with amylopectin and starch granules where the starch granule walls are clearly distinguishable. The combination of xanthan gum and the starches shows larger starch granules with softened granule walls (see Figure 18 for according microscopy pictures) and amylose chains are assumed to be shifted apart by local xanthan gum parts so that a wider-meshed amylose network is created.

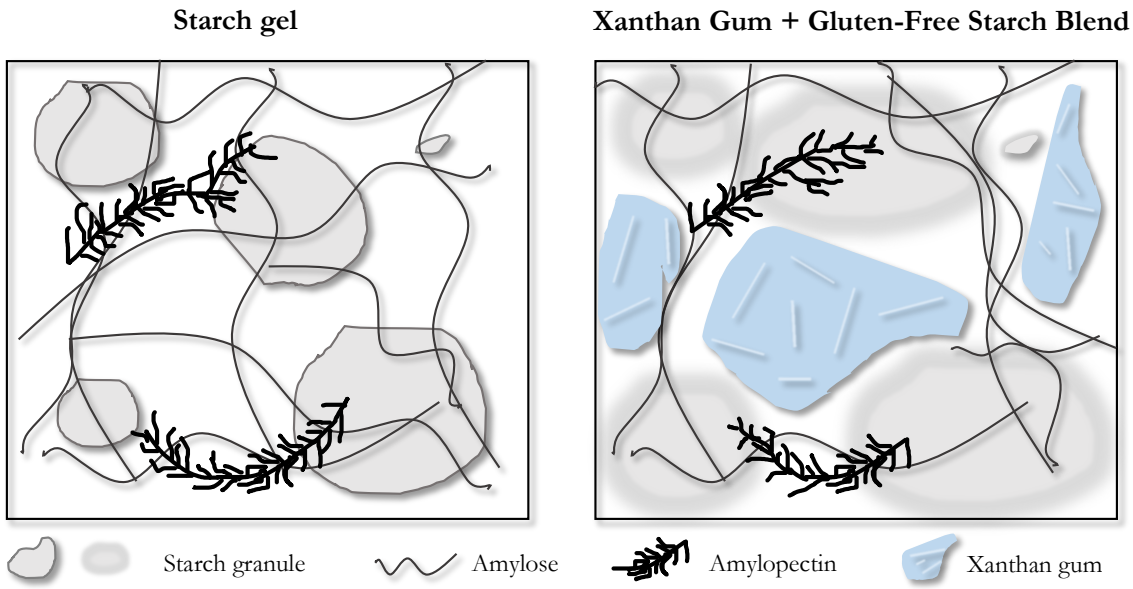

Figure 19: Illustration of the presumed molecular interactions between xanthan gum and gluten-free starches in water-salt solution after heating to 90°C and subsequent cooldown to 25°C. Note: Drawing not to scale.

Transferring these interaction models on their implications on gluten-free bread the lower pasting temperature for the G1XG-St would probably lead to earlier gelatinization of starches during baking which may influence the total baking time and baking temperature. Because of the more closely packed amylose chains crosslinks can be formed more easily which can influence the gelation rate after baking, i.e. amylose chains recrystallize faster under water expulsion which can migrate to the crust and increase retrogradation and staling rate. However, this could be counteracted by the overall higher viscosity and water binding capacity of xanthan gum leading to a probably moister, firmer bread crumb and less water migration to the crust. Also, from the increased moduli values for G1XG-St in the temperature sweep and tanδ it can be assumed that dough and bread will be firmer with xanthan gum.

Moving on with xanthan gum and milk proteins, Figure 20 presents the presumed molecular interactions. The right part of the picture depicts whey proteins hindering the complete coil–helix retransition of some xanthan gum molecules.

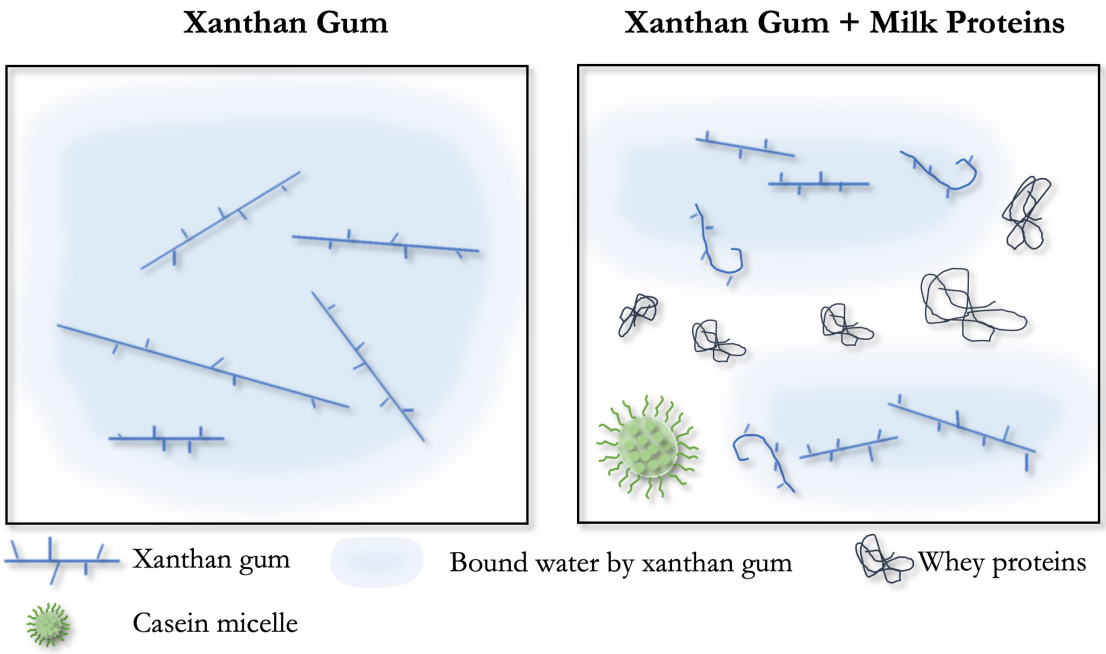

Figure 20: Illustration of the molecular interactions between xanthan gum and milk proteins. Note: Drawing not to scale.

Since the combination of xanthan gum and milk powder did not show great changes compared to xanthan gum in the previous chapter, the observed interactions may be too small to have a measurable implication on bread. This is probably due to the low milk protein concentration. Therefore, no gelling of whey proteins or viscosity increase due to water-binding has been observed as mentioned in chapter 2.4. Referring to the study conducted by Gallagher, Gormley & Arendt (2003), the viscosity of gluten-free breads with skim milk powder increased proportionally with increasing concentration of skim milk powder (0%, 3%, 6%, 9%). This again suggests that the skim milk powder concentration used in this project was too low to observe corresponding effects. In addition, the lack in viscosity increase and water-holding capacity of G1XG-MP would probably not result in additional crumb moistening or water migration reduction regarding staling. Therefore, the addition of skim milk powder as presented in this chapter would not compete for water like xanthan gum or starch in a gluten-free dough or bread. However, milk proteins in general substitute the lack of proteins due to gluten-absence in gluten-free formulations (Kenny et al., 2000). It must be noted that here only assumptions about overall interaction mechanisms of xanthan gum and milk proteins can be made since the state of milk proteins in the used skim milk powder is unknown. Nevertheless, it can be concluded that the overall rheological behaviour of the milk protein-xanthan gum mixture was xanthan-gum driven.

Lastly, Figure 21 illustrates the assumed interaction between xanthan gum and psyllium. Although psyllium polymers are considered to form a pronounced network as visible in the amplitude sweep, the mixture of xanthan gum and psyllium is not assumed to form crosslinks or increase its elastic proportion which could substitute a 3D-network like gluten in bread.

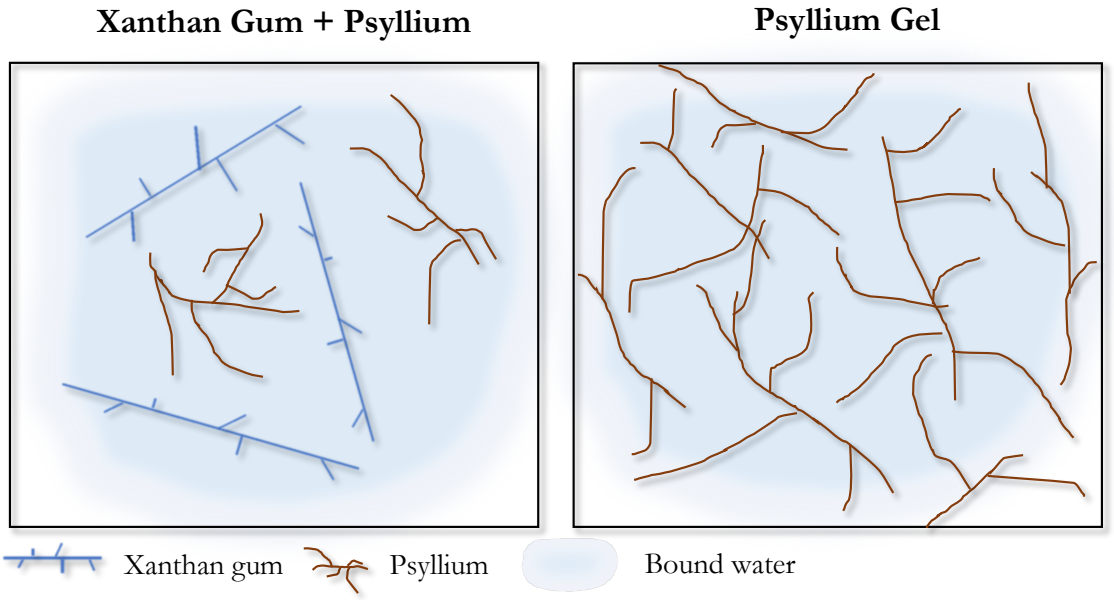

Figure 21: Illustration of the assumed molecular interactions between xanthan gum and psyllium. Note: Drawing not to scale.

However, the usage of xanthan gum + psyllium in gluten-free bread may still be favourable since the mixture can increase the overall viscosity of dough and gas cell wall thickness by a thickening effect through higher water-binding capacity. This can also increase the moisture content of the bread. Moreover, psyllium can contribute to a nutritional improvement of gluten-free bread by its high soluble fibre content.

It must be noted that the transfer from these interactions to bread properties is only conditionally valid, as the formulations are only models and consist of approximately more than 90% water which is not the case in bread formulations. Therefore, the direct influence of xanthan gum on gluten-free dough and bread was analysed in the next chapters.

To sum up, it is assumed that xanthan gum mainly interrupted the network formation of amylose and psyllium by local xanthan gum parts but increased the overall rigidity and viscosity in mixture. In combination with milk proteins, it is suggested that the milk proteins mainly interfered the formation of large xanthan gum-dominated areas. However, all these ingredients can be useful in gluten-free dough and bread for example concerning handling or nutritional benefits.

4.2 Influence of Xanthan Gum on Gluten-Free Dough

4.2.1 Kneading behaviour

G2YXG and G2Y were mixed for 27 minutes in a micromixer to analyse the optimal dough mixing time by observing the kneading behaviour in form of dough resistance over time. The optimal dough development time where dough strands can be extended to the maximum before they disrupt (cohesiveness) would have occurred as a clear maximum in the measurements. This cannot be observed for the two doughs in Appendix D (Figure 30, Figure 31) as the bandwidth of the measurement remains the same over time after adding all ingredients. This indicates that the addition of xanthan gum did not affect dough cohesiveness during mixing concerning the development of a continuous, elastic network but just increased the overall viscosity of a dough as soon as completely hydrated. Therefore, it can be concluded that G2YXG and G2Y cannot be overmixed but undermixed when e.g. starch and hydrocolloids are not properly hydrated. A proper hydrated xanthan gum is important for example concerning the moisture retention in dough and bread.

4.2.2 Moisture retention

The moisture analysis in Figure 22 presents the percentage of total gram water released from the doughs in dependence of time. The slope can be interpreted as the water release rate where both curves resemble a degressive growth over time.

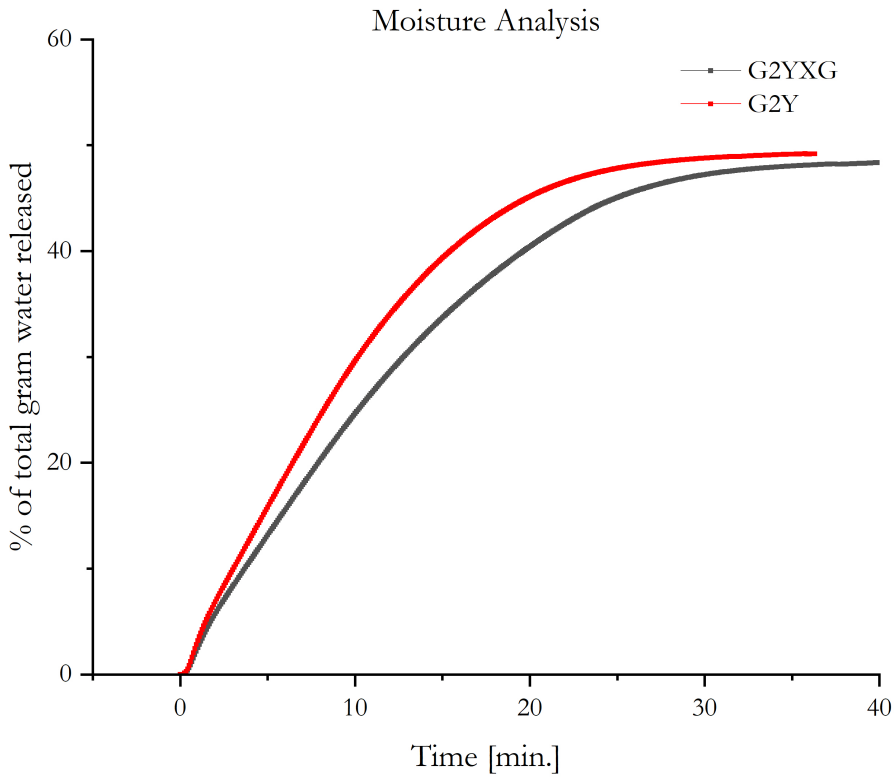

Figure 22: Moisture release of dough with xanthan gum and dough without xanthan gum. Mean graphs are based on triplicates.

Within the first ten minutes Figure 22 and Table 12 show that both curves increase sharply where G2Y shows a significantly higher slope than G2YXG. The significantly higher moisture release rate in the beginning for G2Y may be caused by a higher diffusion of water within the

dough since completed gelatinization probably has not taken place, yet which is otherwise associated with high water absorption in starch granules. Conversely, it can be assumed that G2YXG shows a lower water release rate due to -OH groups of xanthan gum forming hydrogen bonds with water molecules already at room temperature and therefore increased the water-binding capacity as well as viscosity already at the beginning which may have reduced water diffusion. However, this trend cannot be transferred to the total time of halogen drying and time until reaching the plateau value [Time (P)] probably due to progressing gelatinization of starch granules.

Table 12: Percentage of total gram water released (Moisture release) from G2YXG and G2Y (without XG) in the Halogen Moisture Analyzer. The slope refers to minute 0–10 and "Time (P)" refers to the time until the plateau value (97% of final value) was reached. "Time" refers to the time until the final value was reached.

Formulation	Moisture release [%]	Time [min.]	Slope	Time (P) [min.]
G2YXG	48.44 ± 0.15[a]	40:41 ± 2:55[a]	2.456 ± 0.245[a]	28:55 ± 2:18[a]
G2Y	49.14 ± 0.12[b]	34:17 ± 2:27[a]	2.950 ± 0.182[b]	24:10 ± 2:51[a]

The results suggest that the water bound by xanthan gum at room temperature during dough formation significantly reduced the water release rate especially in the beginning of baking. However, the bound water by xanthan gum can be later missing for the starch gelatinization during heating. The lower moisture release rate may lead to a moister bread crumb after baking and during storage, and probably affects final loaf weight. In addition, the water-holding capacity of xanthan gum may also reduce water migration in bread so that less water may migrate to the bread crust during baking. This could reduce staling during storage compared to gluten-free bread without xanthan gum (G3-).

4.2.3 Rheological properties

Rheological analysis of G2XG (Dough with XG) and G2 (Dough without XG) which did not include yeast was performed by a temperature sweep and a subsequent amplitude sweep showing that both doughs were viscoelastic solids ($G' > G''$). Figure 23 and Table 13 present the significantly higher values for G2XG compared to G2- regarding the gel strength and LVR. Overall, it shows a parallel shift of the curve pattern. The higher gel strength could be derived from the explanation for the molecular interaction between xanthan gum and starch in chapter 4.1 where the additional increase in viscosity by xanthan gum and probably the modification of starch granule swelling led to a higher rigidity. However, an increase in starch granule swelling as observed in G1XG-St is an assumption since the competition for water could also lead to more rigid starch granules due to insufficient hydration. The higher LVR for G2XG could be caused by the fact that there were more molecules in the formulation and thus the molecules were packed closer together which thereby could withstand higher strain rates.

Table 13: LVR and gel strength in the amplitude sweep for G2XG and G2-. Statistical analysis by means of a t-test. Different letters in the same row indicate significant differences ($p < 0.05$).

Formulation	**LVR ($G'_{95\%}$)**	**Gel strength (G')**
G2XG	0.37 ± 0.03^{a}	26671.25 ± 1446.40^{a}
G2-	0.25 ± 0.01^{b}	11805.45 ± 188.16^{b}

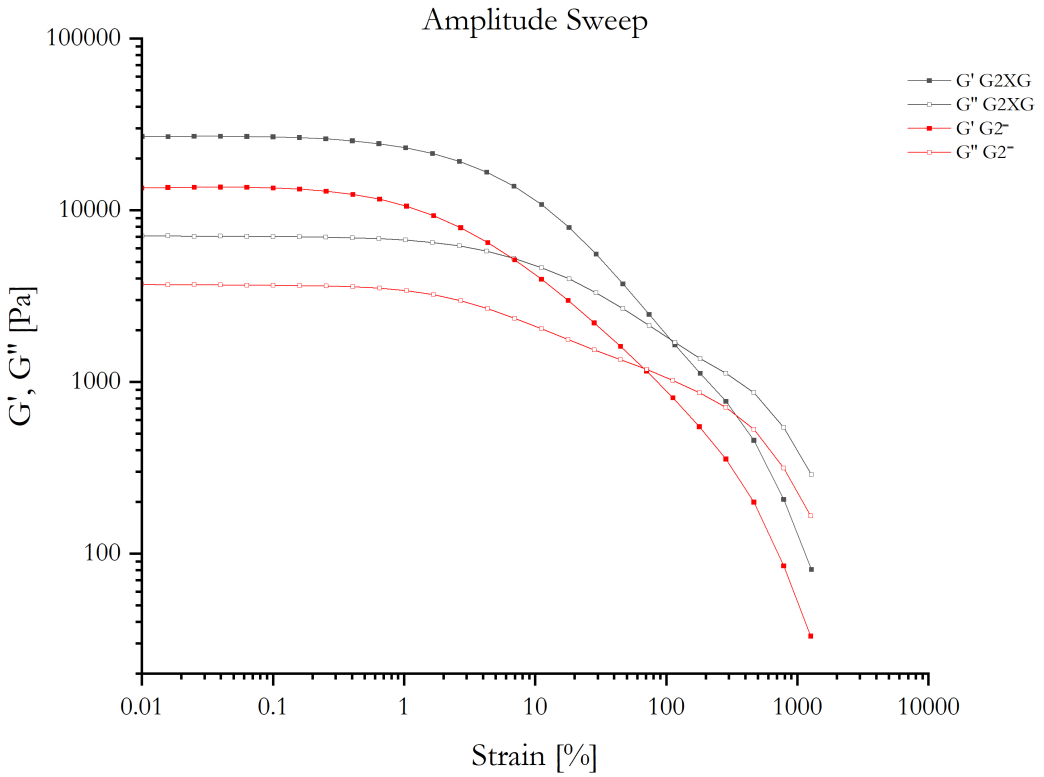

Figure 23: Amplitude sweep of the doughs G2XG and G2- without yeast at 25°C. Mean graphs are based on triplicates.

Outstanding is that the overall curve pattern in Figure 23 resembles the curve pattern of a gluten-containing wheat model dough as shown in Figure 24. Also, the gel strength of G2XG and G2- is almost as high as the doughs in Figure 24 with 80–90% starch and 10–20% gluten.

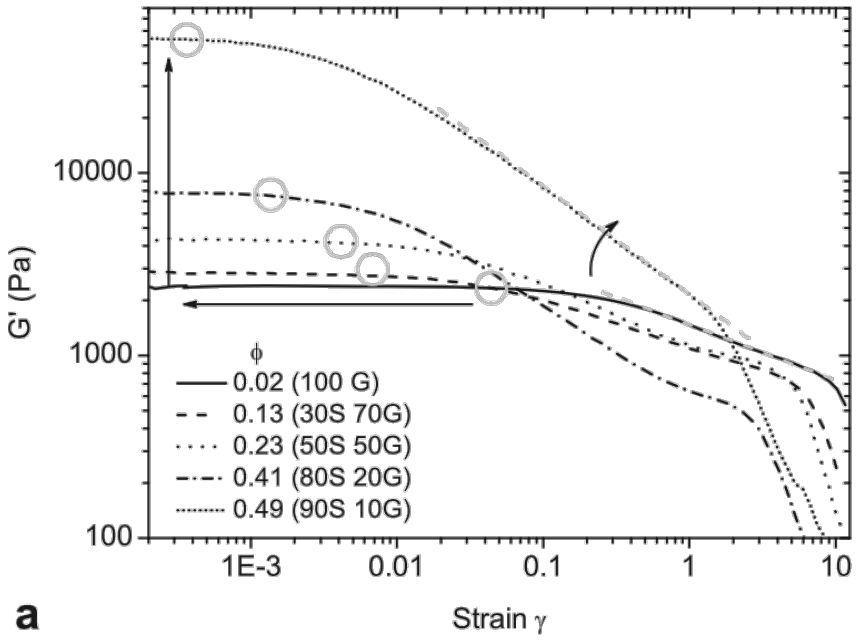

Figure 24: Amplitude sweep of a model dough with different ratios of starch (S) and gluten (G) (Schiedt et al., 2013).

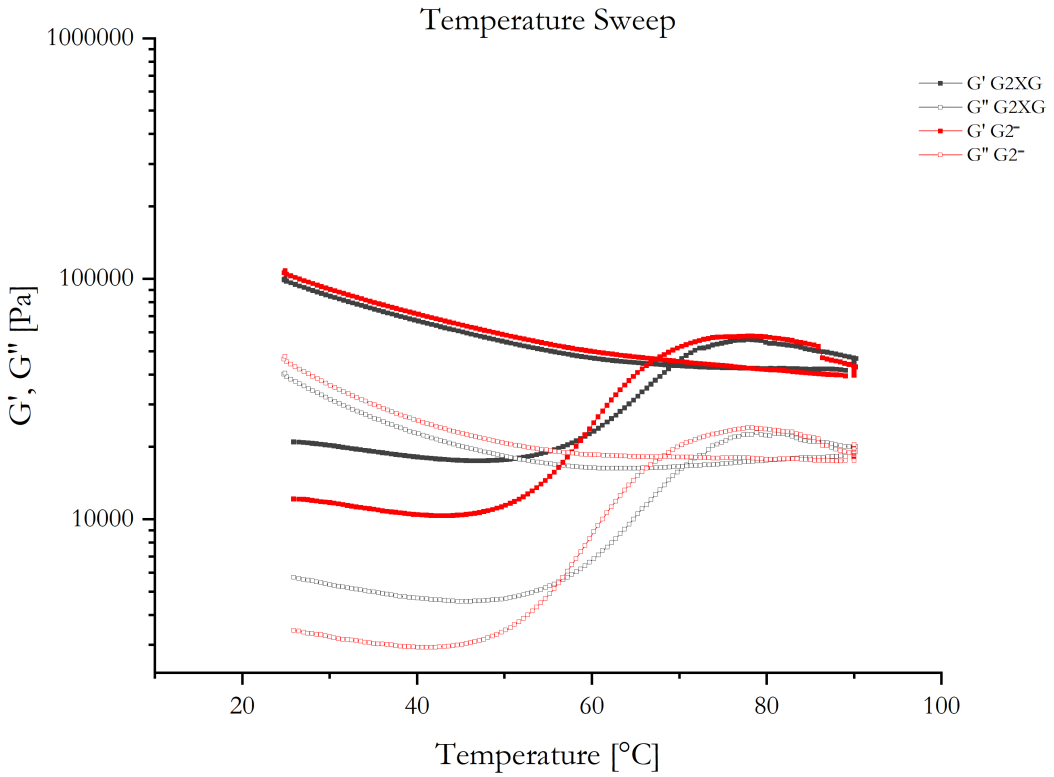

Figure 25: Temperature Sweep of the doughs G2XG and G2- without yeast at 25°C. Mean graphs are based on triplicates for G2- and on duplicates for G2XG.

The curve pattern in Figure 25 for G2XG and G2- resemble broadly the curves of G1St and G1XG-St in Figure 15. Therefore, the explanation of the curve pattern concerning the gelatinization process in chapter 4.1 can be broadly adopted as the doughs mainly consist of starch. As for G1XG-St xanthan gum addition increased the rigidity of G2XG compared to G2- until the beginning of starch gelatinization at around 50°C due to its water-holding capacity which was also observed by Upadhyay, Ghosal & Mehra (2012) in wheat flour dough. However, the storage and loss moduli for the doughs between 50–80°C did not increase that much compared to the model system in G1St and G1XG-St. This may emphasize the difference between the doughs and the model systems concerning water availability and the higher content of solids contributing to less free movement of water molecules to the starch granules. During cooling, the curves resemble each other reaching approximately the same rigidity where the increase in the storage modulus can be caused for example by the short-term retrogradation of amylose and xanthan gum's temperature dependence to some extent. In addition, stiffening of milk protein aggregates by crosslinks during heating and subsequent cooling could also contribute to the increase in rigidity as observed by Lavoisier, Vilgis & Aguilera (2019).

For bread it is important, that there is no imbalance in the ratio between elasticity and viscosity since the elastic proportion is important for gas holding and film development whereas the viscous proportion makes the dough more flexible so that gas can expand (Crockett, Ie & Vodovotz, 2011; Lazaridou et al., 2007). Looking at tanδ for the temperature sweep in Appendix E (Figure 32), tanδ <1 describes the doughs as solid-like. The addition of xanthan gum shifted the balance between elastic and viscous proportions slightly to the viscous proportions of the dough. The reason for this may be that xanthan gum is not able to form a film by an elastic network but increases viscosity by its high water-holding capacity. The slight increase in the viscous proportion and the associated bread property as mentioned in the beginning of the paragraph may indicate a higher gas expansion and thus a higher bread loaf volume which will be investigated in chapter 4.3.1. However, the temperature sweep shows only minor differences in the storage modulus between G2XG and G2- during cooling so that the decrease in elasticity in the tanδ (Appendix E, Figure 32) had very little effect on overall rigidity.

4.2.4 Dough texture

Figure 26 presents the one-cycle compression of the dough with xanthan gum (G2YXG) and without xanthan gum (G2Y) where G2YXG shows a significantly higher stiffness than G2Y (Appendix E, Table 23). The increase in stiffness of G2YXG may be caused by xanthan gum incorporating more polymers to the dough and increasing the viscosity by binding more water as mentioned for the moisture analysis in chapter 4.2.2.

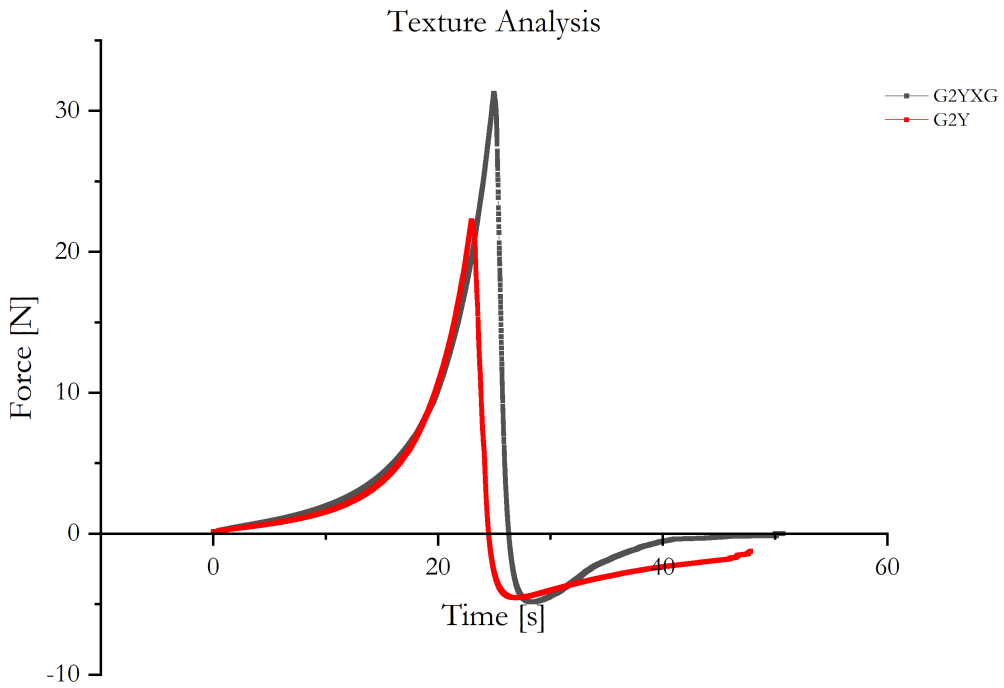

Figure 26: Texture analysis of G2YXG and G.2.2 (Dough without XG). One-cycle compression. Mean graphs are based on triplicates.

Adhesiveness and stringiness were not measurable for G2Y because the dough did not separate from the stamp as can be seen in Figure 26. Looking at Figure 27, G2Y still attaches to both plates and thus can be expanded more than G2YXG which detached from the probe.

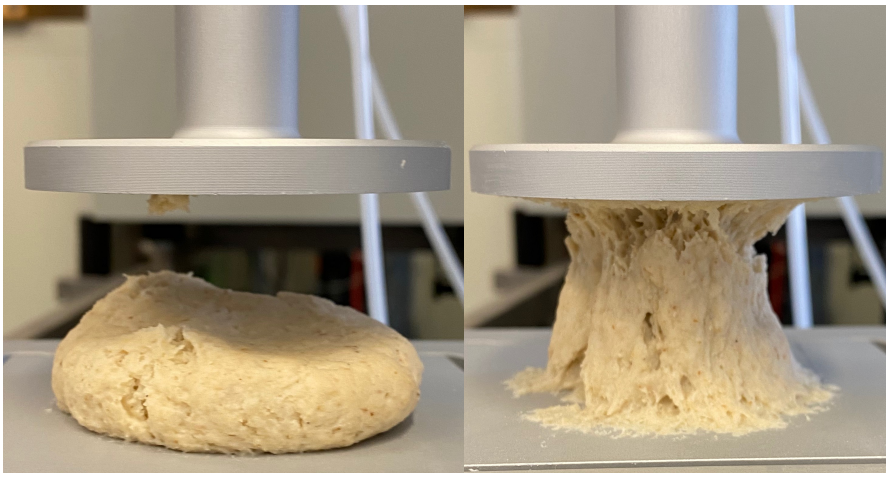

Figure 27: Once-cycle compression texture analysis of G2YXG (left) and G2Y (right).

According to Mezger (2016), the detachment of G2YXG from the probe shows its higher cohesiveness represented in less stringiness probably caused by a higher viscosity. Although stringiness could not have been measured for G2Y, Figure 26 suggests that the distance between the negative peak until reaching 0 N is smaller for G2YXG than for G2Y. In contrast, the attachment of G2Y to both measuring plates indicates lower cohesiveness but higher adhesiveness represented by longer dough strands of G2Y. Again, as the direct measurement of adhesiveness is not possible for G2Y the area under the x-axis in Figure 26 seems to be greater than for G2YXG. An assumption for the higher adhesiveness may be the higher water

ratio in G2Y compared to the water-binding ability of xanthan gum at room temperature which may influence cohesion. Therefore, it is presumed that the lower water ratio in G2YXG resulted in a more cohesive dough than G2Y (Faubion & Hoseney, 1990). In addition, fat is also considered to strongly contribute to adhesiveness since it was found to occur to a higher extent on the dough surface (Velzen et al., 2003). Since fat can be found in both formulations it is assumed that the unbound water in G2Y affected adhesiveness.

From the greater stiffness of the dough with xanthan gum, it may be possible to conclude that the final bread will be firmer than the bread without xanthan gum. Further implications may be a moister bread with a lower water release rate in the beginning of heating which may lead to less water migration to the crust. Moreover, these results are important for bread manufacturers regarding e. g. workability, moulding (pouring, modelling) or pumping during dough processing. For example, a stickier dough is more difficult to remove from machine walls which may even increase food waste due to leftovers on machine walls or higher cleaning costs due to longer cleaning times. In addition, xanthan gum's pseudoplastic behaviour as mentioned in chapter 2.5.2 may also positively affect dough processing due to its shear-thinning property.

To sum up, the viscoelastic behaviour of both gluten-free doughs can be described as viscoelastic solid where xanthan gum functions as a moisturizer and thickener. The water-holding ability of xanthan gum can affect dough rheology by increasing dough rigidity until the start of starch gelatinization. Also, significant differences in moisture release and dough texture concerning stiffness emphasize the mentioned function of xanthan gum.

4.3 Influence of Xanthan Gum on Gluten-Free Bread

4.3.1 Bread specific volume

One hour after taking the bread out of the oven the bread loaf weight was determined which showed significant differences between the bread with xanthan gum (G3XG) and without xanthan gum (G3-; Table 14). The baking loss was 16.60% for G3- and 14.68% for G3XG. This is in accordance with Therdthai & Zhou (2014) who connected a 10–20% baking loss to water release. Referring to the moisture analysis in chapter 4.2.2, this difference in weight might be attributable to the water-holding capacity of xanthan gum which also resulted in a moister dough. However, as G3XG also contained 1.2% more dry matter than G3- and as it was not possible to scrape the whole dough from the bowl due to the stickiness, there is a limitation here. The previously mentioned assumption of xanthan gum contributing to a higher gas expansion and increase in volume based on a minor increase in dough tanδ values (chapter 4.2.3; Appendix E, Figure 32) cannot be confirmed by the results in Table 14. This increase might have been too low to be measurably detected in volume differences. In addition, the high viscosity provided by xanthan gum probably even counteracted gas expansion so that no statistically significant differences in bread volume have been observed. Another reason could be the lack of enough adhesion (chapter 4.2.4) to the bread tin which could have supported dough rise of G3XG. Significant differences in bread specific volume were not found in this study but are in line with the results of other studies conducted by Hager et al. (2012), Encina-Zelada et al. (2018) and Sciarini et al. (2012).

Table 14: Rapeseed Displacement. Statistical analysis by means of a t-test. Different letters in the same row indicate statistically significant differences ($p < 0.05$). Based on quadruplicates.

Formulation	Weight [g]	Volume [ml]	Bread Specific Volume $\left[\frac{ml}{g}\right]$	Baking Loss [%]
G3XG	431.94 ± 2.57[a]	853.00 ± 33.01[a]	1.98 ± 0.08[a]	14.68 ± 0.00[a]
G3-	417.09 ± 2.16[b]	878.50 ± 32.55[a]	2.09 ± 0.10[a]	16.60 ± 0.00[b]

4.3.2 Bread texture

The texture profile analysis for bread without crust in Figure 28 and Table 15 reveals significant higher crumb firmness of bread with xanthan gum (G3XG) compared to bread without xanthan gum (G3-).

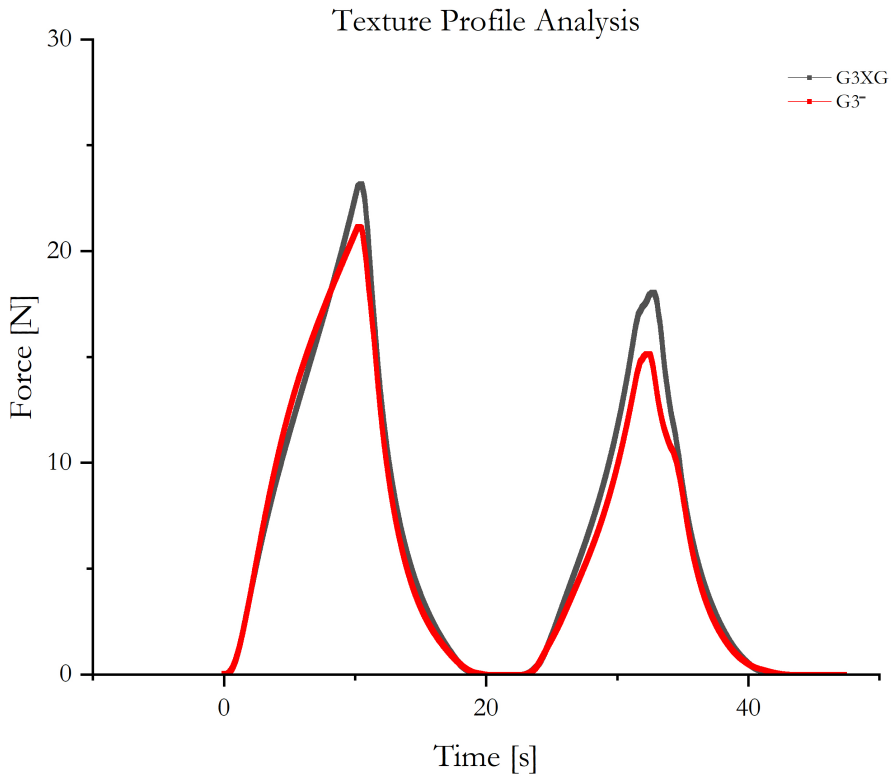

Figure 28: Texture Profile Analysis of bread with and without xanthan gum. Mean graphs are based on measuring three slices from the centre of three replicates (breads) respectively.

Table 15: TPA Parameter Bread without crust. Statistical analysis by means of a t-test. Different letters in the same row indicate statistically significant differences ($p < 0.05$). Resilience and cohesiveness are dimensionless.

Formulation	Firmness [N]	Resilience	Springiness [%]	Cohesiveness	Chewiness [N]
G3XG	23.71 ± 0.45^{a}	0.47 ± 0.19^{a}	98.00 ± 1.57^{a}	0.70 ± 0.01^{a}	16.27 ± 0.46^{a}
G3-	21.92 ± 0.14^{b}	0.39 ± 0.17^{b}	98.42 ± 1.18^{a}	0.61 ± 0.01^{b}	13.09 ± 0.22^{b}

The significantly higher firmness for G3XG confirms the derived bread properties from the temperature sweep (Figure 14) and tanδ (Figure 15) of G1XG-St in chapter 4.1.4 and the results of the dough texture analysis in chapter 4.2.4 showing greater firmness values for dough with xanthan gum. Accordingly, the explanation for xanthan gum incorporating more dry matter to the matrix which needs to be compressed additionally also applies. Rosell, Rojas & Benedito de Barber (2001) argued that the higher crumb firmness is also the result of thicker gas cell walls due to the thickening effect of xanthan gum. This probably requires a higher pressure of gas cells to expand. Therefore, the first bite during the chewing process demands more force to compress the gluten-free bread with xanthan gum.

The overall springiness can be related to the viscoelastic property of the doughs. The non-significant difference in springiness may be explained by the inability of xanthan gum to develop a continuous, elastic network which is associated to withstand deformation by recovery. This also agrees with Armero & Collar (1997) who related elasticity to springiness. Therefore, there is no difference in the extent to which G3XG and G3- recover to their original size in the mouth. Although there is no significant difference in springiness, the resilience as a measure of how fast the bread springs back shows significantly higher values for the bread with xanthan gum. Resilience can be related to the physical quantity momentum $\vec{p}$ [Ns]. The higher values refer to the higher molecular movement during the recovery which is caused by the higher mass due to the addition of xanthan gum and its water binding ability. A reduction in resilience values over time combined with an increase in firmness indicates the progression of retrogradation (Kadan et al., 2001). This suggests, that G3- with its lower resilience values is more prone to starch retrogradation than G3XG.

The significant higher cohesiveness for G3XG confirms the observations in the dough texture analysis in Figure 26. The higher cohesiveness may result from additional water binding by hydrogen bonds between xanthan gum and water molecules which increased the dough viscosity and bread firmness. It is normally associated with a higher specific bread volume (Lazaridou & Biliaderis, 2009) which has not been observed in this study (Table 14), probably because of the lack of gluten and inability of xanthan gum to form an elastic network. When eating bread, the higher cohesiveness of G3XG means that a higher extent of compression needs to be applied with the teeth to disrupt the bread but it also forms a bolus easily which can be swallowed more readily than crumbles which are characterized by lower cohesiveness values and demand less compression (Civille & Szczesniak, 1973; Onyango et al., 2011). Therefore, according to Encina-Zelada et al. (2018) higher cohesion is preferred because less cohesive breads tend to crumble which was also observed for G3- in this degree project.

Since bread is a soft solid, chewiness was used instead of gumminess. Chewiness is a secondary parameter and the product of firmness, cohesiveness and springiness of which firmness has the highest influence (Armero & Collar, 1997). Since there were also significant differences in firmness, the present doughs also show a significant difference in chewiness. The higher values for G3XG indicate a longer time to chew the food until it can be swallowed compared to G3- which probably is the result of a higher solids content and the aforementioned factors concerning firmness, cohesiveness and springiness.

Depending on how much firmness is desired, firmness values could be lowered by varying the gluten-free starch composition in the bread which currently consists mainly of rice starch. Breads consisting of only rice starch have been observed to result in a firmer crumb, lower specific volume and being more susceptible to retrogradation (Kadan et al., 2001). Another option would be the slight decrease in xanthan gum addition since the crumb firmness can increase with higher xanthan gum levels (Lazaridou et al., 2007). Lastly, adjusting the water amount could also lead to a softer bread since it acts as a plasticizer.

Overall, the TPA results show that the gluten-free bread texture of G3XG especially regarding firmness was more affected by the amount of polymers incorporated by xanthan gum than by the plasticizing effect of the bound water. However, these results can differ according to the parameters and probe speeds applied.

4.3.3 Moisture retention of bread

After the bread was cooled to room temperature a moisture analysis was performed with the upper crust, bread crumb from the centre of the slice and a whole slice without the crust. The results in Table 16 show with 21.93% ± 1.00 moisture a significantly higher moisture content in the crust for G3- than for G3XG with 19.13% ± 2.05. To this, also the slope within 0–200s of G3- was significantly higher (Appendix G, Table 24). No significant differences were found between the crumb and slice of the breads and the according slopes.

Table 16: Moisture analysis of bread in percent. Statistical analysis by means of a t-test. Different letters in the same row indicate statistically significant differences ($p < 0.05$). Based on quadruplicates.

Formulation	Crust	Crumb	Slice
G3XG	19.13 ± 2.05[a]	47.54 ± 0.54[a]	47.09 ± 1.19[a]
G3-	21.93 ± 1.00[b]	48.60 ± 0.09[b]	48.37 ± 0.62[a]

The higher moisture in the crust for G3- can be a sign for a higher water migration or diffusion from the centre to the crust as explained in 4.2.2. This can lead to an increased staling rate as shown by the significantly higher slope as a measure of the moisture release rate for the crust. Consequently, G3- may dry out and harden faster than G3XG. Xanthan gum may delay this migration by its water-binding ability and overall thickening effect reflected in the significant lower crust moisture content since water has a plasticizing effect which can therefore slow down crystallization of amylose and amylopectin. The result confirms the assumptions made for bread based on the molecular interaction between xanthan gum and starch in chapter 4.1.4. However, it must be pointed out that the model systems for the first research question consisted mainly out of water which is not the case in dough and bread. Therefore, the assumptions in chapter 4.1.4 can be correct but caution must be paid when transferring to other food systems.

The lower crumb moisture for G3XG was unexpected since the dough with xanthan gum in 4.2.2 had a significant higher moisture. However, the minor difference of approximately 1% may not be caused by systematic error but may originate in the processing for example in temperature irregularities during the baking process in the oven or the time span between single measurements. Here, an analysis of the water activity could provide further information on this.

4.3.4 Visual observations

Figure 29 shows the gluten-free bread with xanthan gum (G3XG) and the gluten-free bread without xanthan gum (G3-) which were baked in a house hold convection oven at 175°C for 50 minutes. Photos from the breads were taken from the aerial view, cross-section and as a macro shot of the crumb.

Figure 29: Gluten-free bread. Above (1–3): G3XG Bread with xanthan gum 1) Loaf from above, 2) Cross-section, 3) Crumb. Below (4–6): Bread without xanthan gum (G3-) 4) Loaf from above, 5) Cross-section, 6) Crumb.

It must be noted that the lighting conditions in Figure 29, 1) were not optimal so there is a shadow over G3XG. In addition, both gluten-free breads cracked during baking indicating inefficient extensibility at the given environmental parameters. This can be counteracted for example by adjusting proofing and/or baking conditions. Looking at the cross-section 5) and 6) in Figure 29, the TPA results for G3- concerning firmness are reflected in the more aerated and open crumb structure of G3- which is considered to lead to a softer bread. The more compact crumb structure in G3XG, Figure 29, 2–3, resulted in a firmer crumb as compared to G3-. In addition, the smaller gas bubbles in G3XG can be the result of thicker gas cell walls due to xanthan gum which may impair gas cell expansion as previously mentioned. Crockett, Ie & Vodovotz (2011) also observed a harder bread crumb with xanthan gum which they attributed to thicker gas cell walls because the firm dough was unable to expand sufficiently. However, this property can be also advantageous concerning the limitation of gas diffusion. It is noticeable that the crumb structure in picture 2) in Figure 29 resembles the observations for a gluten-free bread with 1.5% xanthan gum and a water amount of 90% flour weight in the study conducted by Encina-Zelada et al. (2018). With increasing water content to 110% flour weight, these authors were able to increase the gas cells size of gluten-free bread.

Since further trials about the comparison between different hydrocolloids in gluten-free bread with the same recipe but different conditions conducted by Jungbunzlauer Ladenburg GmbH showed visual differences regarding bread volume between a reference and a bread with 1.2% xanthan gum, care must be taken under which conditions xanthan gum in gluten-free breads will result in improvements. For example, the ratio between the mass of dough and the bread tin volume can be a factor as well as the ratio of water since dough rheology is affected by

water. Further factors include the amount of incorporated xanthan gum, proofing conditions and baking temperature since the last two parameters were not optimized in this study. Also, it must be considered, that the present dough consisted of a starch blend having different gelatinization temperatures and granule sizes. Thus, the rheological behaviour and viscosity are affected by both the proportion of starches and their granule size. To this, the exact ratios of the starch blend used in each sample can differ.

Finally, it can be considered if the ratio of milk powder can be reduced because the interaction of xanthan gum and milk proteins in chapter 4.1 showed no improvement regarding rigidity and viscosity. In addition, people with celiac disease are also prone to have a lactose intolerance due to an intact mucosa so that a removal of milk powder can increase the target group (Hamer, 2005).

4.4 Conclusion

The results show that xanthan gum increased the rigidity and viscosity when combined with the gluten-free starch blend in solution. Likewise, a higher rigidity and viscosity was observed for the mixture of xanthan gum and psyllium whereas no effect of xanthan gum was found in the mixture with milk proteins. The analysis of the viscoelastic dough behaviour revealed the influence of xanthan gum on the increase in dough stiffness and moisture retention. Outstanding is the similarity of the rheological behaviour of the dough with xanthan gum to that of a gluten-containing model dough. The resulting bread properties showed that some assumptions based on the molecular interactions in solution and dough analysis could be confirmed. The bread with xanthan gum was firmer and the water binding-ability of the hydrocolloid yielded less water migration to the bread crust compared to the formulation without xanthan gum. Therefore, xanthan gum can be an option to increase the viscosity of gluten-free doughs and to reduce water migration to the bread crust.

5. Outlook

Future work could consist of analysing the water activity in the gluten-free dough and bread to estimate the free water under the influence of xanthan gum. Also, a sensory analysis would be helpful to find out if xanthan gum significantly affects bread quality characteristic like flavour development or firmness. Based on these results, variations concerning the starch composition, xanthan gum ratio and water content could be used to modify texture properties. Apart from this, the texture properties could be also altered by adjusting manufacturing parameters like proofing time and baking conditions. If needed, the flavour of the gluten-free bread could be intensified by the addition of bread spices like caraway, aniseed, fennel or coriander. Also, since the rheological results of xanthan gum with milk powder were not striking baking trials without the addition of milk powder could be performed. Lastly, a comparison for example in texture between the xanthan gum-containing dough/bread and dough/bread with gluten could be performed to quantify the extent to which xanthan gum contributes to mimic gluten-bread. Here, however, the difficulty would be to create comparable recipes.

It is hoped that these findings will support the development of gluten-free bakery products and help to define optimal conditions in which xanthan gum can fully develop its potential.

References

Abbaszadeh, A. H. et al. (2019). The influence of charge on the multiple thermal transitions observed in xanthan. *Food Hydrocolloids*, *97*, pp. 1-8. https://doi.org/https://doi.org/10.1016/j.foodhyd.2019.105184.

Ai, Y. & Jane, J. l. (2016). Starch: Structure, Property, and Determination. In B. Caballero, P. M. Finglas & F. Toldrá (Eds.), *Encyclopedia of Food and Health* (pp. 165-174). Academic Press. https://doi.org/https://doi.org/10.1016/B978-0-12-384947-2.00657-7.

Ako, K. et al. (2009). Micro-phase separation explains the abrupt structural change of denatured globular protein gels on varying the ionic strength or the pH. *Soft Matter*, *5*(20), pp. 4033-4041. https://doi.org/10.1039/B906860K.

Al-Assaf, S. et al. (2003). Molecular weight, tertiary structure, water binding and colon behaviour of ispaghula husk fibre. *Proceedings of the Nutrition Society*, *62*(1), pp. 211-216. https://doi.org/10.1079/PNS2002216.

Anema, S. G. (2007). Role of κ-Casein in the Association of Denatured Whey Proteins with Casein Micelles in Heated Reconstituted Skim Milk. *Journal of Agricultural and Food Chemistry*, *55*(9), pp. 3635-3642. https://doi.org/10.1021/jf062734m.

Anema, S. G. (2020). The whey proteins in milk: Thermal denaturation, physical interactions, and effects on the functional properties of milk. In M. Boland & H. Singh (Eds.), *Milk Proteins* (3rd ed., pp. 325-384). Academic Press. https://doi.org/https://doi.org/10.1016/B978-0-12-815251-5.00009-8.

Anema, S. G. & Klostermeyer, H. (1997). Heat-Induced, pH-Dependent Dissociation of Casein Micelles on Heating Reconstituted Skim Milk at Temperatures below 100 °C. *Journal of Agricultural and Food Chemistry*, *45*(4), pp. 1108-1115. https://doi.org/10.1021/jf960507m.

Anton, A. A. & Artfield, S. D. (2008). Hydrocolloids in gluten-free breads: a review. *International Journal of Food Sciences and Nutrition*, *59*(1), pp. 11-23. https://doi.org/10.1080/09637480701625630.

Anton Paar GmbH. (n.d.-a). *Amplitude sweeps*. Retrieved 12.06.2021 from https://wiki.anton-paar.com/en/amplitude-sweeps/.

Anton Paar GmbH. (n.d.-b). *Basics of rheology*. Retrieved 10.06.2021 from https://wiki.anton-paar.com/en/basics-of-rheology/#oscilliation-tests-and-viscoelasticity.

Anton Paar GmbH. (n.d.-c). *Temperature-dependent behavior (oscillation)*. Retrieved 10.06.2021 from https://wiki.anton-paar.com/en/temperature-dependent-behavior-oscillation/.

Appell, M. et al. (2018). Amino Acids and Proteins. In *Principles of Food Chemistry* (4th ed., pp. 117-164). Springer International Publishing. https://doi.org/https://doi.org/10.1007/978-3-319-63607-8.

Arendt, E. K. et al. (2008). Gluten-free breads. In E. K. Arendt & F. Dal Bello (Eds.), *Gluten-Free Cereal Products and Beverages* (pp. 289-320). Academic Press. https://doi.org/https://doi.org/10.1016/B978-012373739-7.50015-0.

Armero, E. & Collar, C. (1997). Texture properties of formulated wheat doughs. Relationships with dough and bread technological quality. *Zeitschrift für Lebensmitteluntersuchung und -Forschung A*, *204*(2), pp. 136-145. https://doi.org/10.1007/s002170050050.

Augustin, M. A., Clarke, P. T. & Craven, H. (2003). Powdered Milk. Characteristics of Milk Powders. In B. Caballero (Ed.), *Encyclopedia of Food Sciences and Nutrition* (2nd ed., pp. 4703-4711). Academic Press. https://doi.org/https://doi.org/10.1016/B0-12-227055-X/00956-1.

Barnes, H. A., Hutton, J. F. & Walters, K. (1989a). Linear Viscoelasticity. In H. A. Barnes, J. F. Hutton & K. Walters (Eds.), *Rheology Series* (Vol. 3, pp. 37-54). Elsevier. https://doi.org/https://doi.org/10.1016/B978-0-444-87469-6.50007-X.

Barnes, H. A., Hutton, J. F. & Walters, K. (1989b). Viscosity. In H. A. Barnes, J. F. Hutton & K. Walters (Eds.), *Rheology Series* (Vol. 3, pp. 11-35). Elsevier. https://doi.org/https://doi.org/10.1016/B978-0-444-87469-6.50006-8.

Belitz, H. D., Grosch, W., Schieberle, P. (2009). *Food Chemistry* (4th ed.). Springer, Berlin, Heidelberg. https://doi.org/https://doi.org/10.1007/978-3-540-69934-7.

Belorio, M. & Gómez, M. (2020). Psyllium: a useful functional ingredient in food systems. *Critical Reviews in Food Science and Nutrition*, pp. 1-12. https://doi.org/10.1080/10408398.2020.1822276.

BeMiller, J. N. (2019a). Polysaccharides: Properties. In J. N. BeMiller (Ed.), *Carbohydrate Chemistry for Food Scientists* (3rd ed., pp. 103-157). AACC International Press. https://doi.org/https://doi.org/10.1016/B978-0-12-812069-9.00005-4.

BeMiller, J. N. (2019b). Xanthan. In J. N. BeMiller (Ed.), *Carbohydrate Chemistry for Food Scientists* (3rd ed., pp. 261-269). AACC International Press. https://doi.org/https://doi.org/10.1016/B978-0-12-812069-9.00011-X.

Bercea, M. & Morariu, S. (2020). Real-time monitoring the order-disorder conformational transition of xanthan gum. *Journal of Molecular Liquids*, *309*, pp. 1-8. https://doi.org/https://doi.org/10.1016/j.molliq.2020.113168.

Bourne, M. (1990). Basic Priniciples of Food Texture Measurement. In H. Faridi & J. M. Faubion (Eds.), *Dough Rheology and Baked Product Texture* (1st ed.). Springer, Boston, MA. https://doi.org/https://doi-org.ejp.mpip-mainz.mpg.de/10.1007/978-1-4613-0861-4.

Brunchi, C.-E. et al. (2019). Chain conformation of xanthan in solution as influenced by temperature and salt addition. *Journal of Molecular Liquids*, *287*, pp. 1-8. https://doi.org/https://doi.org/10.1016/j.molliq.2019.111008.

Brunchi, C.-E., Morariu, S. & Bercea, M. (2014). Intrinsic viscosity and conformational parameters of xanthan in aqueous solutions: Salt addition effect. *Colloids and Surfaces B: Biointerfaces*, *122*, pp. 512-519. https://doi.org/https://doi.org/10.1016/j.colsurfb.2014.07.023.

Caggianiello, G., Kleerebezem, M. & Spano, G. (2016). Exopolysaccharides produced by lactic acid bacteria: from health-promoting benefits to stress tolerance mechanisms. *Applied Microbiology and Biotechnology*, *100*(9), pp. 3877-3886. https://doi.org/10.1007/s00253-016-7471-2.

Callet, F., Milas, M. & Rinaudo, M. (1987). Influence of acetyl and pyruvate contents on rheological properties of xanthan in dilute solution. *International Journal of Biological Macromolecules*, *9*(5), pp. 291-293. https://doi.org/https://doi.org/10.1016/0141-8130(87)90068-7.

Carr, C. W. (1956). Studies on the binding of small ions in protein solutions with the use of membrane electrodes. VI. The binding of sodium and potassium ions in solutions of various proteins. *Archives of Biochemistry and Biophysics*, *62*(2), pp. 476-484. https://doi.org/https://doi.org/10.1016/0003-9861(56)90146-1.

Cereals & Grains Association. (2001). *AACC Method 10-05.01: Guidelines for Measurement of Volume by Rapeseed Displacement.* https://www.cerealsgrains.org/resources/Methods/Pages/10BakingQuality.aspx.

Chawla, R. & Patil, G. R. (2010). Soluble Dietary Fiber. *Comprehensive Reviews in Food Science and Food Safety*, *9*(2), pp. 178-196. https://doi.org/https://doi.org/10.1111/j.1541-4337.2009.00099.x.

Chazeau, L., Milas, M. & Rinaudo, M. (1995). Conformations of Xanthan in Solution: Analysis by Steric Exclusion Chromatography. *International Journal of Polymer Analysis and Characterization*, *2*(1), pp. 21-29. https://doi.org/10.1080/10236669508233892.

Christianson, D. D. et al. (1981). Gelatinization of wheat starch as modified by xanthan gum, guar gum, and cellulose gum. *Cereal Chemistry*, *58*(6), pp. 513-517. https://doi.org/https://handle.nal.usda.gov/10113/26085.

Civille, G. V. & Szczesniak, A. S. (1973). Guidelines to training a texture profile panel. *Journal of Texture Studies*, *4*(2), pp. 204-223. https://doi.org/https://doi.org/10.1111/j.1745-4603.1973.tb00665.x.

Clare Mills, E. N. et al. (1990). Characterization of a panel of monoclonal anti-gliadin antibodies. *Journal of Cereal Science*, *11*(2), pp. 89-101. https://doi.org/https://doi.org/10.1016/S0733-5210(09)80113-6.

Côté, G. L. & Finkenstadt, V. L. (2008). A history of carbohydrate research at athe USDA Laboratory in Peoria, Illinois. *Bulletin for the history of chemistry*, *33*(2), pp. 103-111. https://doi.org/http://acshist.scs.illinois.edu/bulletin_open_access/v33-2/v33-2%20p103-111.pdf.

Coultate, T. (2002). Polysaccharides. In T. P. Coultate (Ed.), *Food: The Chemistry of its Components* (4th ed., pp. 41-72). The Royal Society of Chemistry. https://doi.org/10.1039/9781847550903-00041.

Coultate, T. (2009). *Food: The Chemistry of its Components* (5th ed.). The Royal Society of Chemistry.

Coupland, J. N. (2014). *An Introduction to the Physical Chemistry of Food*. Springer, New York, NY. https://doi.org/https://doi.org/10.1007/978-1-4939-0761-8.

Crockett, R., Ie, P. & Vodovotz, Y. (2011). How do xanthan and hydroxypropyl methylcellulose individually affect the physicochemical properties in a model gluten-free dough? *Journal of Food Science*, *76*(3), pp. E274-E282. https://doi.org/10.1111/j.1750-3841.2011.02088.x.

Cui, S. W. & Wang, Q. (2005). Functional Properties of Carbohydrates: Polysaccharide Gums. In Y. H. Hui & F. Sherkat (Eds.), *Handbook of Food Science, Technology, and Engineering - 4 Volume Set* (1st ed., pp. 4-1 - 4-18). CRC Press. https://doi.org/https://doi.org/10.1201/b15995.

Dalgleish, D. G., Senaratne, V. & Francois, S. (1997). Interactions between α-Lactalbumin and β-Lactoglobulin in the Early Stages of Heat Denaturation. *Journal of Agricultural and Food Chemistry*, *45*(9), pp. 3459-3464. https://doi.org/10.1021/jf970113a.

Ebermann, R. & Elmadfa, I. (2011). Tierische Lebensmittel. In *Lehrbuch Lebensmittelchemie und Ernährung* (pp. 279-336). Springer Vienna. https://doi.org/10.1007/978-3-7091-0211-4_11.

Edwards, W. P. (2007). Science. In *The Science of Bakery Products* (pp. 11-55). The Royal Society of Chemistry. https://doi.org/10.1039/9781847557797-00011.

Eidam, D. et al. (1995). Formation of Maize Starch Gels Selectively Regulated by the Addition of Hydrocolloids. *Starch - Stärke*, *47*(10), pp. 378-384. https://doi.org/https://doi.org/10.1002/star.19950471003.

Eliasson, A.-C. (2006). *Carbohydrates in Food*. CRC Press LLC. http://ebookcentral.proquest.com/lib/lund/detail.action?docID=262273

Encina-Zelada, C. R. et al. (2018). Combined effect of xanthan gum and water content on physicochemical and textural properties of gluten-free batter and bread. *Food Research International*, *111*, pp. 544-555. https://doi.org/https://doi.org/10.1016/j.foodres.2018.05.070.

Farahnaky, A. et al. (2010). The impact of concentration, temperature and pH on dynamic rheology of psyllium gels. *Journal of Food Engineering*, *100*(2), pp. 294-301. https://doi.org/https://doi.org/10.1016/j.jfoodeng.2010.04.012.

Faubion, J. M. & Hoseney, R. C. (1990). The Viscoelastic Properties of Wheat Flour Doughs. In H. Faridi & J. M. Faubion (Eds.), *Dough Rheology and Baked Product Texture* (pp. 29-66). Springer US. https://doi.org/10.1007/978-1-4613-0861-4_2.

Fischer, M. H. et al. (2004). The gel-forming polysaccharide of psyllium husk (Plantago ovata Forsk). *Carbohydrate Research*, *339*(11), pp. 2009-2017. https://doi.org/https://doi.org/10.1016/j.carres.2004.05.023.

Fitzpatrick, P. et al. (2013). Control of the properties of xanthan/glucomannan mixed gels by varying xanthan fine structure. *Carbohydrate Polymers*, *92*(2), pp. 1018-1025. https://doi.org/https://doi.org/10.1016/j.carbpol.2012.10.049.

Fox, P. F. (2003). Milk Proteins: General and Historical Aspects. In P. F. Fox & P. L. H. McSweeney (Eds.), *Advanced Dairy Chemistry-1 Proteins* (pp. 1-48). Springer US. https://doi.org/10.1007/978-1-4419-8602-3_1.

Fox, P. F. et al. (2015). *Dairy Chemistry and Biochemistry* (2nd ed.). Springer, Cham. https://doi.org/https://doi.org/10.1007/978-3-319-14892-2.

Franco, E. A. N. et al. (2020). Psyllium (Plantago ovata Forsk): From evidence of health benefits to its food application. *Trends in Food Science & Technology*, *96*, pp. 166-175. https://doi.org/https://doi.org/10.1016/j.tifs.2019.12.006.

Fratelli, C. et al. (2018). Modelling the effects of psyllium and water in gluten-free bread: An approach to improve the bread quality and glycemic response. *Journal of Functional Foods*, *42*, pp. 339-345. https://doi.org/https://doi.org/10.1016/j.jff.2018.01.015.

Galindo, E. & Albiter, V. (1996). High-Yield Recovery of Xanthan by Precipitation with Isopropyl Alcohol in a Stirred Tank. *Biotechnology Progress*, *12*(4), pp. 540-547. https://doi.org/https://doi.org/10.1021/bp9600445.

Gallagher, E., Gormley, T. R. & Arendt, E. K. (2003). Crust and crumb characteristics of gluten free breads. *Journal of Food Engineering*, *56*(2-3), pp. 153-161. https://doi.org/https://doi.org/10.1016/S0260-8774(02)00244-3.

Gallagher, E., Gormley, T. R. & Arendt, E. K. (2004). Recent advances in the formulation of gluten-free cereal-based products. *Trends in Food Science & Technology*, *15*(3), pp. 143-152. https://doi.org/https://doi.org/10.1016/j.tifs.2003.09.012.

Galván, Z. R. N. et al. (2018). Rheological Properties of Aqueous Dispersions of Xanthan Gum Containing Different Chloride Salts Are Impacted by both Sizes and Net Electric Charges of the Cations. *Food Biophysics*, *13*(2), pp. 186-197. https://doi.org/10.1007/s11483-018-9524-9.

Gan, Z. et al. (1989). Some effects of non-endosperm components of wheat and of added gluten on wholemeal bread microstructure. *Journal of Cereal Science*, *10*(2), pp. 81-91. https://doi.org/https://doi.org/10.1016/S0733-5210(89)80037-2.

García-Ochoa, F. et al. (2000). Xanthan gum: production, recovery, and properties. *Biotechnology Advances*, *18*(7), pp. 549-579. https://doi.org/https://doi.org/10.1016/S0734-9750(00)00050-1.

Gibiński, M. et al. (2006). Thickening of sweet and sour sauces with various polysaccharide combinations. *Journal of Food Engineering*, *75*(3), pp. 407-414. https://doi.org/https://doi.org/10.1016/j.jfoodeng.2005.04.054.

Goff, D. (2014). Milk Proteins: Functional Ingredients in Food. In P. Williams & G. Phillips (Eds.), *Gums and Stabilisers for the Food Industry 17: The Changing Face of Food Manufacture: The Role of Hydrocolloids* (pp. 11-18). Royal Society of Chemistry. https://doi.org/ https://doi.org/10.1039/9781782621300-00011.

Goff, H. D. & Guo, Q. (2020). The Role of Hydrocolloids in the Development of Food Structure. In F. Spyropoulos, A. Lazidis & I. Norton (Eds.), *Handbook of Food Structure Development* (pp. 1-28). The Royal Society of Chemistry. https://doi.org/10.1039/9781788016155-00001.

Goulding, D. A., Fox, P. F. & O'Mahony, J. A. (2020). Milk proteins: An overview. In M. Boland & H. Singh (Eds.), *Milk Proteins* (3rd ed., pp. 21-98). Academic Press. https://doi.org/https://doi.org/10.1016/B978-0-12-815251-5.00002-5.

Gras, P. W. et al. (2001). Gluten protein functionality in wheat flour processing: a review. *Australian Journal of Agricultural Research*, *52*(12), pp. 1311-1323. https://doi.org/https://doi.org/10.1071/AR01068.

Gras, P. W., Carpenter, H. C. & Anderssen, R. S. (2000). Modelling the Developmental Rheology of Wheat-Flour Dough using Extension Tests. *Journal of Cereal Science*, *31*(1), pp. 1-13. https://doi.org/https://doi.org/10.1006/jcrs.1999.0293.

Grubbs, F. E. (1950). Sample Criteria for Testing Outlying Observations. *The Annals of Mathematical Statistics*, *21*(1), pp. 27-58, 32. https://doi.org/ https://doi.org/10.1214/aoms/1177729885.

Guo, Q. et al. (2009). Microstructure and rheological properties of psyllium polysaccharide gel. *Food Hydrocolloids*, *23*(6), pp. 1542-1547. https://doi.org/https://doi.org/10.1016/j.foodhyd.2008.10.012.

Hager, A.-S. et al. (2012). Investigation of product quality, sensory profile and ultrastructure of breads made from a range of commercial gluten-free flours compared to their wheat counterparts. *European Food Research and Technology*, *235*(2), pp. 333-344. https://doi.org/10.1007/s00217-012-1763-2.

Hamer, R. J. (2005). Coeliac Disease: Background and biochemical aspects. *Biotechnology Advances*, *23*(6), pp. 401-408. https://doi.org/https://doi.org/10.1016/j.biotechadv.2005.05.005.

Haque, A., Morris, E. R. & Richardson, R. K. (1994). Polysaccharide substitutes for gluten in non-wheat bread. *Carbohydrate Polymers*, *25*(4), pp. 337-344. https://doi.org/https://doi.org/10.1016/0144-8617(94)90060-4.

Haque, A., Richardson, R. K. & Morris, E. R. (1993). Xanthan-like „weak gel" rheology from dispersions of ispaghula seed husk. *Carbohydrate Polymers*, *22*(4), pp. 223-232. https://doi.org/https://doi.org/10.1016/0144-8617(93)90124-M.

Hemar, Y. et al. (2001). Viscosity, microstructure and phase behavior of aqueous mixtures of commercial milk protein products and xanthan gum. *Food Hydrocolloids*, *15*(4), pp. 565-574. https://doi.org/https://doi.org/10.1016/S0268-005X(01)00077-7.

Herzog, M. H., Francis, G. & Clarke, A. (2019). ANOVA. In M. H. Herzog, G. Francis & A. Clarke (Eds.), *Understanding Statistics and Experimental Design : How to Not Lie with Statistics* (pp. 67-82). Springer International Publishing. https://doi.org/10.1007/978-3-030-03499-3_6.

Hines, M. E. & Foegeding, E. A. (1993). Interactions of α-lactalbumin and bovine serum albumin with β-lactoglobulin in thermally induced gelation. *Journal of Agricultural and Food Chemistry*, *41*(3), pp. 341-346. https://doi.org/10.1021/jf00027a001.

Houben, A., Höchstötter, A. & Becker, T. (2012). Possibilities to increase the quality in gluten-free bread production: an overview. *European Food Research and Technology*, *235*(2), pp. 195-208. https://doi.org/10.1007/s00217-012-1720-0.

Huber, K., McDonald, A. & BeMiller, J. N. (2005). Carbohydrate Chemistry. In Y. H. Hui & F. Sherkat (Eds.), *Handbook of Food Science, Technology, and Engineering - 4 Volume Set* (1st ed., pp. 1-1 - 1-23). CRC Press. https://doi.org/https://doi.org/10.1201/b15995.

Izydorczyk, M. S. (2009). Arabinoxylans. In G. O. Phillips & P. A. Williams (Eds.), *Handbook of Hydrocolloids* (2nd ed., pp. 653-692). Woodhead Publishing. https://doi.org/https://doi.org/10.1533/9781845695873.653.

Jansson, P.-E., Kenne, L. & Lindberg, B. (1975). Structure of the extracellular polysaccharide from *xanthomonas campestris*. *Carbohydrate Research*, *45*(1), pp. 275-282. https://doi.org/https://doi.org/10.1016/S0008-6215(00)85885-1.

Kadan, R. S. et al. (2001). Texture and other Physicochemical Properties of Whole Rice Bread. *Journal of Food Science*, *66*(7), pp. 940-944. https://doi.org/https://doi.org/10.1111/j.1365-2621.2001.tb08216.x.

Kalpić, D., Hlupić, N. & Lovrić, M. (2011). Student's t-Tests. In M. Lovric (Ed.), *International Encyclopedia of Statistical Science* (pp. 1559-1563). Springer Berlin Heidelberg. https://doi.org/10.1007/978-3-642-04898-2_641.

Kang, K. S. & Pettitt, D. J. (1993). Xanthan, Gellan, Welan and rhamsan. In R. L. Whistler & J. N. Bemiller (Eds.), *Industrial Gums* (3rd ed., pp. 341-397). Academic Press. https://doi.org/https://doi.org/10.1016/B978-0-08-092654-4.50017-6.

Kasapis, S. (2005). Composition and Structure-Function Relationships in Gums. In Y. H. Hui & F. Sherkat (Eds.), *Handbook of Food Science, Technology, and Engineering - 4 Volume Set* (1st ed., pp. 92-91 - 92-19). CRC Press. https://doi.org/https://doi.org/10.1201/b15995.

Kelly, A. L., O'Connell, J. E. & Fox, P. F. (2003). Manufacture and Properties of Milk Powders. In P. F. Fox & P. L. H. McSweeney (Eds.), *Advanced Dairy Chemistry-1 Proteins* (pp. 1027-1061). Springer US. https://doi.org/10.1007/978-1-4419-8602-3_29.

Kenny, S. et al. (2000). Incorporation of dairy ingredients into wheat bread: effects on dough rheology and bread quality. *European Food Research and Technology*, *210*(6), pp. 391-396. https://doi.org/10.1007/s002170050569.

Lavoisier, A., Vilgis, T. A. & Aguilera, J. M. (2019). Effect of cysteine addition and heat treatment on the properties and microstructure of a calcium-induced whey protein cold-set gel. *Current Research in Food Science*, *1*, pp. 31-42. https://doi.org/https://doi.org/10.1016/j.crfs.2019.10.001.

Lazaridou, A. & Biliaderis, C. G. (2009). Gluten-Free Doughs: Rheological Properties, Testing Procedures – Methods and Potential Problems. In *Gluten-Free Food Science and Technology* (pp. 52-82). https://doi.org/https://doi.org/10.1002/9781444316209.ch5.

Lazaridou, A. et al. (2007). Effects of hydrocolloids on dough rheology and bread quality parameters in gluten-free formulations. *Journal of Food Engineering*, *79*(3), pp. 1033-1047. https://doi.org/10.1016/j.jfoodeng.2006.03.032.

Levine, H. & Finley, J. W. (2018). Texture. In J. M. deMan, J. W. Finley, W. J. Hurst & C. Y. Lee (Eds.), *Principles of Food Chemistry* (4th ed.). Springer, Cham.

Mandala, I. G. & Palogou, E. D. (2003). Effect of preparation conditions and starch/xanthan concentration on gelation process of potato starch systems. *International Journal of Food Properties*, *6*(2), pp. 311-328. https://doi.org/10.1081/JFP-120017818.

Mariotti, M. et al. (2009). The role of corn starch, amaranth flour, pea isolate, and Psyllium flour on the rheological properties and the ultrastructure of gluten-free doughs. *Food Research International*, *42*(8), pp. 963-975. https://doi.org/https://doi.org/10.1016/j.foodres.2009.04.017.

McGee, H. (2004). *On Food and Cooking: The Science and Lore of the Kitchen*. Scribner.

Melton, L. D., Mindt, L. & Rees, D. A. (1976). Covalent structure of the extracellular polysaccharide from Xanthomonas campestris: evidence from partial hydrolysis studies. *Carbohydrate Research*, *46*(2), pp. 245-257. https://doi.org/https://doi.org/10.1016/S0008-6215(00)84296-2.

Mettler-Toledo GmbH. (2016). *Method Collection. Food Industry. Moisture Methods*. Retrieved 01.07.2021 from https://www.mt.com/de/de/home/library/applications/laboratory-weighing/moisture-content-in-food.html.

Mezger, T. G. (2014). *Angewandte Rheologie*. Anton Paar GmbH.

Mezger, T. G. (2016). *Das Rheologie Handbuch: Für Anwender von Rotations- und Oszillations-Rheometern*. Vincentz Network.

Milas, M., Reed, W. F. & Printz, S. (1996). Conformations and flexibility of native and re-natured xanthan in aqueous solutions. *International Journal of Biological Macromolecules*, *18*(3), pp. 211-221. https://doi.org/https://doi.org/10.1016/0141-8130(95)01080-7.

Milas, M. & Rinaudo, M. (1986). Properties of xanthan gum in aqueous solutions: Role of the conformational transition. *Carbohydrate Research*, *158*, pp. 191-204. https://doi.org/https://doi.org/10.1016/0008-6215(86)84017-4.

Mohammad, K. S. & Fox, P. F. (1987). Heat induced microstructural changes in casein micelles before and after heat coagulation. *New Zealand Journal of Dairy Science and Technology*, *22*(3), pp. 191 - 204. https://doi.org/https://eurekamag.com/research/005/551/005551230.php.

Moreno, R. (2001). Rheology. In K. H. J. Buschow, R. W. Cahn, M. C. Flemings, B. Ilschner, E. J. Kramer, S. Mahajan & P. Veyssière (Eds.), *Encyclopedia of Materials: Science and Technology* (pp. 8192-8196). Elsevier. https://doi.org/https://doi.org/10.1016/B0-08-043152-6/01468-6.

Morris, E. R. (2019). Ordered conformation of xanthan in solutions and "weak gels": Single helix, double helix – or both? *Food Hydrocolloids*, *86*, pp. 18-25. https://doi.org/https://doi.org/10.1016/j.foodhyd.2017.11.036.

Ngemakwe, P. N., Le Roes-Hill, M. & Jideani, V. (2015). Advances in gluten-free bread technology. *Food Science and Technology International*, *21*(4), pp. 256-276. https://doi.org/10.1177/1082013214531425.

Niba, L. (2005). Carbohydrates: Starch. In Y. H. Hui & F. Sherkat (Eds.), *Handbook of Food Science, Technology, and Engineering - 4 Volume Set* (1st ed., pp. 3-1 - 3-17). CRC Press. https://doi.org/https://doi.org/10.1201/b15995.

Nie, S., Cui, S. W. & Xie, M. (2018). Psyllium Polysaccharide. In S. Nie, S. W. Cui & M. Xie (Eds.), *Bioactive Polysaccharides* (pp. 395-443). Academic Press. https://doi.org/https://doi.org/10.1016/B978-0-12-809418-1.00008-3.

Nie, S.-P. et al. (2014). Review of the Physicochemical Properties and Structural Characteristics of Psyllium and its Relative Bioactivity. In *Gums and Stabilisers for the Food Industry 17: The Changing Face of Food Manufacture: The Role of Hydrocolloids* (pp. 79-89). The Royal Society of Chemistry. https://doi.org/10.1039/9781782621300-00079.

Nordqvist, D. & Vilgis, T. A. (2011). Rheological Study of the Gelation Process of Agarose-Based Solutions. *Food Biophysics*, *6*(4), pp. 450-460. https://doi.org/10.1007/s11483-011-9225-0.

O'Mahony, J. A. & Fox, P. F. (2013). Milk Proteins: Introduction and Historical Aspects. In P. L. H. McSweeney & P. F. Fox (Eds.), *Advanced Dairy Chemistry: Volume 1A: Proteins: Basic Aspects* (4th ed., pp. 43-85). Springer US. https://doi.org/10.1007/978-1-4614-4714-6_2.

Onyango, C. et al. (2011). Modification of gluten-free sorghum batter and bread using maize, potato, cassava or rice starch. *LWT - Food Science and Technology*, *44*(3), pp. 681-686. https://doi.org/https://doi.org/10.1016/j.lwt.2010.09.006.

Palaniraj, A. & Jayaraman, V. (2011). Production, recovery and applications of xanthan gum by Xanthomonas campestris. *Journal of Food Engineering*, *106*(1), pp. 1-12. https://doi.org/https://doi.org/10.1016/j.jfoodeng.2011.03.035.

Park, J. M. et al. (1992). Effects of protein charge heterogeneity in protein-polyelectrolyte complexation. *Macromolecules*, *25*(1), pp. 290-295. https://doi.org/10.1021/ma00027a047.

Pawar, H. & Varkhade, C. (2014). Isolation, characterization and investigation of Plantago ovata husk polysaccharide as superdisintegrant. *International Journal of Biological Macromolecules*, *69*, pp. 52-58. https://doi.org/https://doi.org/10.1016/j.ijbiomac.2014.05.019.

Perten Instruments. (n.d.-a). *Perten Instruments Method Description TVT Method 01-03.02.* .

Perten Instruments. (n.d.-b). *Perten Instruments Method Description TVT Method 03-01.02.* .

Preichardt, L. D. et al. (2011). The role of xanthan gum in the quality of gluten free cakes: improved bakery products for coeliac patients. *International Journal of Food Science & Technology*, *46*(12), pp. 2591-2597. https://doi.org/https://doi.org/10.1111/j.1365-2621.2011.02788.x.

Rahman, M. S. et al. (2021). Measurement of Instrumental Texture Profile Analysis (TPA) of Foods. In M. S. Khan & M. S. Rahman (Eds.), *Techniques to Measure Food Safety and Quality: Microbial, Chemical, and Sensory* (pp. 427-465). Springer International Publishing. https://doi.org/10.1007/978-3-030-68636-9_17.

Rao, M. A. (2014). *Rheology of Fluid, Semisolid, and Solid Foods: Principles and Applications* (3rd ed.). Springer, Boston, MA. https://doi.org/https://doi.org/10.1007/978-1-4614-9230-6.

Rosell, C. M., Rojas, J. A. & Benedito de Barber, C. (2001). Influence of hydrocolloids on dough rheology and bread quality. *Food Hydrocolloids*, *15*(1), pp. 75-81. https://doi.org/https://doi.org/10.1016/S0268-005X(00)00054-0.

Rüegg, M., Moor, U. & Blanc, B. (1977). A calorimetric study of the thermal denaturation of whey proteins in simulated milk ultrafiltrate. *Journal of Dairy Research*, *44*(3), pp. 509-520. https://doi.org/10.1017/S002202990002046X.

Ryan, K. N. et al. (2012). Stability and mechanism of whey protein soluble aggregates thermally treated with salts. *Food Hydrocolloids*, *27*(2), pp. 411-420. https://doi.org/https://doi.org/10.1016/j.foodhyd.2011.11.006.

Saha, D. & Bhattacharya, S. (2010). Hydrocolloids as thickening and gelling agents in food: a critical review. *Journal of Food Science and Technology*, *47*(6), pp. 587-597. https://doi.org/10.1007/s13197-010-0162-6.

Sahin, S. & Sumnu, S. G. (2006). *Physical Properties of Food* (1st ed.). Springer, New York. https://doi.org/https://doi.org/10.1007/0-387-30808-3.

Schiedt, B. et al. (2013). Short- and Long-Range Interactions Governing the Viscoelastic Properties during Wheat Dough and Model Dough Development. *Journal of Texture Studies*, *44*(4), pp. 317-332. https://doi.org/https://doi.org/10.1111/jtxs.12027.

Schuppan, D., Junker, Y. & Barisani, D. (2009). Celiac Disease: From Pathogenesis to Novel Therapies. *Gastroenterology*, *137*(6), pp. 1912-1933. https://doi.org/https://doi.org/10.1053/j.gastro.2009.09.008.

Sciarini, L. S. et al. (2010). Effect of hydrocolloids on gluten-free batter properties and bread quality. *International Journal of Food Science & Technology*, *45*(11), pp. 2306-2312. https://doi.org/10.1111/j.1365-2621.2010.02407.x.

Sciarini, L. S. et al. (2012). Incorporation of several additives into gluten free breads: Effect on dough properties and bread quality. *Journal of Food Engineering*, *111*(4), pp. 590-597. https://doi.org/https://doi.org/10.1016/j.jfoodeng.2012.03.011.

Sherman, P. (1969). A Texture Profile of Foodstuffs Based upon Well-defined Rheological Properties. *Journal of Food Science*, *34*(5), pp. 458-462. https://doi.org/https://doi.org/10.1111/j.1365-2621.1969.tb12804.x.

Singh, H. & Flanagen, J. (2005). Milk Proteins. In Y. H. Hui & F. Sherkat (Eds.), *Handbook of Food Science, Technology, and Engineering - 4 Volume Set* (1st ed., pp. 26-21 - 26-23). CRC Press. https://doi.org/https://doi.org/10.1201/b15995.

Singh, H. & Havea, P. (2003). Thermal Denaturation, Aggregation and Gelation of Whey Proteins. In P. F. Fox & P. L. H. McSweeney (Eds.), *Advanced Dairy Chemistry—1 Proteins: Part A / Part B* (pp. 1261-1287). Springer US. https://doi.org/10.1007/978-1-4419-8602-3_34.

Sosulski, F. W. & Cadden, A. M. (1982). Composition and Physiological Properties of Several Sources of Dietary Fiber. *Journal of Food Science*, *47*(5), pp. 1472-1477. https://doi.org/https://doi.org/10.1111/j.1365-2621.1982.tb04964.x.

Stathopoulos, C. E. (2008). Dairy-based ingredients. In E. K. Arendt & F. Dal Bello (Eds.), *Gluten-Free Cereal Products and Beverages* (pp. 217-236). Academic Press. https://doi.org/https://doi.org/10.1016/B978-012373739-7.50012-5.

Sworn, G. (2009). Xanthan gum. In G. O. Phillips & P. A. Williams (Eds.), *Handbook of Hydrocolloids* (2nd ed., pp. 186-203). Woodhead Publishing. https://doi.org/https://doi.org/10.1533/9781845695873.186.

Taggart, P. & Mitchell, J. R. (2009). Starch. In G. O. Phillips & P. A. Williams (Eds.), *Handbook of Hydrocolloids* (2nd ed., pp. 108-141). Woodhead Publishing. https://doi.org/https://doi.org/10.1533/9781845695873.108.

Therdthai, N. & Zhou, W. (2014). Manufacture. In *Bakery Products Science and Technology* (pp. 473-488). https://doi.org/https://doi.org/10.1002/9781118792001.ch27.

Upadhyay, R., Ghosal, D. & Mehra, A. (2012). Characterization of bread dough: Rheological properties and microstructure. *Journal of Food Engineering*, *109*(1), pp. 104-113. https://doi.org/https://doi.org/10.1016/j.jfoodeng.2011.09.028.

Vaclavik, V. A., Christian, E., W. & Campbell, T. (2021). *Essentials of Food Science* (5th ed.). Springer, cham. https://doi.org/https://doi.org/10.1007/978-3-030-46814-9.

Vardhanabhuti, B. & Allen Foegeding, E. (2008). Effects of dextran sulfate, NaCl, and initial protein concentration on thermal stability of β-lactoglobulin and α-lactalbumin at neutral pH. *Food Hydrocolloids*, *22*(5), pp. 752-762. https://doi.org/https://doi.org/10.1016/j.foodhyd.2007.03.003.

Velzen, E. et al. (2003). Factors Associated with Dough Stickiness as Sensed by Attenuated Total Reflectance Infrared Spectroscopy. *Cereal Chemistry*, *80*, pp. 378-382. https://doi.org/10.1094/cchem.2003.80.4.378.

Veraverbeke, W. S. & Delcour, J. A. (2002). Wheat Protein Composition and Properties of Wheat Glutenin in Relation to Breadmaking Functionality. *Critical Reviews in Food Science and Nutrition*, *42*(3), pp. 179-208. https://doi.org/10.1080/10408690290825510.

Verheul, M., Roefs, S. P. F. M. & de Kruif, K. G. (1998). Kinetics of Heat-Induced Aggregation of β-Lactoglobulin. *Journal of Agricultural and Food Chemistry*, *46*(3), pp. 896-903. https://doi.org/10.1021/jf970751t.

Wang, Q. & Wood, P. J. (2005). Carbohydrates: Physical Properties. In Y. H. Hui & F. Sherkat (Eds.), *Handbook of Food Science, Technology, and Engineering - 4 Volume Set* (1st ed., pp. 2-1 - 2-18). CRC Press. https://doi.org/https://doi.org/10.1201/b15995.

Ward, F. M., Hanway, W. H. & Ward, R. (2005). Food Gums: Functional Properties and Applications. In Y. H. Hui & F. Sherkat (Eds.), *Handbook of Food Science, Technology, and Engineering - 4 Volume Set* (1st ed., pp. 139-131 - 139-116). CRC Press. https://doi.org/https://doi.org/10.1201/b15995.

Whaley, J. K., Templeton, C. & Anvari, M. (2019). Rheological Testing for Semisolid Foods: Traditional Rheometry. In H. S. Joyner (Ed.), *Rheology of Semisolid Foods* (1st ed., pp. 63-96). Springer International Publishing. https://doi.org/10.1007/978-3-030-27134-3_3.

Wyatt, N. B. & Liberatore, M. W. (2009). Rheology and viscosity scaling of the polyelectrolyte xanthan gum. *Journal of Applied Polymer Science*, *114*(6), pp. 4076-4084. https://doi.org/https://doi.org/10.1002/app.31093.

Xanthan gum, 21 C.F.R. § 172.695 (2021). https://www.ecfr.gov/current/title-21/chapter-I/subchapter-B/part-172/subpart-G/section-172.695.

Zandonadi, R. P., Botelho, R. B. A. & Araújo, W. M. C. (2009). Psyllium as a Substitute for Gluten in Bread. *Journal of the American Dietetic Association*, *109*(10), pp. 1781-1784. https://doi.org/https://doi.org/10.1016/j.jada.2009.07.032.

Zhang, J. et al. (2019). Review of isolation, structural properties, chain conformation, and bioactivities of psyllium polysaccharides. *International Journal of Biological Macromolecules*, *139*, pp. 409-420. https://doi.org/10.1016/j.ijbiomac.2019.08.014.

Zhang, Y. et al. (2018). Comparative study on the interaction between native corn starch and different hydrocolloids during gelatinization. *International Journal of Biological Macromolecules*, *116*, pp. 136-143. https://doi.org/https://doi.org/10.1016/j.ijbiomac.2018.05.011.

Zheng, H. (2019). Introduction: Measuring Rheological Properties of Foods. In H. S. Joyner (Ed.), *Rheology of Semisolid Foods* (1st ed., pp. 3-30). Springer, Cham. https://doi.org/https://doi.org/10.1007/978-3-030-27134-3_1.

Zheng, H. et al. (2000). Rheological Properties of Dough During Mechanical Dough Development. *Journal of Cereal Science*, *32*(3), pp. 293-306. https://doi.org/https://doi.org/10.1006/jcrs.2000.0339.

Ziemichód, A., Wójcik, M. & Różyło, R. (2019). Seeds of Plantago psyllium and Plantago ovata: Mineral composition, grinding, and use for gluten-free bread as substitutes for hydrocolloids. *Journal of Food Process Engineering*, *42*(1), p. e12931. https://doi.org/https://doi.org/10.1111/jfpe.12931.

List of Figures

List of Tables

Appendices

Appendix A

Table 17: Moisture content of dry ingredients presented as average.

Dry ingredient	**Moisture content [%]**
Xanthan gum	11.13 ± 0.23
Psyllium	7.29 ± 0.04
Gluten-free starch mix	10.53 ± 0.16
Milk powder	3.34 ± 0.04

Appendix B

Table 18: Composition of the gluten-free doughs and breads with yeast for Goal 2 (Micro mixer, Texture Profile Analysis and Moisture Analysis) and Goal 3. G2YXG & G3XG = Dough/Bread with xanthan gum, G2Y & G3 = Dough/Bread without xanthan gum. Recipe provided by Jungbunzlauer Ladenburg GmbH. *Premixed starch blend. Variations in the composition of the premixed starch blend may occur.

Ingredient	**G2YXG & G3XG**	**G2Y & G3-**
	Percentage [%]	**Percentage [%]**
White rice flour*	18.55	18.78
Brown rice flour*	5.79	5.87
Potato starch*	5.41	5.48
Tapioca flour*	2.32	2.35
Oat flour*	9.29	9.41
Non-fat milk powder	4.07	4.13
Psyllium husk	1.21	1.22
Xanthan gum	1.21	-
GdL	0.53	0.55
Sodium bicarbonate	0.24	0.25
Sub4Salt	0.73	0.75
SSL	0.41	0.42
Sugar	1.98	2.00
Yeast	0.61	0.61
Water	38.35	38.81
Whole eggs	7.41	7.50
Butter	1.86	1.89
SUM	100.00	100.00

Table 19: Composition of the gluten-free doughs without yeast for the rheological measurements in Goal 2. Recipe provided by Jungbunzlauer Ladenburg GmbH. *Pre-mixed starch blend. Variations in the composition of the premixed starch blend may occur.

Ingredient	**G2XG**	**G2-**
	Percentage [%]	**Percentage [%]**
White rice flour*	18.67	18.89
Brown rice flour*	5.83	5.90
Potato starch*	5.45	5.51
Tapioca flour*	2.33	2.36
Oat flour*	9.35	9.47
Non-fat milk powder	4.11	4.15
Psyllium husk	1.21	1.23
Xanthan gum	1.21	-
GdL	0.55	0.55
Sodium bicarbonate	0.25	0.25
Sub4Salt	0.75	0.75
SSL	0.41	0.42
Sugar	1.99	2.01
Yeast	-	-
Water	38.58	39.05
Whole eggs	7.45	7.54
Butter	1.88	1.90
SUM	100.00	100.00

Appendix C

Table 20: LVR and gel strength of the amplitude sweep for G1XG and G1XG-MP. Statistical analysis by means of a t-test. Different letters in the same row indicate statistically significant differences ($p < 0.05$).

Formulation	LVR for $G'_{95\%}$	Gel strength (LVR)
G1XG	30.18 ± 0.57^{a}	3.86 ± 0.14^{a}
G1XG-MP	28.66 ± 1.82^{a}	3.88 ± 0.20^{a}

Table 21: Characteristic viscosity-profile-temperatures for G1XG and G1XG-MP. Statistical analysis by means of a t-test. Different letters in the same row indicate statistically significant differences ($p < 0.05$).

Formulation	Viscosity start (25°C) [Pa.s]	Viscosity (90°C, 5 min.) [Pa.s]	Final viscosity (25°C) [Pa.s]
G1XG	0.03 ± 0.00^{a}	0.02 ± 0.00^{a}	0.03 ± 0.00^{a}
G1XG-MP	0.03 ± 0.00^{a}	0.02 ± 0.00^{a}	0.03 ± 0.00^{a}

Table 22: Characteristic viscosity-profile-temperatures for G1XG and G1XG-Ps. Statistical analysis by means of a t-test. Different letters in the same row indicate statistically significant differences ($p < 0.05$).

Formulation	Viscosity start (25°C) [Pa.s]	Viscosity (90°C, 5 min.) [Pa.s]	Final viscosity (25°C) [Pa.s]
G1XG	0.03 ± 0.00^{a}	0.02 ± 0.00^{a}	0.03 ± 0.00^{a}
G1XG-Ps	0.04 ± 0.00^{b}	0.04 ± 0.00^{b}	0.09 ± 0.00^{b}

Appendix D

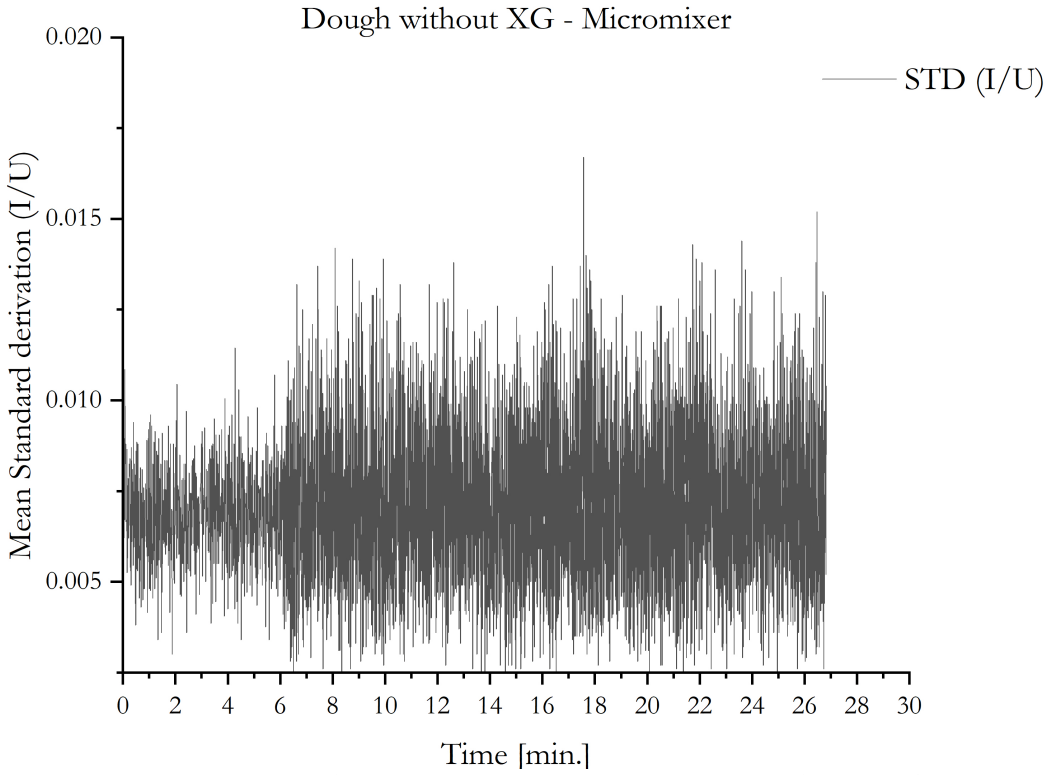

Figure 30: Mixing of G2YXG in the micromixer for 27 min. Mean graph is based on duplicates.

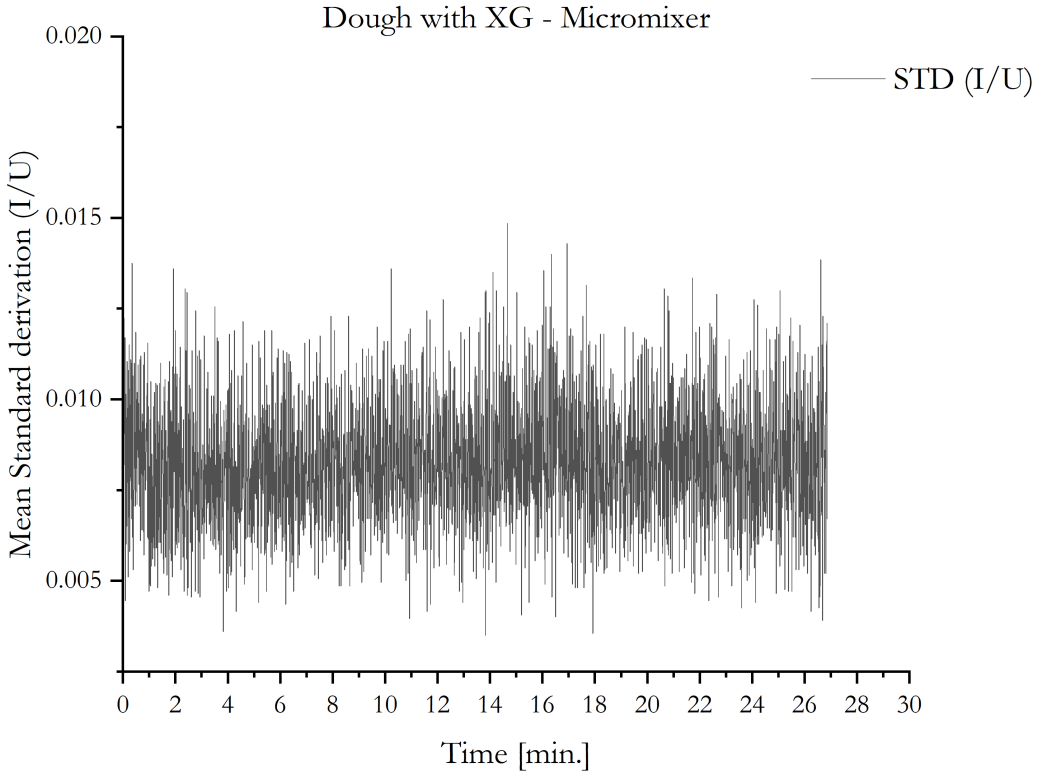

Figure 31: Mixing of G2Y in the micromixer for 27 min. Mean graph is based on duplicates.

Appendix E

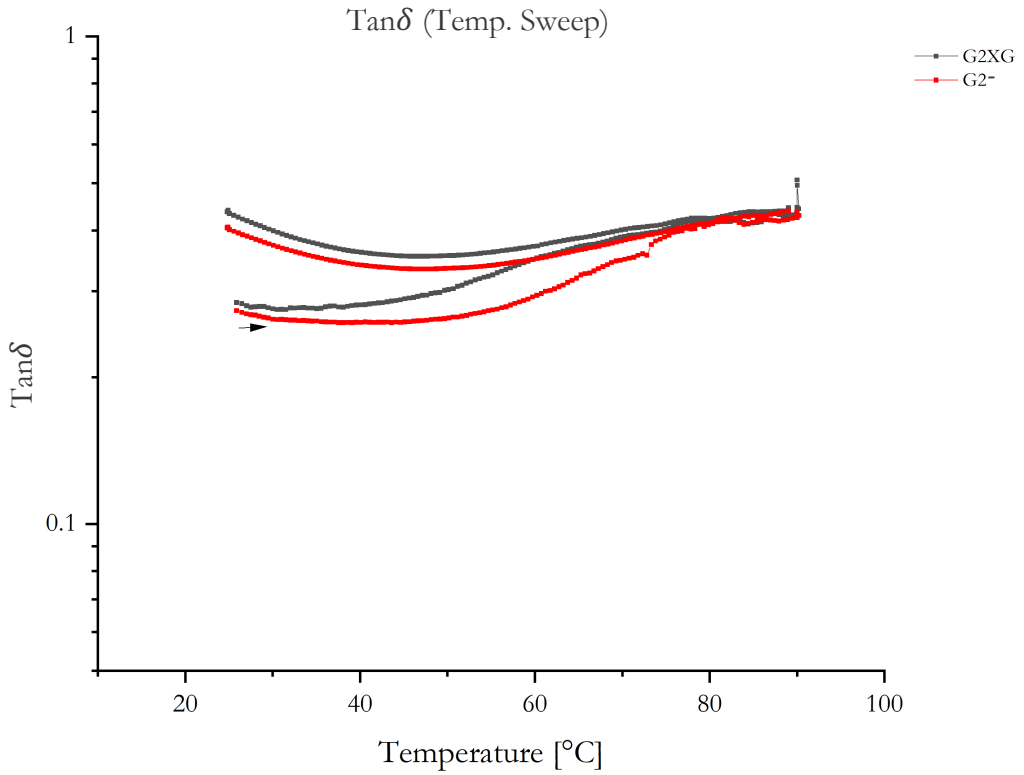

Figure 32: Tanδ of the temperature sweep for G2XG and G2-.

Table 23: Texture analysis parameter mean values. Adhesiveness and stringiness could not have been measured since G2Y got stuck to the cylinder probe. Statistical analysis by means of a t-test. Different letters in the same row indicate statistically significant differences ($p < 0.05$).

Formulation	Firmness [N]	Stickiness [N]	Adhesiveness [mm^2]	Stringiness [mm]
G2YXG	32.13 ± 0.36^a	-4.86 ± 0.25^a	33.99 ± 3.85	13.91 ± 0.77
G2Y	23.92 ± 0.78^b	-4.60 ± 0.26^a	-	-

Appendix G

Table 24: Slopes for the halogen moisture analysis of the bread with xanthan gum (G3XG) and without xanthan gum (G3). Statistical analysis by means of a t-test. Different letters in the same row indicate statistically significant differences ($p < 0.05$).

Formulation	Slope Crust (200s)	Slope Crumb (500s)	Slope Slice (1000s)
G3XG	0.05 ± 0.01^{a}	0.05 ± 0.00^{a}	0.03 ± 0.00^{a}
G3-	0.08 ± 0.04^{b}	0.05 ± 0.01^{a}	0.04 ± 0.00^{a}